pennsylvania
DEPARTMENT OF TRANSPORTATION

Bridge Resiliency in Rain Events

FINAL REPORT

December 10, 2021

By Kewei Gao
Clay Naito, Ph.D., P.E.
Muhannad Sulieman, Ph.D.
Richard Weisman, Ph.D.
Nick Crociata

ATLSS Research Center
Lehigh University

COMMONWEALTH OF PENNSYLVANIA
DEPARTMENT OF TRANSPORTATION

WORK ORDER # 003

Technical Report Documentation Page

1. Report No. FHWA-PA-2021-013-E04005-003	**2. Government Accession No.**	**3. Recipient's Catalog No.**
4. Title and Subtitle Bridge Resiliency in Rain Events		**5. Report Date** December 10, 2021
		6. Performing Organization Code
7. Author(s) Kewei Gao Clay Naito, Ph.D., P.E. Muhannad Sulieman, Ph.D. Richard Weisman, Ph.D. Nick Crociata		**8. Performing Organization Report No.**
9. Performing Organization Name and Address ATLSS Research Center 117 ATLSS Drive Lehigh University Bethlehem, PA 18015		**10. Work Unit No. (TRAIS)**
		11. Contract or Grant No. **E04005 WO 003**
12. Sponsoring Agency Name and Address The Pennsylvania Department of Transportation Bureau of Planning and Research Commonwealth Keystone Building 400 North Street, 6th Floor Harrisburg, PA 17120-0064		**13. Type of Report and Period Covered** Final Report 2020 - 2021
		14. Sponsoring Agency Code

15. Supplementary Notes
This report combines ATLSS Reports 21-01, 21-02 and 21-03.

16. Abstract

A study was conducted to understand the failure mechanisms of backfill materials around bridge abutments and pipe culverts during flood events. A review of standard backfill materials and construction practices used by PennDOT was conducted. Sample backfill materials were characterized for erosion potential. The erosion patterns of currently used backfill materials and construction methods were simulated/scaled in the laboratory and subjected to water flow conditions simulating current design floods and future flood projections based on the recently developed Extreme Weather Vulnerability Study. Based on the observed patterns of failure, proposed construction practices are examined in the laboratory with the objective of reducing failure during flood events.

17. Key Words Resilience, Extreme Rain Events, Structural Backfill, Embankment, Culvert		**18. Distribution Statement** No restrictions. This document is available from the National Technical Information Service, Springfield, VA 22161	
19. Security Classif. (of this report) Unclassified	**20. Security Classif. (of this page)** Unclassified	**21. No. of Pages** 158	**22. Price**

ACKNOWLEDGMENTS

The contents of this report reflect the views of the authors who are responsible for the facts and the accuracy of the data presented herein. The contents do not necessarily reflect the official views or policies of the US Department of Transportation, Federal Highway Administration, or the Commonwealth of Pennsylvania at the time of publication. This report does not constitute a standard, specification or regulation.

This work was sponsored by the Pennsylvania Department of Transportation and the U.S. Department of Transportation, Federal Highway Administration.

ABSTRACT

A study was conducted to understand the failure mechanisms of backfill materials around bridge abutments and pipe culverts during flood events. A review of standard backfill materials and construction practices used by PennDOT was conducted. Sample backfill materials were characterized for erosion potential. The erosion patterns of currently used backfill materials and construction methods were simulated/scaled in the laboratory and subjected to water flow conditions simulating current design floods and future flood projections based on the recently developed Extreme Weather Vulnerability Study. Based on the observed patterns of failure, proposed construction practices are examined in the laboratory with the objective of reducing failure during flood events.

This report summarizes the results of Task 1.1 to 1.3. Task 1.1 provides a summary of the state of the practice for construction of backfill used by the state Departments of Transportation, a summary of standard backfill materials used and properties (gradation curves) other states relative to Pennsylvania, resistance of materials to piping, slumping, and erosion with respect to PA materials, and backfill characterization of the materials used in the experimental program. Task 1.2 discusses the development of the test program on embankments and embankments with bridge openings. The experimental results are summarized, and recommendations are provided for construction details to improve the resilience of structural backfill under extreme rain events. Task 1.3 provides an assessment of erosion of culvert backfills. The development of the culvert test program and the experimental results are summarized. Recommendations are provided for construction details to improve the resilience of structural backfill under extreme rain events.

TABLE OF CONTENTS

LIST OF FIGURES

1. BACKGROUND

Pennsylvania State Climate Summaries report that precipitation, especially extreme precipitation, have been increasing during the last two decades in Pennsylvania (Frankson et al., 2017). The temperatures in Pennsylvania have also risen in the winter and spring (Frankson et al., 2017; Reidmiller et al., 2017). More frequent precipitation and higher temperatures have led to an increase of snowmelt in Spring, which results in an increased risk for extreme floods. Extreme floods can lead to overtopping of bridge embankments when the flow exceeds the capacity of the bridge opening or for cases where the openings may be obstructed due to debris. Cases of erosion of backfill material around a bridge abutment due to intense flood events and overtopping have been observed throughout Pennsylvania in recent years (Figure 1.1 and Figure 1.2).

Figure 1.2 Erosion of backfill material and culvert failure caused by overtopping (courtesy of PennDOT)

Local materials consisting of compacted fine soils have been widely used as the backfill material for embankments. Cohesionless fine sands, however, are easily erodible (Briaud, 1997). For cases where the bridge opening is obstructed, the low permeability of fine soils can result in the accumulation of water upstream, which leads to an increased water head differential upstream and downstream of the embankment. Piping (the movement of water and soil particles through the

embankment) and slope stability issues are more likely with the large head differential resulting in the initiation of erosion and a progressive failure of the embankment.

Layered soil-cement, concrete blocks and gabions have been applied to prevent the erosion (DeGroot, 1976; Hewlett et al., 1987; Powledge & Dodge, 1985). However, the cost of these conventional methods are relatively high (Powledge et al., 1989). Methods with lower costs, such as Riprap and Geobags, have been shown to provide surface protection of the backfill material which increase the geotechnical stability of the embankment (Korkut et al., 2007; Morales et al., 2008). For example, geotextile was applied to prevent erosion by allowing for drainage and dissipation of pore water pressure (Carroll Jr et al., 1992). However, there is a lack of fundamental research on erosion of bridge structural backfill materials during flood events and cases where the embankment is overtopped. Limited research has been conducted to investigate the effect of combining the use of aggregates, riprap (also referred to as rock lining within this report) and geotextile to enhance the erosion resistance under extreme flood events.

To help understand the issues involved in the erosion of backfill materials, this report provides an overview of the following:

- Summary of state of the practice for construction of backfill for State Departments of Transportation
- Summary of standard backfill materials used in the U.S. Bridge Practice
- Erosion resistance of materials with respect to PA materials
- Characterization of Backfill Material Used in Experimental Study

2. EROSION MECHANISM

Erosion of embankments, dams, and levees can be defined as the detachment of the particles away from the soil under the action of a fluid flow (Briaud et al., 2019; Sterpi, 2003). There are two forms of erosion: surface erosion and internal erosion. (Adamo et al., 2020; Briaud et al., 2019; Sterpi, 2003). Internal erosion refers to the movements of soil particles transported within the body of the embankment when subjected to an eroding fluid (Wan & Fell, 2004). Surface erosion mainly occurs on the surface of the soil due to the drag shear force and uplift normal force driven by fluids (Briaud et al., 2019).

The internal erosion can be further divided into two types: piping and suffusion (Briaud et al., 2019). Suffusion refers to the detachment of finer soils exiting the coarser particles driven by the water flow (Briaud et al., 2019; Sterpi, 2003; Yang et al., 2019). Piping is a form of seepage erosion at a high exit gradient due to the high water head difference between upstream and downstream (Briaud et al., 2019; Ojha et al., 2003). Fluid percolates through the embankment and transport the fines, which are free to move, leads to the loss of fines (Ojha et al., 2003). The continuous loss of the fines cause the formation of flow channels in the embankment, which leads to the piping failure and the settlement of the embankment (Cividini et al., 2009; Yang et al., 2019). Densely packed soils and soils with large mean grain size (D_{50}), which have higher seepage velocity and piping resistance are recommended to mitigate the internal erosion (Fell & Fry, 2007).

The surface erosion of sand and gravel due to water flow is related to the water velocity (Briaud et al., 2008). Figure 2.1 describes a free body diagram of a soil particle subjected to a water flow (Briaud, 2008). The drag force created by water flow and the normal force from surrounding particles determine the movement of a soil particle. As the water flows, the relative motion between soil and water creates shear force on the eroding surface and the shear force increase as the flow velocity increases (Briaud et al., 2001). The normal force also changes with the fluctuation of flow based on Bernoulli's principle, which states that the static pressure or the potential energy of the fluid decreases as the increase of the fluid velocity (Hewitt, 2004). Erosion is initiated when the particle starts to move as the combination of shear force and the uplift force created by water flow become large enough to overcome the resultant force by friction and the self-weight of the soil particle. The critical shear stress (τ_c) is defined as the threshold shear stress at which the erosion starts, and the critical velocity (V_c) is defined as the flow velocity when the erosion initiates. For cohesionless materials (sand and gravel), the critical velocity (Equation 1) and the critical shear stress (Equation 2) are related to the mean grain size (D_{50}) (Figure 2.2 and Figure 2.3).

$$V_c = 0.35(D_{50})^{0.45} \qquad \text{Equation 1}$$

$$\tau_c = D_{50} \qquad \text{Equation 2}$$

When the mean grain size of the soil is larger than 0.5 mm, the critical velocity and the critical shear stress increase with the increase of the mean grain size. Thus, the soil with larger grain size has higher erosion resistance and is preferred to resist the water erosion.

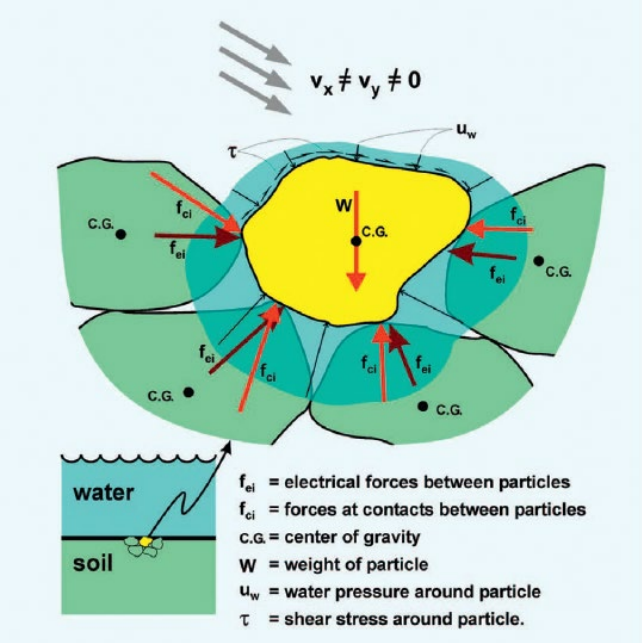

Figure 2.1 Free body diagram of a soil particle under a water flow (Briaud, 2008)

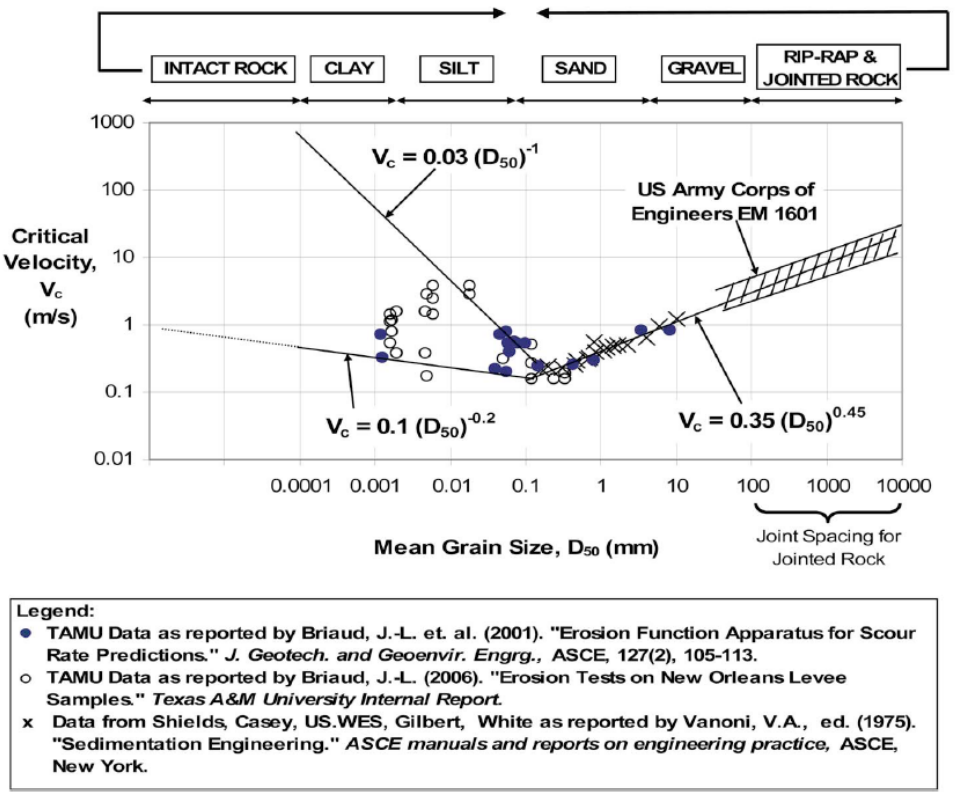

Figure 2.2 Critical velocity as function of mean grain size (Briaud, 2008)

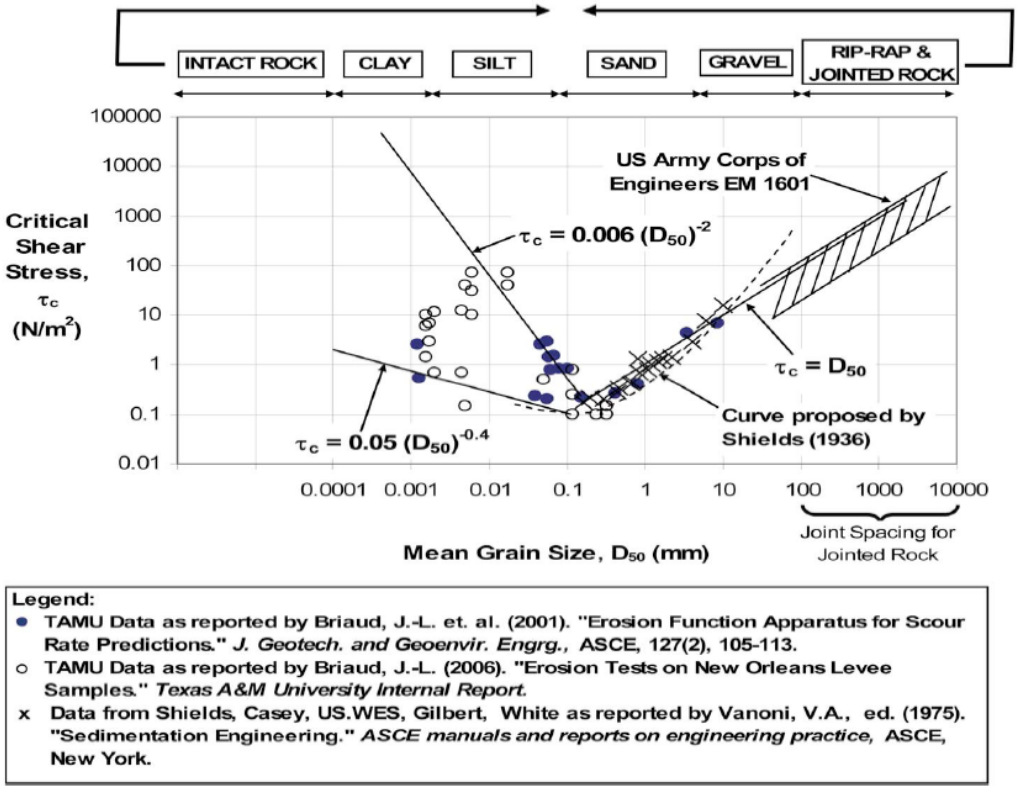

Figure 2.3 Critical shear stress as function of mean grain size (Briaud, 2008)

Ideally structural backfills should consist of materials that are capable of being compacted, have no time dependent properties, are resistant to erosion and are elastic (Kimmerling, 2002; White et al., 2005). Therefore, for example, organic soils (e.g. organic waste, wood, coal and charcoal) and highly organic soils (e.g. peat and muck) are not recommended as the structural backfill material in the embankment design (Kimmerling, 2002). Structural backfill materials behind the bridge abutment are commonly compacted granular soil or compacted granular soil with geosynthetics reinforcement (Zevgolis & Bourdeau, 2007). The compacted granular material, which can be called "high-quality granular soil", has been successfully used by Washington State Department of Transportation (WSDOT), the New Mexico Department of Transportation, and the Minnesota Department of Transportation behind the bridge abutment (Abu-Hejleh et al., 2014). The compaction level is based on the standard Proctor test per AASHTO T99, and with a suggested moisture content of ±2% of the optimum moisture content. Federal Highway Administration (FHWA) recommends that well graded soil be used for structural backfill to ease compaction and ensure proper drainage (Samtani & Nowatzki, 2006). The region behind the abutment shall consist of structural backfill material as illustrated in Figure 3.1.

Structural backfill near the bridge abutment is designed to prevent deformations of the bridge approach which often occur when using in-situ soils (Briaud, 1997; Helwany et al., 2007; Long et al., 1998; Wahls, 1990). The gradation of the structural backfill, which is recommended by FHWA are listed in Table 3.1 (Samtani & Nowatzki, 2006). Gravels and sands are recommended based on the gradation shown in Table 3.1. Fines (grain size smaller than 0.075 mm) are not recommended because of the expected consolidation settlement and poor drainage (Samtani & Nowatzki, 2006).

Table 3.1 Structural backfill gradation recommended by FHWA

Size (mm)	101.6	0.4191	0.075
Sieve	4-inch	No.40	No.200
Federal Highway Administration	100	0-70	0-15

In the case of embankment overtopping, structural backfills are below the water level. This decreases the frictional shearing resistance between soil particles due to the decrease or loss of effective stress, which may lead to the slope failure (Samtani & Nowatzki, 2006). Geosynthetics (Geogrid and Geotextile) are recommended to increase the internal resisting forces to mitigate embankment instability problems as shown in Figure 3.2 (Samtani & Nowatzki, 2006).

Geosynthetic Reinforced Soil (GRS) has been used behind the bridge abutment due to low cost and simplicity of design and construction (Adams et al., 2011). The conceptual design of the GRS backfill is shown in Figure 3.3. However, this design is mainly focusing on reducing settlement (Han & Gabr, 2002; Han et al., 2012; Han & Akins, 2002). Geotextiles have also been used to increase the shear strength of the soil, mitigate the lateral earth pressure applied to the bridge abutment, reduce the differential settlement of approach slabs, minimize erosion, and improve drainage (Haeri et al., 2000; Kramer & Sajer, 1991; Palmeira & Gardoni, 2002). Geotextile is recommended for subsurface drainage and embankment erosion control (GDOT, 2013; Iowa, 2012; LaDOTD, 2016; Tennessee, 2015). Geogrids are recommended to reinforce granular backfill materials behind retaining walls (Iowa, 2012; LaDOTD, 2016; ODOT, 2005; Tennessee, 2015).

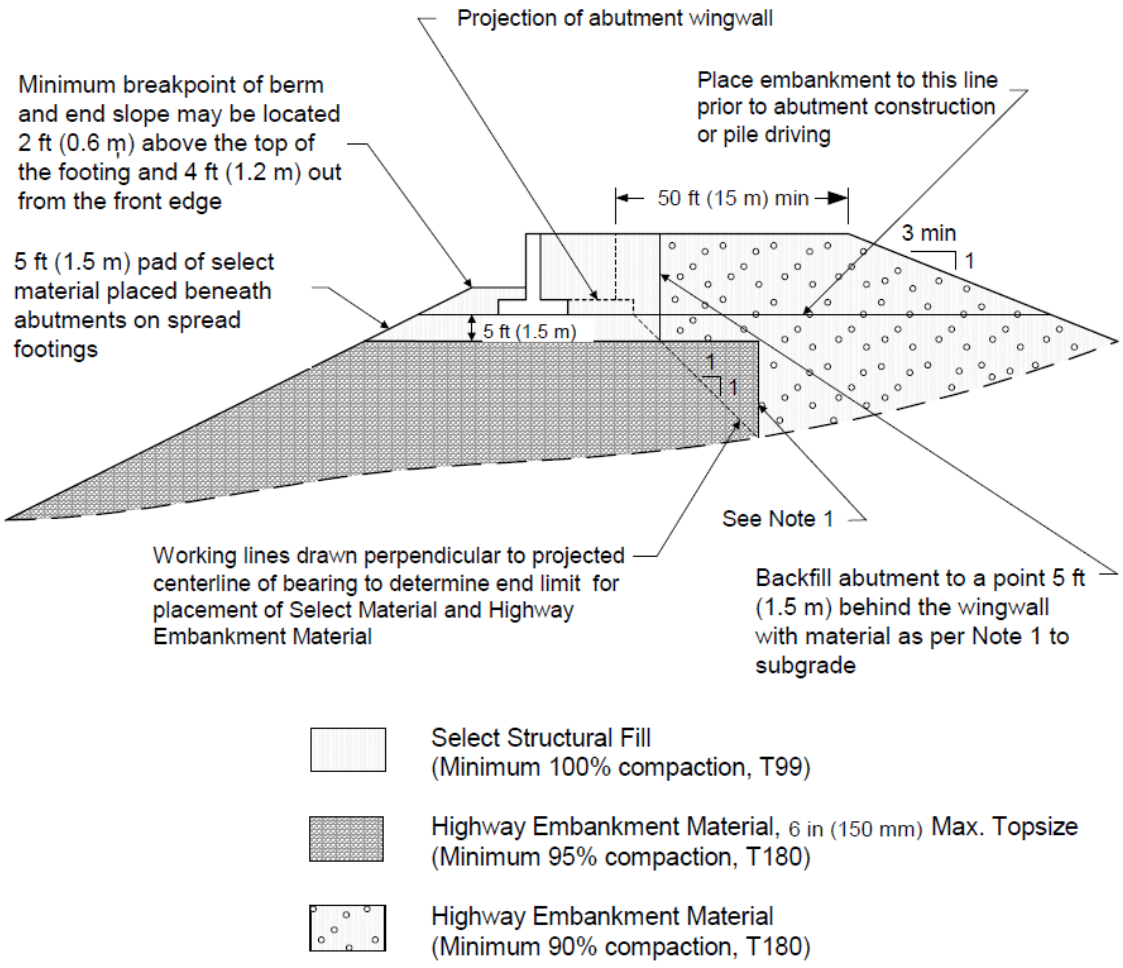

Figure 3.1: FHWA highway embankment material use (Samtani & Nowatzki, 2006)

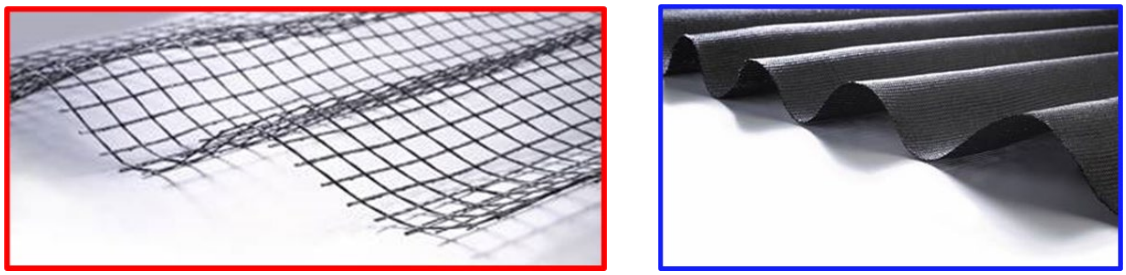

Figure 3.2: Geosynthetics (a) Geogrid, (b) Geotextile
[https://gagneandson.com/products/landscape/accessories/fabrics-grids-adhesives/]

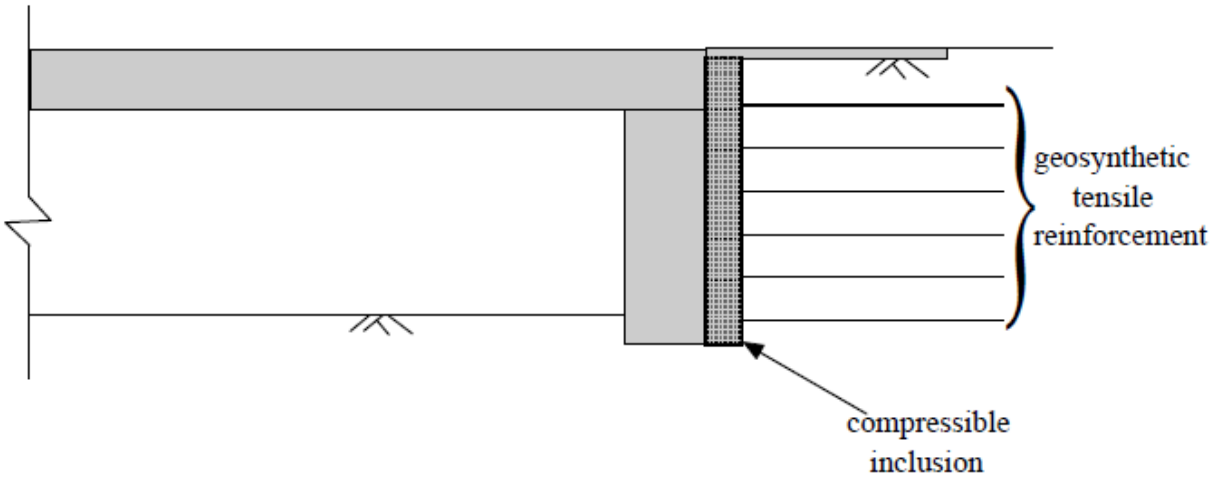

Figure 3.3 GRS backfill behind bridge abutment (Horvath, 2000)

3.1. CURRENT AND PROPOSED PENNDOT RECOMMENDATIONS

Pennsylvania Department of Transportation recommendations are outlined in PennDOT Publication 408/2020 (PennDOT, 2020) and PennDOT RC-Drawings (PennDOT, 2010). The various materials specified are summarized in this section.

3.1.1. Structural Backfill

Excavation or obtaining material used for structure backfill is specified in PennDOT Publication 408/2020 Section 205.2. Materials including AASHTO No. 1, No. 2A, No. 3, No. 5 or No. 57 Coarse Aggregate gradation, meeting at least Type C quality requirements and as specified in Section 703.2 in Pub 408/2020-2, Table B (Table 3.2) and 703.2 Table C (Table 3.3) are allowed.

PennDOT Publication 408/2020 Section 206.2.1.c: Material consisting of natural or synthetic mineral aggregates having less than or equal to 70% of the material passing the 3/8-inch sieve (greater than or equal 30% retained on the 3/8-inch sieve) and less than 20% passing the No. 200 sieve. Also includes AASHTO Nos. 8 or 57 coarse aggregate, or PennDOT Nos. 2A or OGS coarse

aggregate meeting the requirements specified in Section 703.2, select granular material (2RC) meeting the requirements specified in Section 703.3, and structure backfill.

PennDOT RC-Drawings-14M indicates that: Portions of slopes below the 500-year floodplain elevation must use AASHTO No.8 Coarse Aggregate for the reinforced backfill.

Table 3.2 Coarse aggregate quality requirements (PennDOT Publication 408/2020-2 Section 703.2 Table C)

	Type A	Type B	Type C	Type S
Soundness, Max. %	10	12	20	16
Abrasion, Max. %	45	45	55	55
Freeze-Thaw Loss, Max %	—	—	—	7.0(6)
Thin and Elongated Pieces, Max. %	15	20	—	—
Material Finer Than 75 µm (No. 200) Sieve, Max. %	—(1)	—(1)	10	10
Crushed Fragments, Min. %	55(2)	55(2)	50	50
Compact Bulk Density (Unit Weight), lbs./cu. ft.	70	70	70	70
Deleterious Shale, Max. %	2	2	10	10
Clay Lumps, Max. %	0.25	0.25	3	3
Friable Particles, Max. % (excluding shale)	1.0	1.0	—	—
Coal or Coke, Max. %	1	1	5	5
Glassy Particles, Max. %	4 or 10(3)	4 or 10(3)	—	—
Iron, Max. %	3(5)	3(5)	3(5)	3(5)
Absorption, Max. %	3.0(4)	3.5(4)	—	2(4)
Total of Deleterious Shale, Clay Lumps, Friable Particles, Coal, or Coke Allowed, Max. %	2	2	15	15

Notes:

(1) Section 703.2(c)4.
(2) Section 703.2(c)5.
(3) Section 703.2(c)9.
(4) Gravel only for Types A and B. as specified in Section 703.2(c)2. All natural aggregates for Type S.
(5) Section 703.2(c)10..
(6) Natural coarse aggregates with an absorption less than 2% are considered freeze thaw resistant and not subject to testing according to AASHTO T 103, Procedure A. Natural aggregates with an absorption exceeding 2% shall be considered freeze thaw resistant if either their sodium sulfate soundness level is less than 16% or their AASHTO T 103 freeze thaw loss after 25 cycles (coarse fraction) does not exceed 7.0%. Type S 2A aggregate may be supplied where Type 2A aggregate for purposes other than subbase is specified at no additional cost to the Department.
(7) Test methods to determine the quality requirements of Table B as specified in Section 703.2 (c).

Table 3.3 Size and grading requirements for coarse aggregates based on laboratory sieve tests, square openings (PennDOT Publication 408/2020-2 Section 703.2, Table C)

AASHTO Number	Total Percent Passing														
	100 mm (4")	90 mm (3 1/2")	63 mm (2 1/2")	50 mm (2")	37.5 mm (1 1/2")	25.0 mm (1")	19.0 mm (3/4")	12.5 mm (1/2")	9.5 mm (3/8")	4.75 mm (No. 4)	2.36 mm (No. 8)	1.18 mm (No. 16)	300 µm (No. 50)	150 µm (No. 100)	75 µm (No. 200) ***
1	100	90-100	25-60		0-15		0-5								
3			100	90-100	35-70	0-15		0-5							
467				100	95-100		35-70		10-30	0-5					
5					100	90-100	20-55	0-10	0-5						
57					100	95-100		25-60		0-10	0-5				
67						100	90-100		20-55	0-10	0-5				
7							100	90-100	40-70	0-15	0-5				
8								100	85-100	10-30	0-10	0-5			
89								100	90-100	20-55	5-30	0-10	0-5		
9									100	85-100	10-40	0-10	0-5		
10									100	85-100				10-30	
2A**				100			52-100		36-70	24-50	16-38*	10-30			
OGS**				100			52-100		36-65	8-40		0-12			

* Applies only for asphalt mixtures.
** PennDOT Number – Only Type C and Type S will be listed in Bulletin 14.
*** For 75 µm (No. 200), see Table D.

3.1.2. Riprap (Rock Lining)

Riprap (Rock Lining) is allowed in PennDOT Publication 408/2020 Section 223.2(m): The description of the material properties is indicated in Section 850.2. The required gradation of Rock lining is shown in Table 3.4.

PennDOT RC-Drawings-14M also indicates that: Placing Rock Lining and AASHTO No.1 Coarse Aggregate in lifts should not exceed 4.5 feet. No more than 3 wire mesh forms are to be exposed before covering with AASHTO No. 1 Coarse Aggregate and Rock Lining; Minimum required thickness of Rock Lining is 2.5 times the top size of rock specified of rock lining, measured perpendicular to the slope face.

Table 3.4 Rock lining size and gradation (PennDOT Publication 408/2020 Section 850.2)

Percent Passing (Square Openings)						
Class, Size No. (NCSA)	**R-8****	**R-7****	**R-6**	**R-5**	**R-4**	**R-3**
Rock Size, inches						
42	100*					
30		100*				
24	15-50		100*			
18		15-50		100*		
15	0-15					
12		0-15	15-50		100*	
9				15-50		
6			0-15		15-50	100*
4				0-15		
3					0-15	15-50
2						0-15
Nominal Placement Thickness, inches	48	36	30	24	18	12

* Maximum allowable rock size.
** Use Class 4, Type A geotextile

3.1.3. Geosynthetics

Geosynthetic is allowed in RC-Drawings-14M (PennDOT, 2019) for the soil slope reinforcement. Figure 3.4 shows the structure of an example of the Geosynthetic reinforced soil slope (Type C slope defined in RC-Drawings-14M). Type C slope has the maximum slope angle of 1.25(H):1(V). The surface of the slope consists of a layer of Rock lining to mitigate the surface erosion. The inner (core) part of the slope was reinforced by Primary Geosynthetic (Geogrid) and Secondary Geosynthetic (Geotextile). Between the Geosynthetic-reinforced slope and the Rock lining, there is a layer of AASHTO No.1 Coarse Aggregate. Details are shown in the later paragraphs.

RC-Drawings-14M notes that when using a No.8 Coarse Aggregate reinforced backfill, the Class 4, Type A Geotextile secondary reinforcement must wrap around the No.8 Coarse Aggregate, at both the slope face and at the back of the reinforced backfill. The secondary reinforcement wraps must be embedded a minimum of 4 feet into the next reinforcement layer. Primary Geosynthetic Reinforcement consists of a Geogrid meeting the requirements of publication 408, sections 738.1 and 738.2 Class 1, Type A or B. Primary geosynthetics are required to be placed in continuous strips perpendicular to the slope face. The maximum allowable vertical spacing of primary geosynthetics is 18 inches. Two layers of secondary reinforcement are placed evenly spaced between layers of primary reinforcement. Vertical spacing between all secondary layers, and between secondary and primary layers above or below, is 6 inches (PennDOT, 2020).

PennDOT Publication 408/2020 Section 738.1: Provide geogrid listed in Bulletin 15 and conforming to the following requirements. Geogrids must be manufactured from either PVC coated polyester (PET), high density polyethylene (HDPE), or polypropylene (PP) polymer according to the class indicated. No post-consumer recycled material is allowed in polymer resins used in the manufacturing of geogrid products. Requirements for the polymers are indicated in Table 3.5.

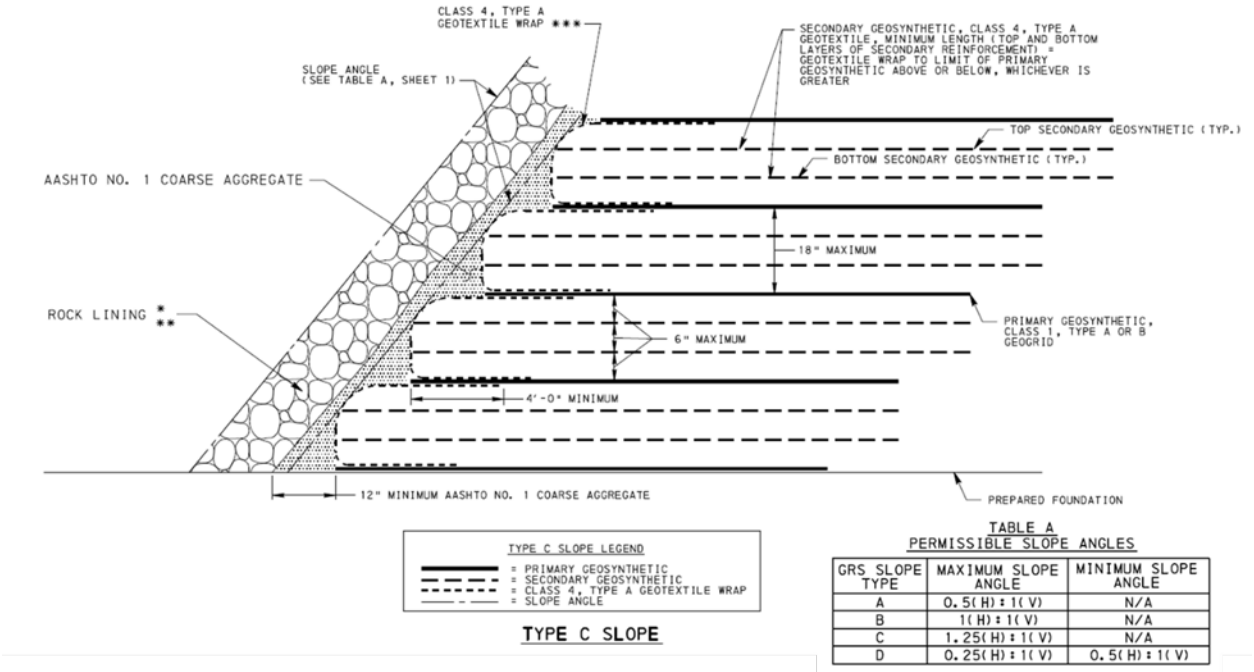

Figure 3.4 Geosynthetic reinforced Type C soil slope (PennDOT RC-Drawings-14M)

Table 3.5 Requirements for Geogrid Polymers (PennDOT Publication 408/2020 Section 738.1, Table A)

Property	Units	Test Method	PET	HDPE	PP
Carboxyl End Group (CEG) Content of PET Yarns	mmol/kg	GRI:GG7[2]	< 30.0	N/A	N/A
Number Average Molecular Weight (M_n) of PET Yarns	-	GRI:GG8[2]	25,000	N/A	N/A
PVC Coating	Except for manufacturing selvedge edges, the PVC coating for PET geogrids must be continuous with no more than 0.03% of the surface area having uncoated, unbound fiber bundles as determined according to ASTM D610.			N/A	N/A
Carbon Black Content[3]	%	ASTM D1603 or ASTM D4218	N/A	2.0 to 3.0	2.0 to 3.0
Melt Flow Index	g/10 min	ASTM D1238 using Condition190/2.16 for HDPE and Condition 230/2.16 for PP	N/A	0.50	0.25
Density	g/cm^3	ASTM D792 or ASTM D1505	N/A	0.940	0.955
Oxidative Induction Time	min	ASTM D3895	N/A	100.0	100.0
Resistance to UV Degradation[4]	%	ASTM D4355 and ASTM D6637 (Method B)	N/A	95	95

Notes:

1. All values are minimum average roll values (MARV), except for CEG for PET polymer which is a maximum average roll value. The maximum average roll value is determined mathematically the same as a MARV, except the value is a maximum.
2. GRI is a reference for the Geosynthetic Institute, formerly known as the Geosynthetic Research Institute.
3. For buried applications only. Do not use geogrids with long-term exposure to UV radiation.
4. A sample is exposed to 500 hours of UV radiation according to ASTM D 4355. The sample is then tested to determine the ultimate tensile strength in the machine direction (MD) for uniaxial geogrids and both the machine and cross machine directions (MD and XD) for biaxial geogrids. The value is calculated by dividing ultimate tensile strength of the UV exposed material by the ultimate tensile strength of the virgin material, and multiplying by 100. Ultimate tensile strengths of all samples are determined according to ASTM D6637, Method B. For biaxial geogrids the minimum required value must be met in both the MD and XD.

PennDOT Publication 408/2020 Section 738.2: Geogrid notes that uniaxial Geogrid reinforcement is for use in geosynthetic reinforced soil (GRS) slopes or geosynthetic reinforced mechanically stabilized earth (MSE) walls. Physical requirements of values and test methods for geogrid properties are indicated in Table 3.6.

Table 3.6 Requirements Class 1 Geogrids – Uniaxial Geogrid Reinforcement (PennDOT Publication 408/2020 Section 738.2, Table B)

Design Parameter	Units	Test Method	Type A	Type B
Polymer Type	-	N/A	PVC Coated PET	Integrally Formed[5] HDPE
Ultimate Tensile Strength	lbs/ft	ASTM D6637 (Method B)	Design Specific	
Tensile Strength at 10 percent elongation, (T_{10})	lbs/ft	ASTM D6637 (Method B)	Design Specific	
Creep Reduction Factor, (RF_C)[1] (determined for a 100 year design life)	-	AASHTO R 69, ASTM D5262, and ASTM D6992	1.60	2.60
Installation Damage Reduction Factor, (RF_{ID})[1, 2]	-	GRI:GG4 (method a or b as appropriate), ASTM D5818, and ASTM D6637	1.30	1.30
Durability Reduction Factor, (RF_D)[1]	-	N/A	1.20	1.10
Overall minimum required reduction factor (RF_{OV})[1, 3, 6]	-	N/A	2.50	3.70
Machine Direction (MD) Aperture Size	in.	N/A	0.60 to 6.0	0.60
Cross Machine Direction (XD) Aperture Size	in.	N/A	0.50	0.50
Rib Section Area Ratio[4]	-	N/A	0.30	0.30
Percent Open Area	%	N/A	45.0	45.0

Notes:
1. Value indicated is the minimum required reduction factor. If product specific data values are higher, the product specific data values must be used.
2. Installation Damage Reduction Factor (RF_{ID}) is valid for a maximum aggregate particle size of 0.5 inch.
3. $RF_{OV} = RF_C \times RF_{ID} \times RF_D$
4. Rib Section Area Ratio = Minimum XD Rib Section Area / Minimum MD Rib Section Area
5. Manufactured by a punched-drawn process.
6. Maximum allowable strain of the geogrid is five percent for the 100 year design live when applying the minimum required overall reduction factor (RF_{OV}).

Secondary reinforcement consists of Class 4, Type A Geotextile meeting the requirements of PennDOT Publication 408/2020, section 735. PennDOT Publication 408/2020 Section 735: Use fabric consisting of long chain polymeric filaments or yarns such as polyethylene, polyamide, polyvinyledene-chloride, polypropylene, or polyester formed into a stable network so that the filaments or yarns retain their relative position to each other. Use fabric structures as noted in Table 3.7.

Table 3.7 Geotextile Physical Requirements (PennDOT Publication 408/2020 Section 735, Table A)

Fabric Properties	Test Method	Construction Class				
		Class 1	Class 3		Class 4	
		Subsurface Drainage	Sediment Control		Separation and Erosion Control	Stabilization and GRS Abutments
			Type A	Type B	Type A	Type C
Fabric Structure	N/A	Woven Monofilament	Woven Slit Film	Woven Slit Film	Non-woven Needle Punched	Woven Polypropylene
Weight, oz/sy	ASTM D5261	N/A	N/A	N/A	12.0 min	N/A
Grab Tensile Strength, lbs.(3)	ASTM D4632	365 min MD x 190 min XD	185 min MD and XD	115 min MD and XD	305 min MD and XD	N/A
Grab Tensile Elongation, %(3),(5)	ASTM D4632	22 to 34 MD x 9 to 26 XD	13 to 31 MD and XD	13 to 31 MD and XD	50 min MD and XD	N/A
Ultimate Wide Width Tensile Strength, lb/ft	ASTM D4595	N/A	N/A	N/A	N/A	4,800 min MD and XD
Wide Width Tensile Strength @ 2% Strain, lb/ft	ASTM D4595	N/A	N/A	N/A	N/A	Design Specific(4)
Puncture, lbs. (2-in flat- end rod)	ASTM D6241	660 min	700 min	440 min	830 min	1,700 min
Trapezoid Tear Strength, lbs.	ASTM D4533	95 min MD x 75 min XD	70 min MD and XD	50 min MD and XD	110 min MD and XD	170 min MD and XD
Apparent Opening Size, mm (Sieve No.)	ASTM D4751	0.30 to 0.60 (No. 50 to No. 30 sieve)(5)	0.21 to 0.43 (No. 70 to No. 40 sieve)(5)	0.30 to 0.60 (No. 50 to No. 30 sieve)(5)	0.15 max	0.425 to 0.85 (No. 40 to No. 20 sieve)(5)
Percent Open Area, %	COE CW-02215	9.0 to 12.0(5)	N/A	N/A	N/A	N/A
Permittivity, sec^{-1}	ASTM D4491	1.9 min	0.05 min(5)	0.05 min(5)	0.70 min	0.40 min(5)
Water Flow Rate, g/min/sf	ASTM D4491	130 min	N/A	N/A	N/A	25 min
Ultraviolet Resistance Strength Retention, %	ASTM D4355	90 @ 500 hrs min	70 @ 500 hrs min	70 @ 500 hrs min	70 @ 500 hrs min	70 @ 500 hrs min

(1) The numerical values indicate the required minimum or maximum (as indicated) average values for ten test specimens. No more than 20% of the individual specimens may have a value less than the required minimum value or greater than the required maximum value (as indicated), except as noted (see Note 5).
(2) MD = Machine Direction, XD = Cross Machine Direction
(3) Test conducted using 1/32 inch thick neoprene pads on grip faces having a Shore A durometer value of 70±5.
(4) Wide width tensile strength at 2% strain in both the machine and cross machine directions (MD x XD), must be greater than or equal to required design tensile strength.
(5) The numerical values indicate the allowable range or required minimum (as indicated) based upon the numerical average of all test specimens from a sample.

In summary, the properties of soil, the design of the reinforced structural backfill configurations behind the bridge abutment consist of: (1) AASHTO #57 coarse aggregates used for the structural backfill based on the PennDOT RC-Drawings-12M and RC-Drawings-14M; AASHTO #8 coarse aggregates are recommended for Geosynthetic-Reinforced Backfill based on the PennDOT RC-Drawings-14M; (2) R-4 Rock lining is recommended for use as rock lining to protect the surface of the slope based on the PennDOT RC-Drawings-14M; (3) Primary Geosynthetic Reinforcement consists of a Geogrid meeting the requirements of PennDOT Publication 408/2020 Sections 738.1 and 738.2 Class 1, Type A or B; Secondary reinforcement consists of Class 4, Type A Geotextile meeting the requirements of PennDOT Publication 408/2020 Section 735 and are used to wrap and reinforce the #8 Coarse Aggregates; (4) embankment material (originally from the site) can be used away from the structural backfill. Details of the design are included in Figure 3.5 and Figure 3.6.

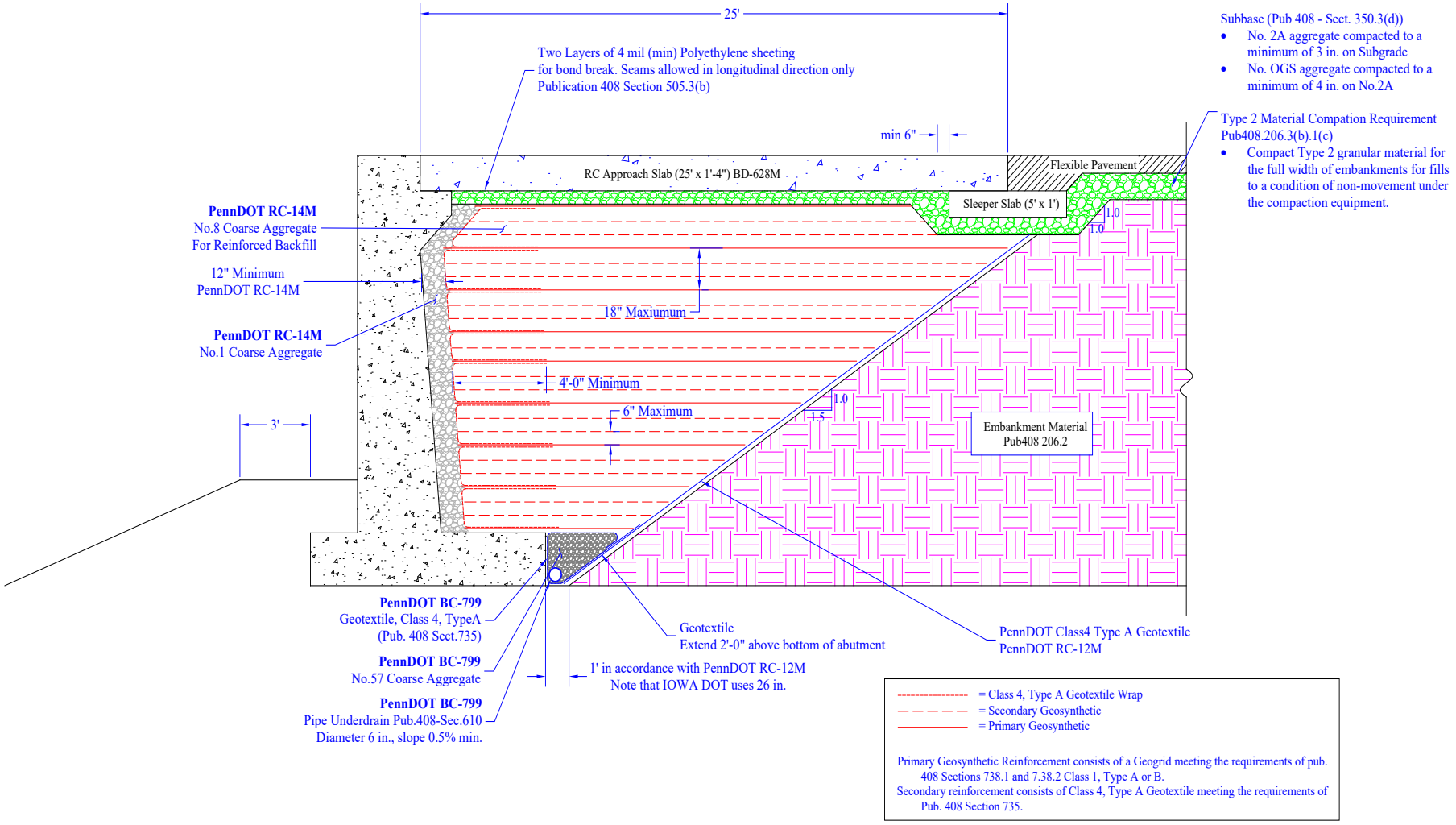

Figure 3.5 Structural backfill design based on PennDOT Publication 408/2020 and PennDOT RC-Drawings-14M

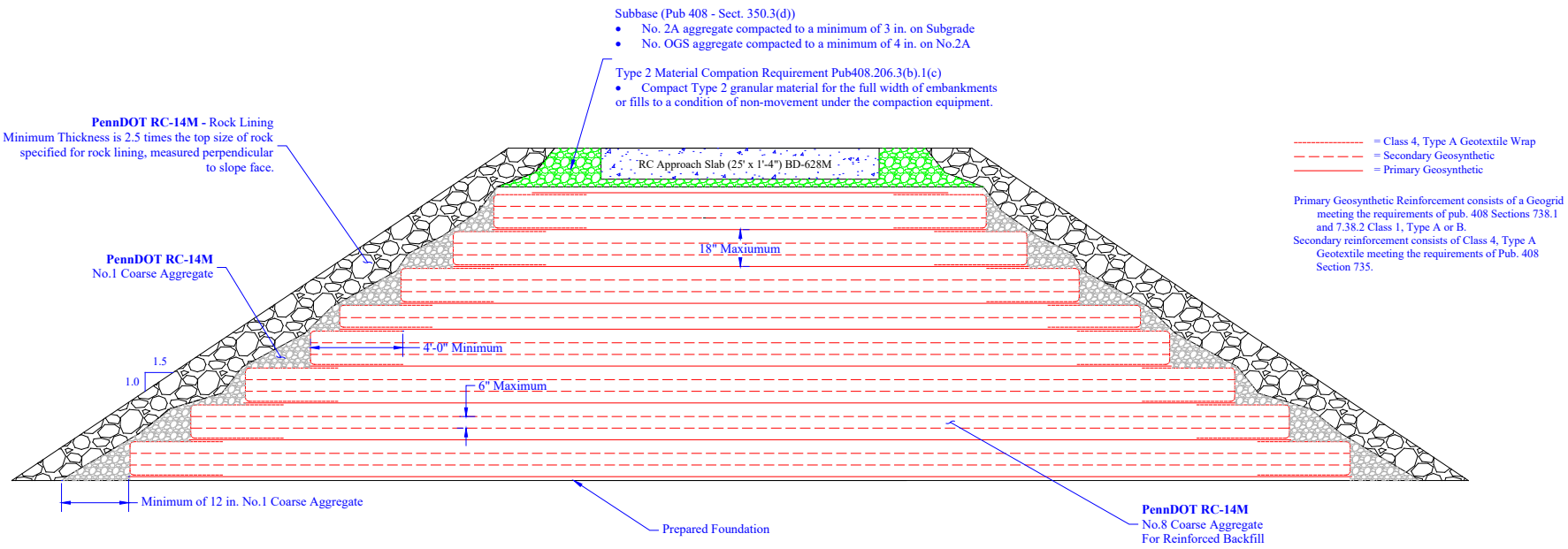

Figure 3.6 Reinforced abutment design based on PennDOT Publication 408/2020 and PennDOT RC-Drawings-14M

PennDOT RC-Drawings-12M defines the Structural Backfill as the backfill at the structures (bridge abutments, box and arch culverts, and wingwalls). Structural backfill is defined as the backfill materials and backfilling excavations for bridges, box culverts, retaining walls, and structural plate pipes and pipe arches (Wisconsin DOT, 2021). Structural backfill materials are intended to be used as backfill adjacent to the structures (Minnesota Department of Transportation, 2018). Selected granular materials are recommended for the use of abutment backfill to avoid the bridge approach distress (Kramer & Sajer, 1991). In order to ensure an adequate foundation for such structures (concrete abutment, wing wall, box culverts, retaining walls, foundations, and substructures), backfill material must meet certain specifications and be compacted by acceptable methods to adequate density. The use of poor soils as a bed for a structure and the failure to adequately compact soils can lead to premature failure (LaDOTD, 2014). The backfills at the structures are specialized but not specifically referred to as structural backfill by some DOTs (Indiana DOT, 2013; Kentucky Department of Transportation, 2012; Oklahoma DOT, 2009).

Most of the DOTs recommend to use granular material with minimal fines (e.g., particle sizes passing sieve No. 200 (0.075 mm)) at the structure (Hoppe, 1999; Illinois DOT, 2016; Indiana DOT, 2013; Kentucky Department of Transportation, 2012; LaDOTD, 2016; Mekkawy et al., 2005; Minnesota Department of Transportation, 2018; MoDOT, 2018; ODOT, 2005; Oklahoma DOT, 2009; PennDOT, 2020; Tennessee, 2015; White et al., 2005; Wisconsin DOT, 2021). The construction practices of eighteen states are summarized based on their requirements for structural backfills (Figure 4.1 to Figure 4.4). Most states provide a number of gradations that are acceptable for use. The mean grain size (D_{50}), which represents the soil diameter where 50% of the distribution has a smaller particle size and 50% has a larger particle size is also determined for the various DOT requirements. The major size of the backfill materials can be roughly estimated based on the D_{50} value. A summary of the gradation of recommended embankment materials along with their D_{50} values are provided in Table 4.1. From the gradations in Table 4.1, we can see that most DOTs allow no fines or only small amount of fines in the structural backfill design to prevent the gradual loss of fine particles which leads to progressive erosion and piping failure (Sterpi, 2003).

Table 4.1 State DOT Embankment Gradations							
Size (mm)	76.2	25.4	4.75	2.36	0.15	0.075	D_{50} (mm)
Sieve	3-in.	1-in.	No.4	No.8	No.100	No.200	
IOWA DOT (2005)	100	---	---	20-100	---	0 - 10	0.34 ~ 9.0
Wisconsin DOT Type A (2021)	100	---	100	0-75	0-15	0 - 8	0.75 ~ 3.2
Michigan DOT Class II (2021)	100	60-100	50-100	---	0-35	0 - 7	0.31 ~ 5.0
New York DOT (2015)	---	100	0-70	---	---	0 - 15	1.2 ~ 12
Minnesota DOT (2018)	100	100	0-50	---	---	0 - 4	4.9 ~ 12
Missouri DOT (2018)	---	100	0-10	---	---	0 - 5	10 ~ 11
Ohio DOT (2008)	---	100	---	---	---	0 - 20	0.7 ~ 1.3
Colorado DOT (2019)	100	100	30-100	---	---	5 - 20	0.36 ~ 7.9
Kansas DOT (2007)	100	100	0-60	---	---	0 - 5	2.1 ~ 11
Illinois DOT (2016)	100	100	50-100	---	---	0 - 4	0.45 ~ 4.8
Oklahoma DOT (2009)	100	100	0-45	---	---	0 - 10	0.55 ~ 4.8
Tennessee DOT (2015)	100	100	35-55	---	---	4 - 15	3.0 ~ 7.0
Indiana DOT (2012)	100	90-100	20-70	---	---	0 - 8	1.2 ~ 10
Virginia DOT (1999)	100	100	15-30	---	---	0 - 14	7.7 ~ 9.3
South Carolina DOT (2006)	100	100	30-50	---	---	0 - 12	4.9 ~ 7.8
Louisiana DOT (2016)	100	100	---	---	---	0 - 10	1.0 ~ 1.5
Kentucky DOT (2012)	100	100	0-30	---	---	0 - 5	8.0 ~ 10.8
Montana DOT (2014)	100	100	20-40	---	---	0 - 8	6.1 ~ 9.0
PennDOT #8 (2020)	100	100	10 – 30	0 – 10	---	0 – 2	5.2~7.0
PennDOT #57 (2020)	100	95–100	0 – 10	0 – 5	---	0 – 2	11 ~ 18
Size (mm)	100	90	63	37.5	19	---	---
Sieve	4-in.	3.5-in.	2.5-in.	1.5-in.	0.75-in.	---	---
PennDOT No.1 (2020)	100	90-100	25-60	0-15	0-5	---	---
Size (mm)	50	19	9.5	4.75	2.36	1.18	---
Sieve	2-in.	0.75-in.	0.375-in.	NO.4	No.8	No.16	---
PennDOT No.2A (2020)	100	52-100	36-70	24-50	16-38	10-30	---
Gradation of Rock lining used by PennDOT (2020)							
Size (mm)	304.8	152.4	76.2	50.8	37.5	25	---
Sieve	12-in.	6-in.	3-in.	2-in.	1.5-in.	1-in.	---
R-4	100	15-50	0-15	---	---	---	---
R-3	---	100	15-50	0-15	---	---	---
R-2	---	---	---	100	15-50	0-15	---

As noted previously, PennDOT Publication 408 Section 206 and PennDOT RC-12M specify that #57 coarse aggregates shall be used for structural backfill applications, and AASHTO #8 coarse aggregates shall be used for Geosynthetic-Reinforced backfill applications. The gradation of AASHTO #8 coarse aggregates is within the range of the recommendations of most DOTs. The gradation of AASHTO #57 coarse aggregates is larger than what other DOTs recommend, which provides higher erosion resistance under extreme flood.

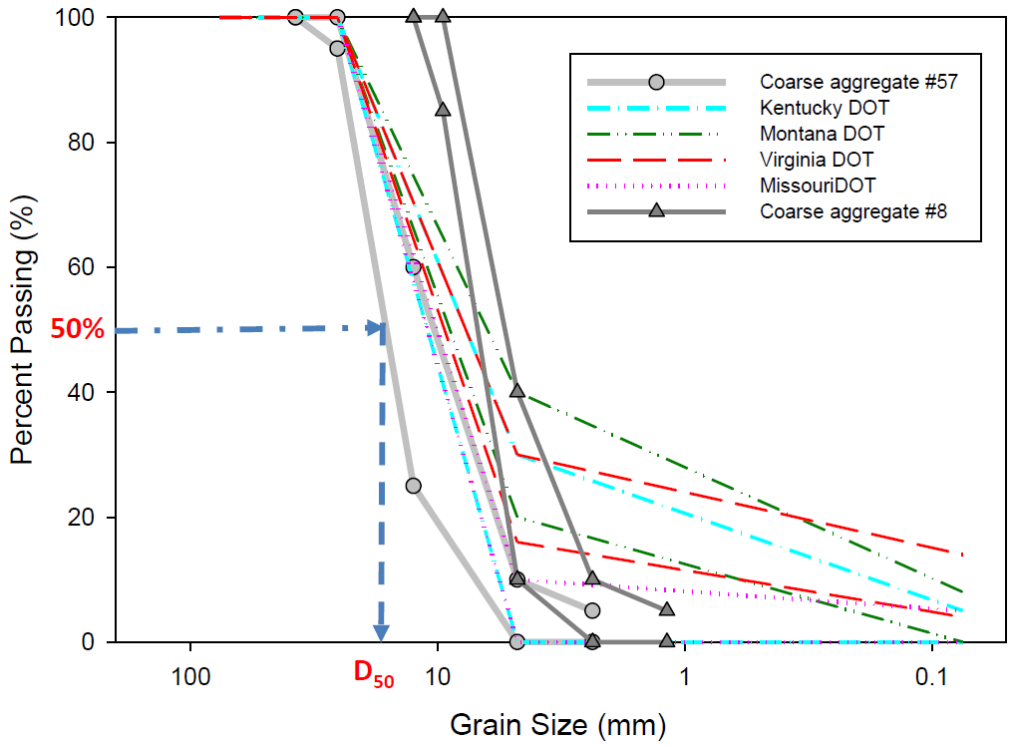

Figure 4.1 Gradations of backfill material currently used by selected states in the US (1)

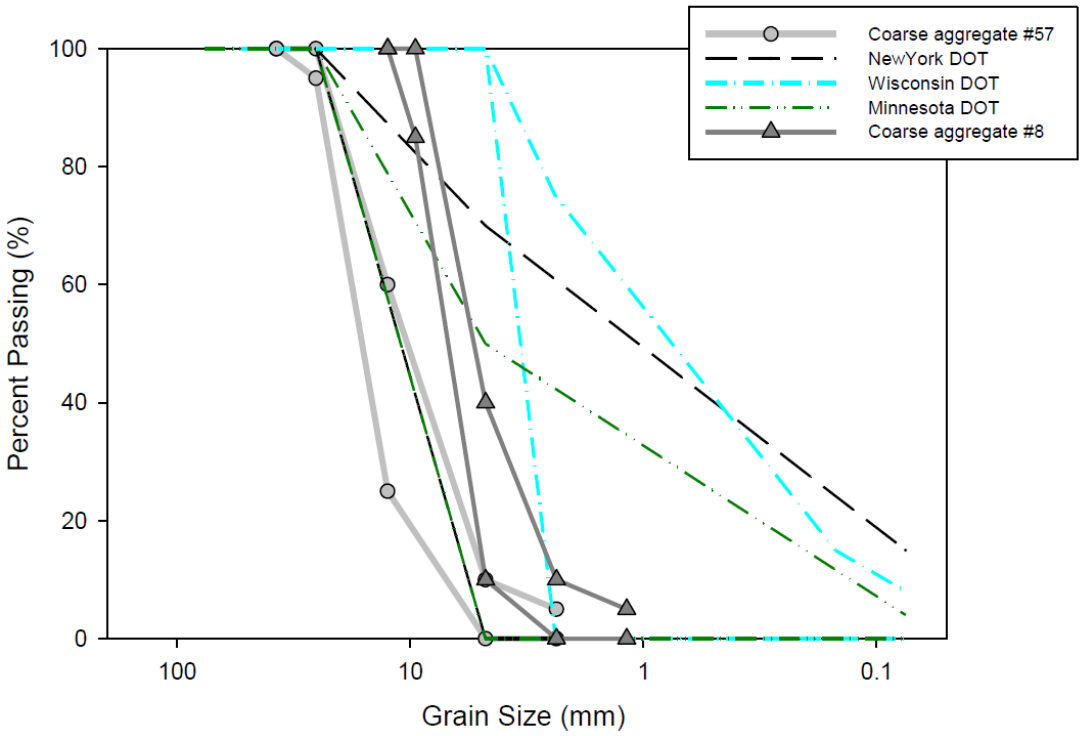

Figure 4.2 Gradations of backfill material currently used by selected states in the US (2)

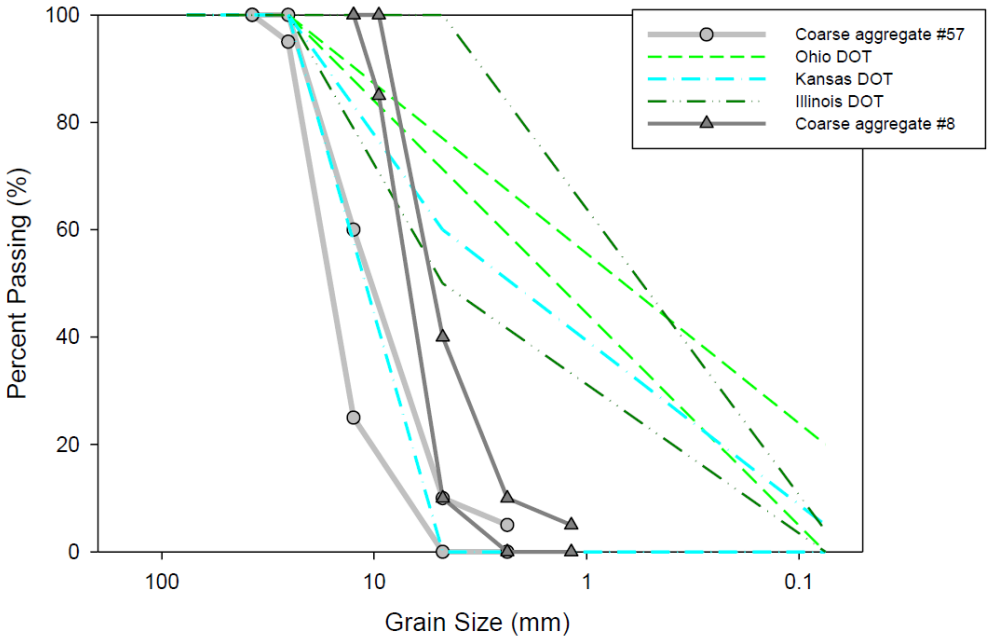

Figure 4.3 Gradations of backfill material currently used by selected states in the US (3)

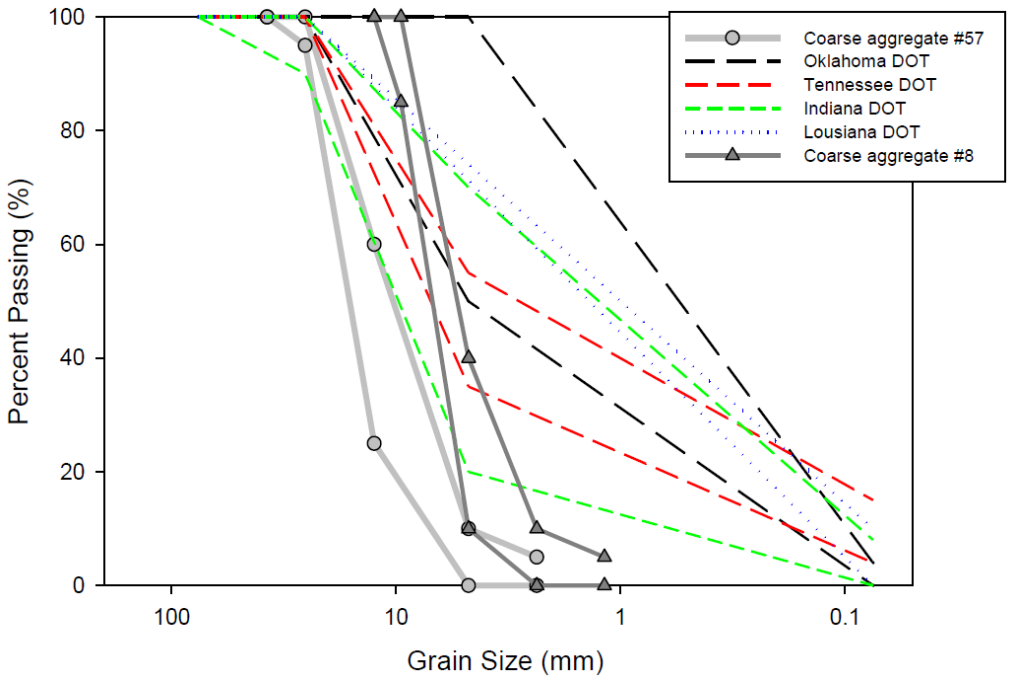

Figure 4.4 Gradations of backfill material currently used by selected states in the US (4)

Given that coarse aggregates (AASHTO #8 and #57) are recommended as the structural backfill by PennDOT, and Rock linings are commonly used in field for the surface erosion mitigation (Morales et al., 2008), the critical velocity and the critical shear stress of the AASHTO #8, #57, #2A coarse aggregates, and Rock linings which are calculated based on the equations shown in Figure 2.2 and Figure 2.3 are summarized in Table 4.2. The function of critical shear stress (Equation 2) and critical velocity (Equation 1) versus mean grain size of backfill materials recommended by PennDOT are included in this chapter (Figure 4.6 and Figure 4.7). As previously discussed, the resistance of the backfill materials to surface erosion increases as the mean grain sizes increase. With R-4 stone eroding at approximately five times the surface velocity as that of #8 coarse aggregate.

Table 4.2 Critical velocity and critical shear stress of selected AASHTO coarse aggregates and Rock lining

Aggregate size	Mean grain size, D50 (mm)	Critical velocity (m/s)	Critical shear stress (N/m^2)
#8	5.2~7	0.73~0.84	5.2~7
#57	10~18	0.99~1.29	10~18
#2A	4.75~18	0.71~1.29	4.75~18
R-2 Rock lining	37.5~46	1.79~1.96	37.5~46
R-3 Rock lining	76.2~100	2.46~2.78	76.2~100
R-4 Rock lining	152.4~200	3.36~3.80	152.4~200

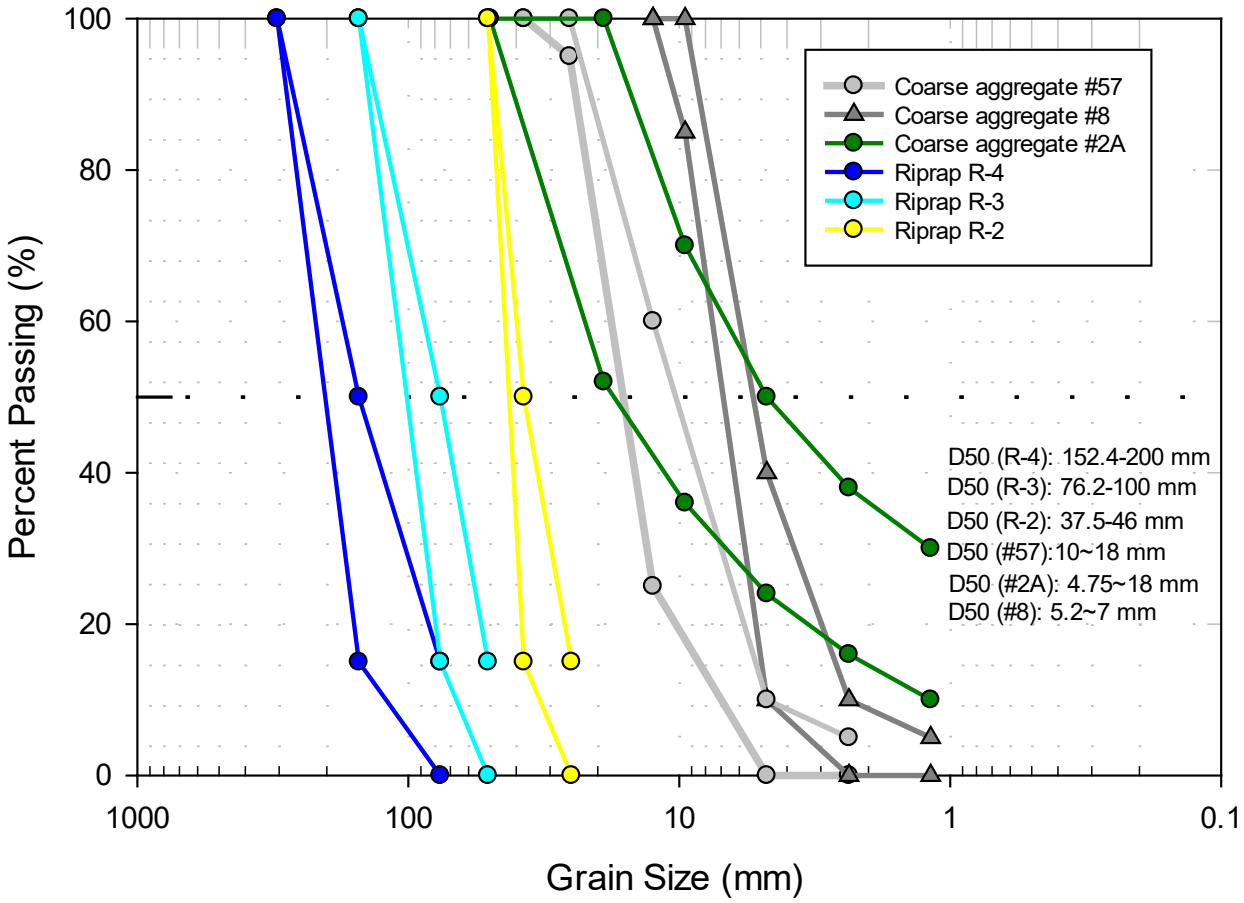

Figure 4.5 Gradations of AASHTO #8, 57, 2A coarse aggregates and R-2, R-3, R-4 Riprap

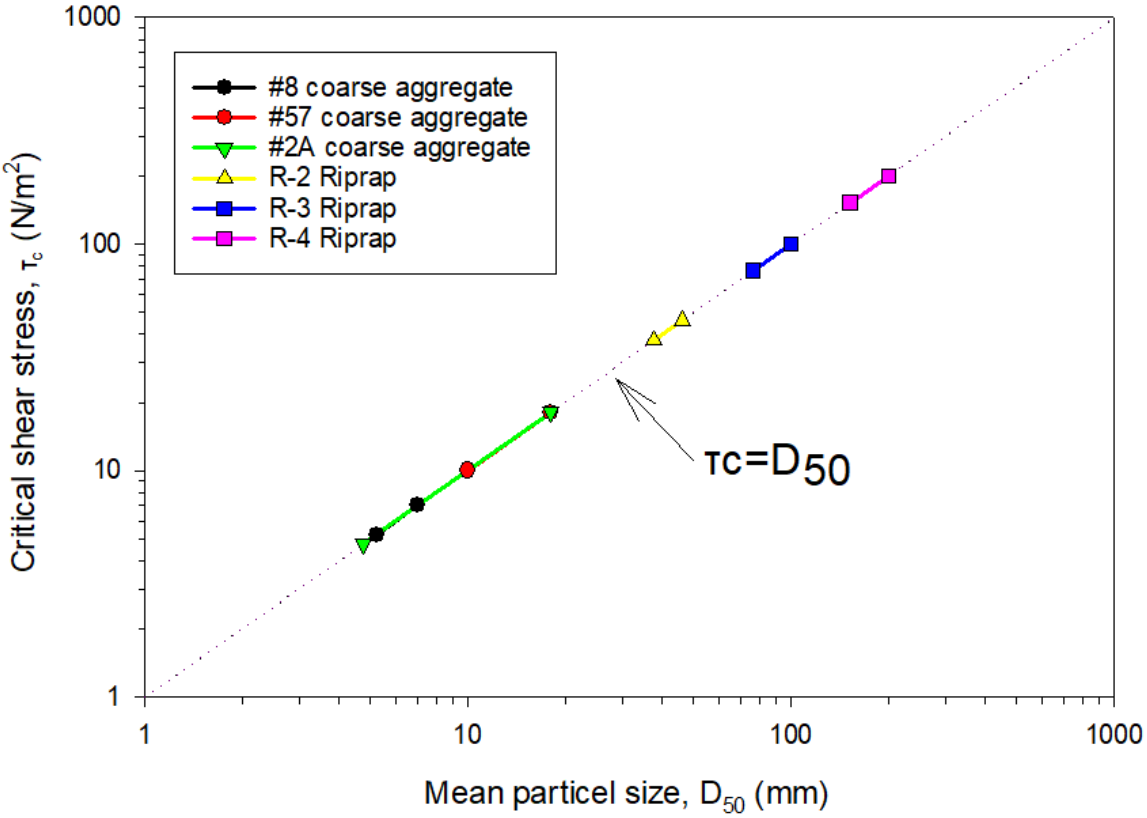

Figure 4.6 Critical shear stress as function of mean grain size from PennDOT standard

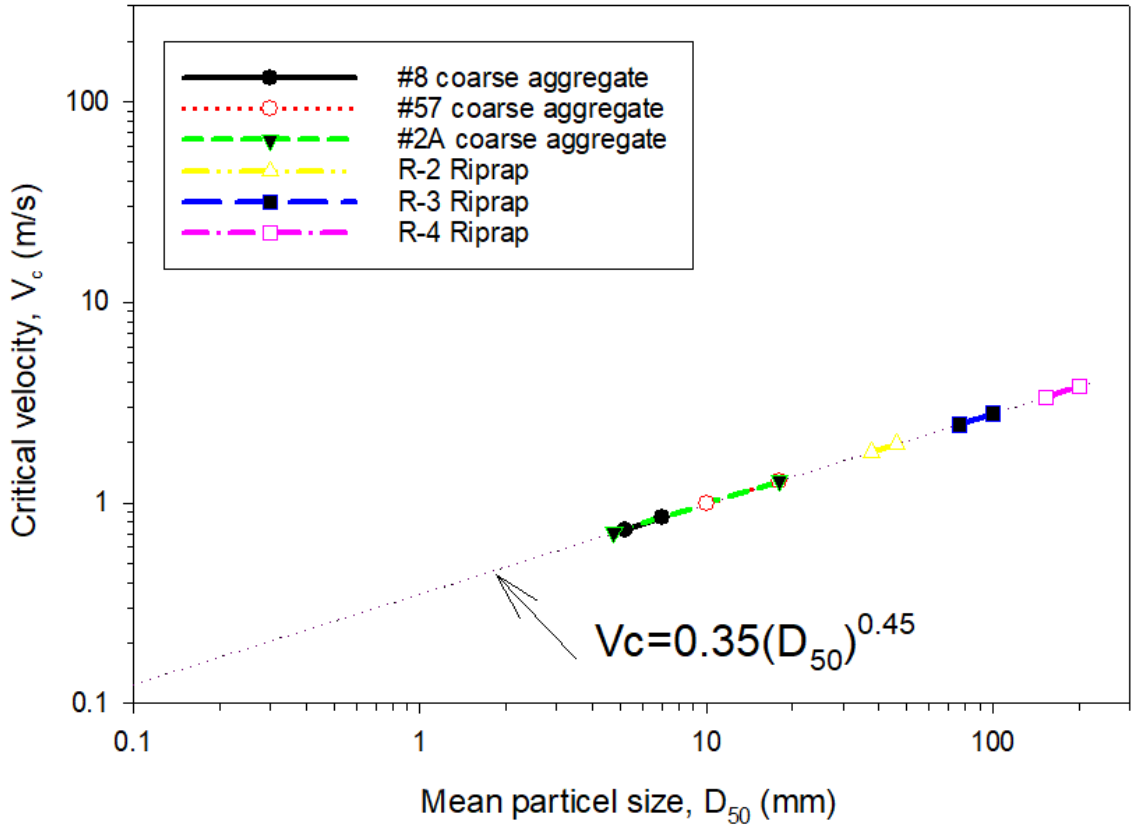

Figure 4.7 Critical velocity as function of mean grain size from PennDOT standard

5. MATERIAL PROPERTIES USED IN EXPERIMENTAL PROGRAM

The materials used in the experimental program are aligned with recommendations provided by PennDOT standards. The recommended properties of the structural backfill material, Rock lining, and Geosynthetics used in the experimental program are summarized in Table 5.1.

Table 5.1 Material properties used in the experimental program and recommended in practice

Gradation of structural backfill used by in experimental program							
Size (mm)	76.2	25.4	4.75	2.36	0.15	0.075	D_{50} (mm)
Sieve	3-in.	1-in.	No.4	No.8	No.100	No.200	
PennDOT #8 (2020)	100	100	10 – 30	0 – 10	---	0 – 2	5.2~7.0
PennDOT #57 (2020)	100	95–100	0 – 10	0 – 5	---	0 – 2	11 ~ 18
Size (mm)	50	19	9.5	4.75	2.36	1.18	D_{50} (mm)
Sieve	2-in.	0.75-in.	0.375-in.	NO.4	No.8	No.16	
PennDOT No.2A (2020)	100	52-100	36-70	24-50	16-38	10-30	4.75~18
Gradation of Rock lining used by in experimental program							
Size (mm)	304.8	152.4	76.2	50.8	37.5	25	---
Sieve	12-in.	6-in.	3-in.	2-in.	1.5-in.	1-in.	---
R-4	100	15-50	0-15	---	---	---	---
R-2	---	---	---	100	15-50	0-15	---

Material properties of Geosynthetics used in experimental program			
Secondary Geosynthetic: Class 4, Type A Geotextile		Primary Geosynthetic: Class 1, Type A Geogrid	
Manufacturer	TenCate Geosynthetics	Manufacturer	TenCate Geosynthetics
Name	Mirafi E1200	Name	Miragrid 2XT
Fabric Structure	Non-woven Needle Punched	Polymer Type	PVC Coated PET
Weight, oz/sy	12.0 min	Ultimate Tensile Strength (lbs/ft)	2000
Grab Tensile Strength, lbs.	305 min, MD and XD	Creep Reduction Factor, (RFC) (determined for a 100-year design life)	1.60
Grab Tensile Elongation,%	50 min, MD and XD	Installation Damage Reduction Factor, (RFID)	1.30
Ultimate Wide Width Tensile Strength, lb/ft	N/A	Durability Reduction Factor, (RFD)	1.20
Wide Width Tensile Strength @ 2% Strain, lb/ft	N/A	Overall minimum required reduction factor (RFOV)	2.50
Puncture, lbs. (2-in flat- end rod)	830 min	Machine Direction (MD) Aperture Size	0.60 to 6.0

Trapezoid Tear Strength, lbs.	10 min, MD and XD	Cross Machine Direction (XD) Aperture Size	0.50
Apparent Opening Size, mm (Sieve No.)	0.15 max	Rib Section Area Ratio	0.30
Percent Open Area, %	N/A	Percent Open Area	45.0
Water Flow Rate, g/min/sf	N/A	---	---
Permittivity, sec^{-1}	0.70 min	---	---
Ultraviolet Resistance Strength Retention, %	70 @500 hrs min	---	---

5.1. GRADATION

Sieve analyses were conducted to investigate the gradation of the materials utilized in the experimental program. This includes embankment material, #8 coarse aggregate, #57 coarse aggregate, #2A coarse aggregate, and R-2 Rock lining (Figure 5.1). The gradation diagram for each material is summarized in Figure 5.2. The mean particle diameter (D_{50}) of the embankment material is 3.7 mm, the mean diameter of the #8 coarse aggregate is 6.9 mm, the mean diameter of the #2A coarse aggregate is 9.1 mm, the mean diameter of the #57 coarse aggregate is from 11 mm, and the mean diameter of R-2 Rock lining is 40 mm. The gradations of all the backfill materials are within the range recommended by PennDOT, which is shown in Figure 5.3 (PennDOT, 2020).

Figure 5.1 #8 coarse aggregate, #57 coarse aggregate, #2A coarse aggregate, R-2 Rock lining, and Embankment material

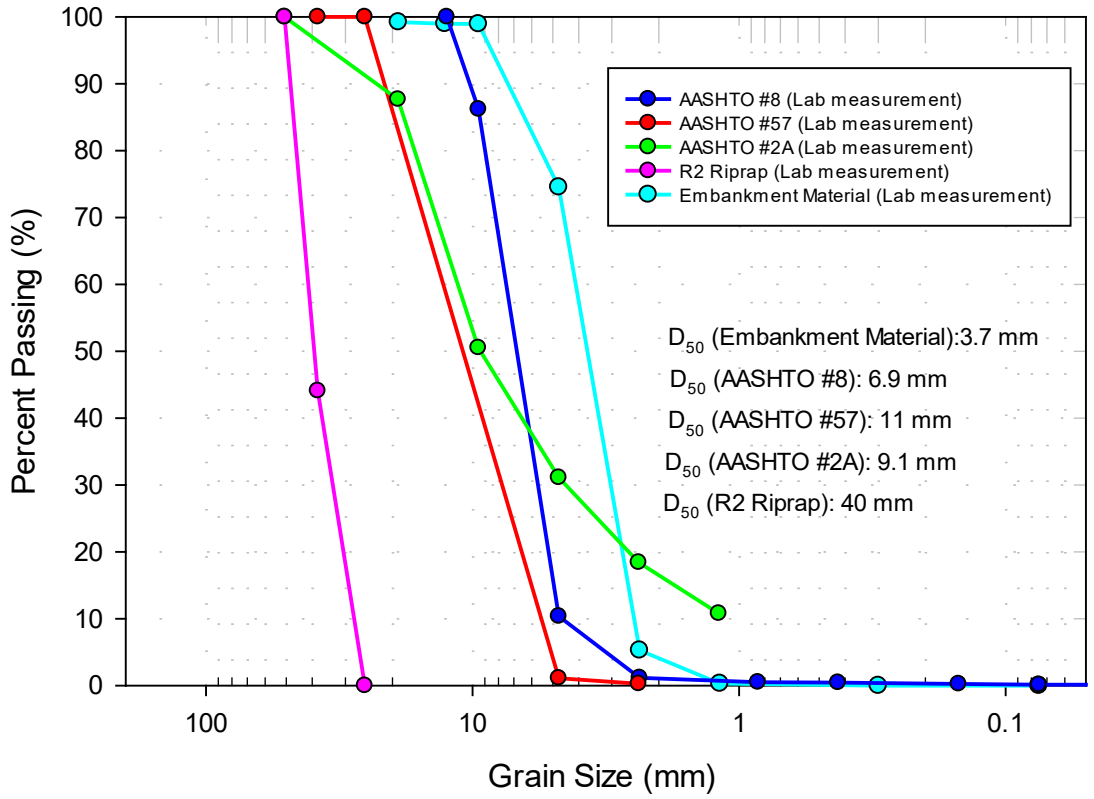

Figure 5.2 Measured gradation of embankment material, #8 coarse aggregate, #57 coarse aggregate, #2A coarse aggregate, and R-2 Rock lining

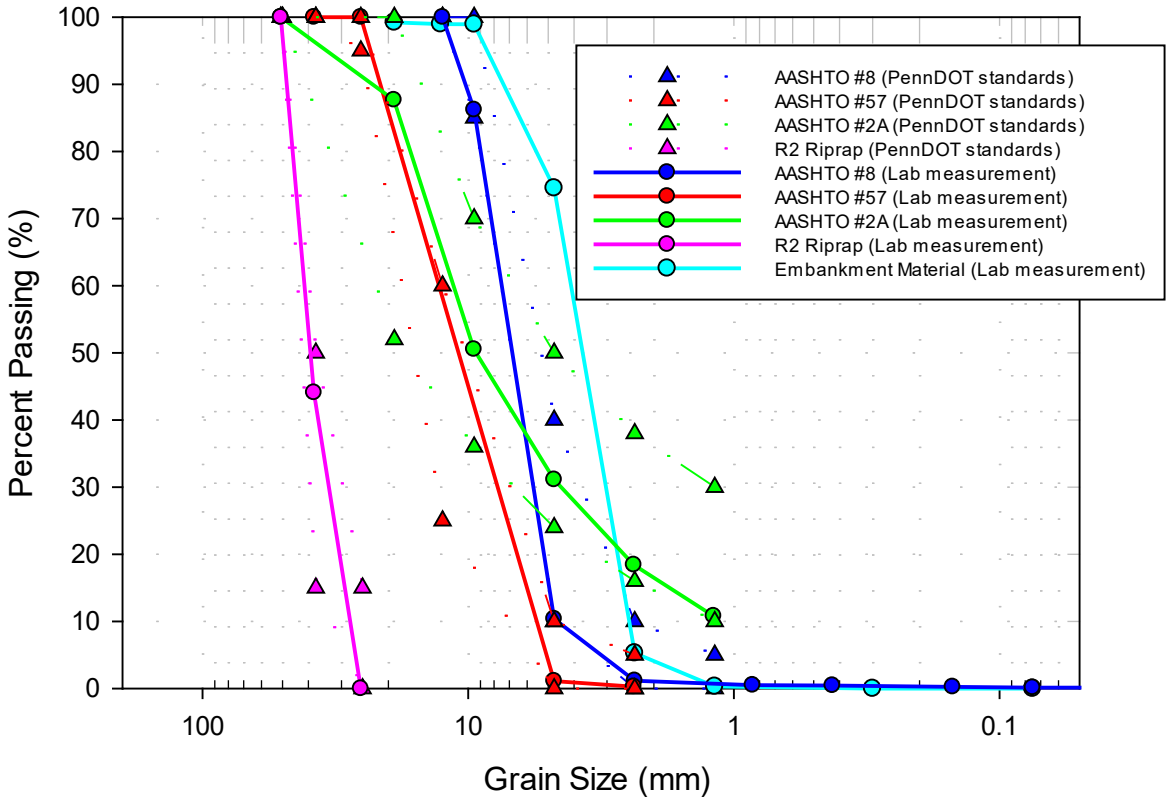

Figure 5.3 Gradations measured in lab and required in PennDOT Standard

MAXIMUM DRY DENSITY

The maximum dry density of AASHTO #8 coarse aggregate, #2A coarse aggregate, and embankment material, which were utilized for the majority of laboratory testing, were determined using the standard Proctor compaction test according to AASHTO T99 (AASHTO, 2019). The Proctor Compaction Test consists of a mold holding a cylinder of soil with a rammer that tightly compacts the soil within the mold. Each layer of soil is impacted with the ram 25 times. This test is used to measure the optimal moisture content that is needed to achieve the maximum dry density of the compacted soil.

The maximum dry unit weight of the #8 coarse aggregate was approximately 105.3 pcf at the optimum moisture content of 2.6% from the proctor test (Figure 5.4). The average dry unit weight measured at different moisture content was 104.0 pcf. Sieve analyses were conducted before and after compaction and plotted in Figure 5.5 and Figure 5.6. From Figure 5.5 and Figure 5.6, we can see that the percent of material passing sieve No. 4 increase between 6% and 13%.

The maximum dry unit weight of the #2A coarse aggregate was approximately 141.0 pcf at the optimum moisture content of 6.61% from the proctor test (Figure 5.7). The average dry unit weight measured at different moisture content was 136.3 pcf.

The maximum dry unit weight of the embankment material was approximately 109.9 pcf at the optimum moisture content of 6.55% from the proctor test (Figure 5.8). The average dry unit weight measured at different moisture content was 109.3 pcf.

The maximum dry unit weight is achieved when the material is at the optimum moisture content during compaction. Compaction behind the bridge abutment, however, is not recommended by PennDOT (from PennDOT Pub408, Section 206.3(b)1.c). This is a good approach as compaction will increase the passive pressure developed which may affect the integrity of the bridge abutment (Naji et al., 2020). Consequently, compaction was not applied during the structural backfill construction in laboratory testing program.

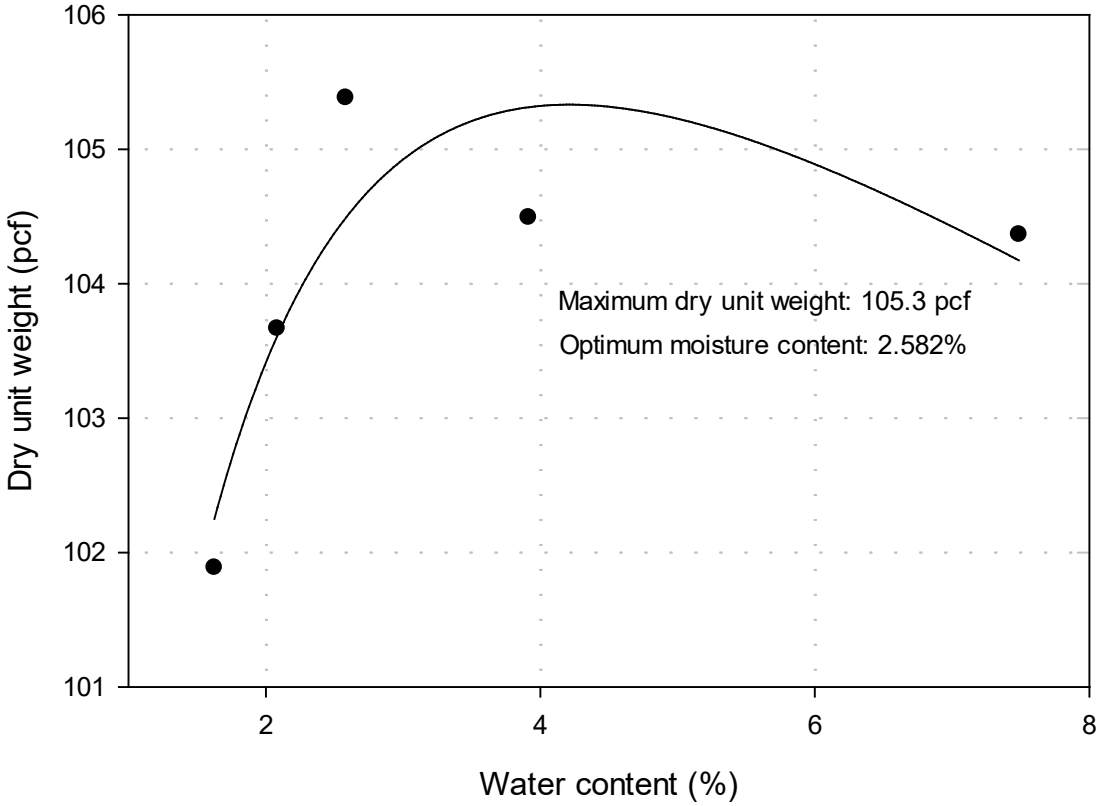

Figure 5.4 Proctor soil compaction test for #8 coarse aggregates

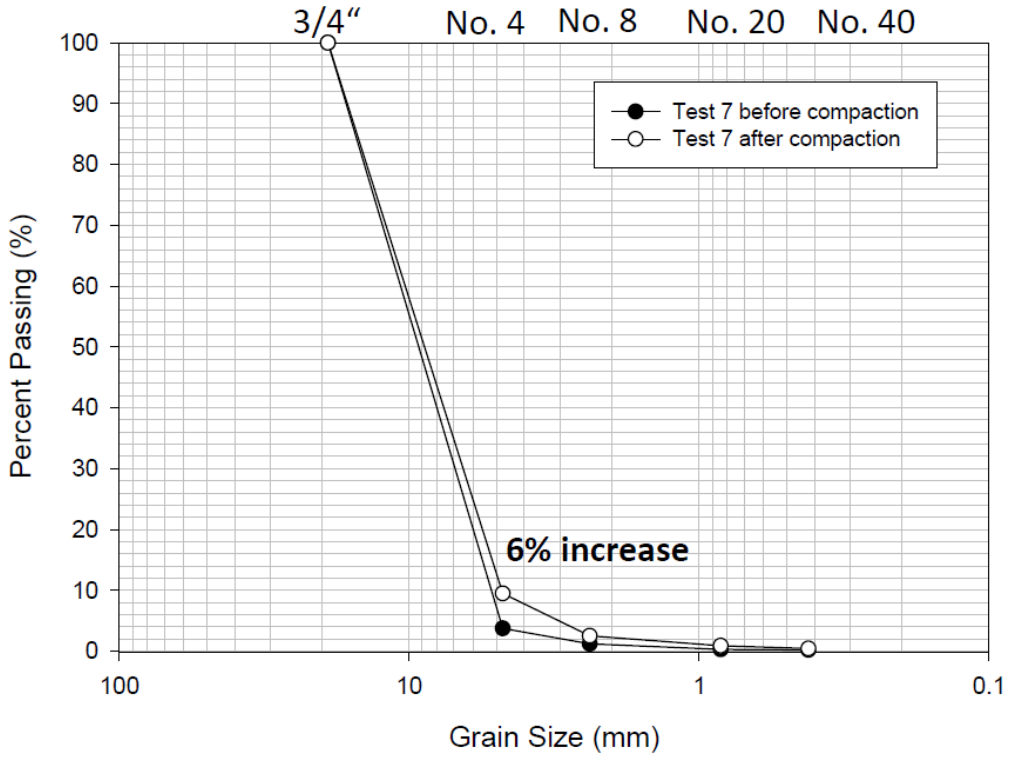

Figure 5.5 Change of gradation before and after compaction for #8 coarse aggregate (Test 7)

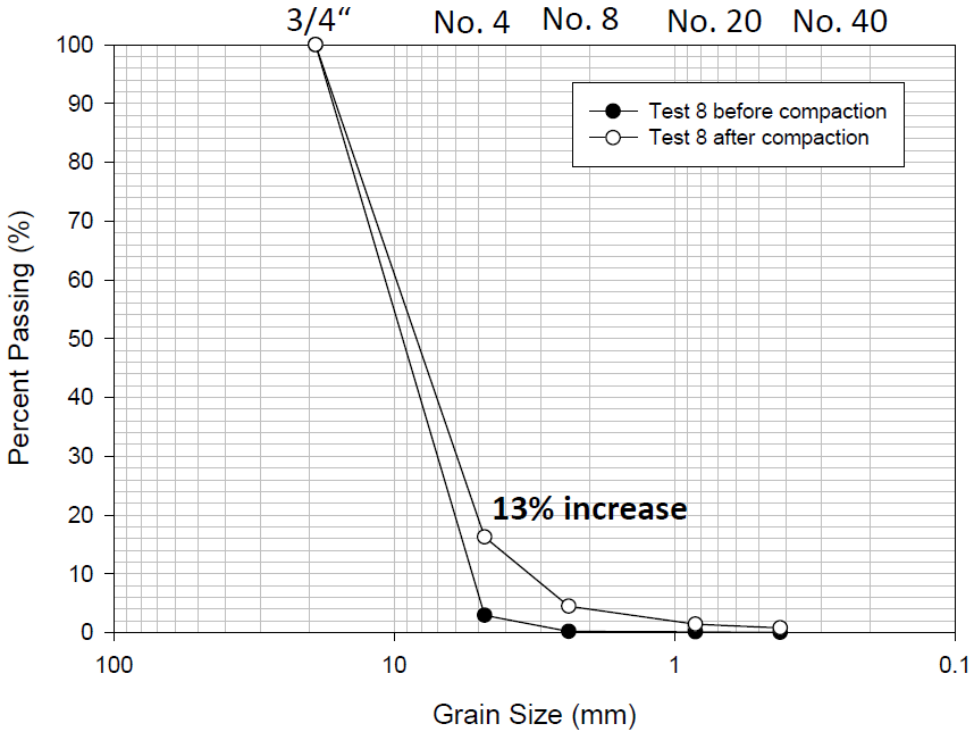

Figure 5.6 Change of gradation before and after compaction for #8 coarse aggregate (Test 8)

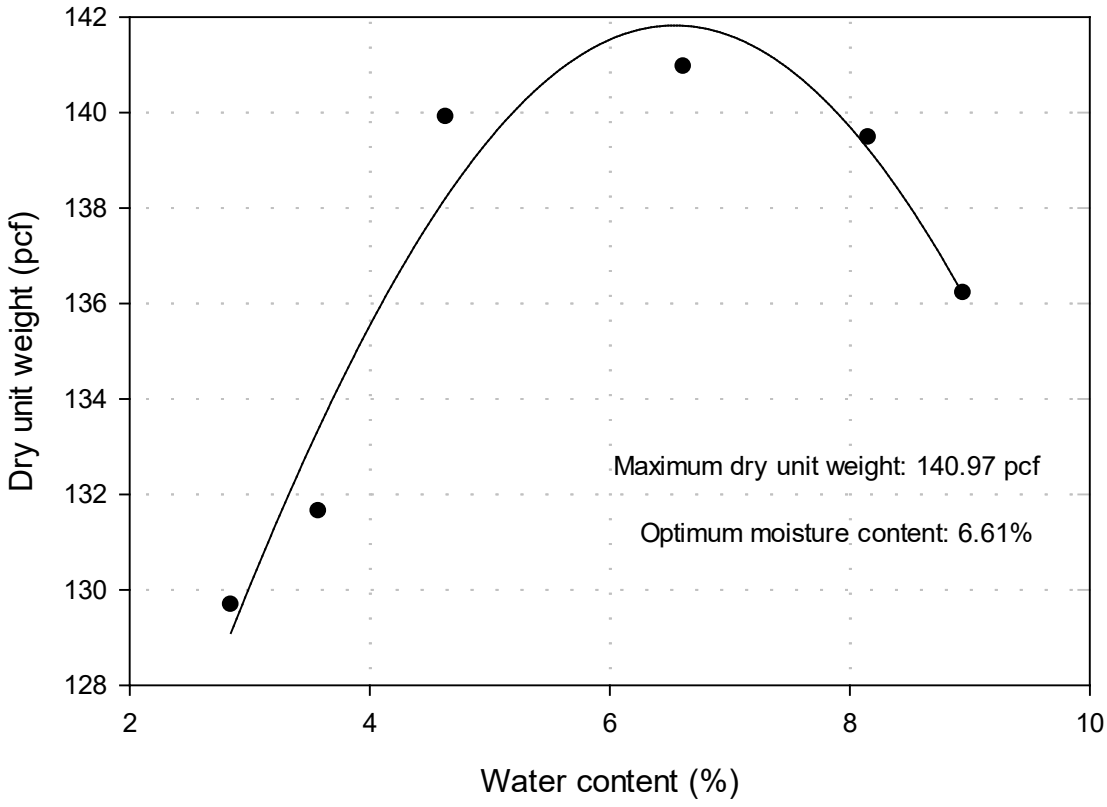

Figure 5.7 Proctor soil compaction test for #2A coarse aggregates

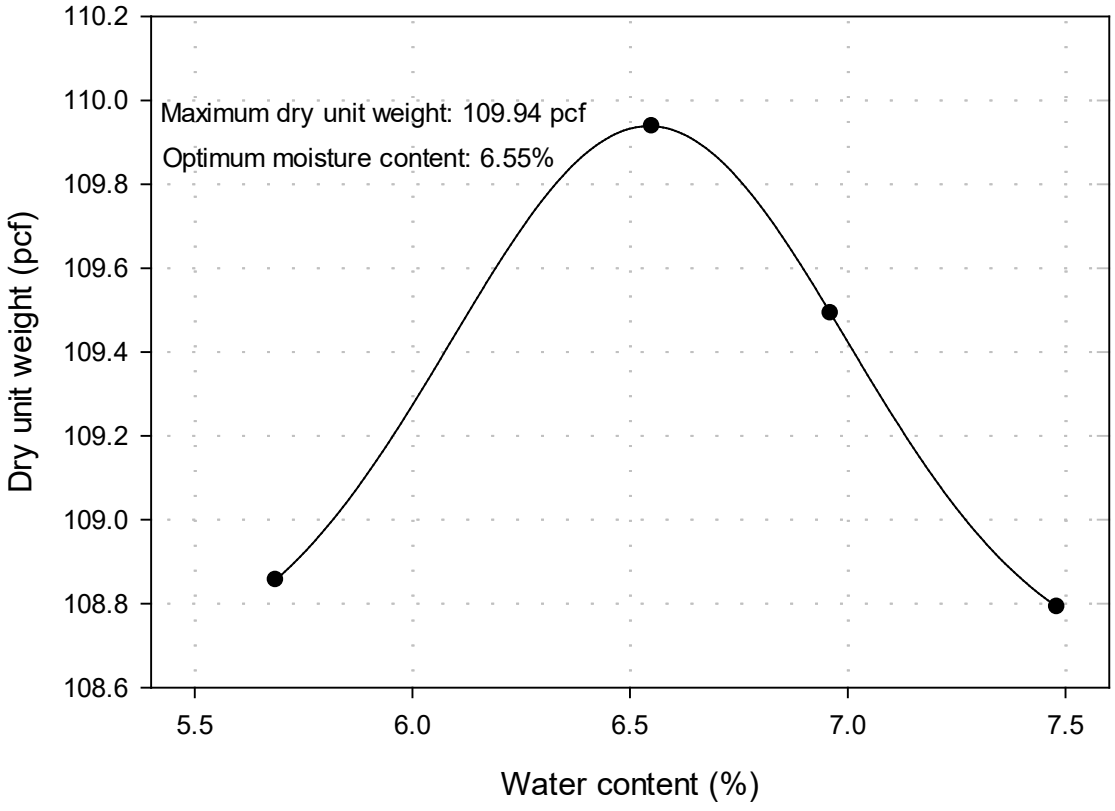

Figure 5.8 Proctor soil compaction test for embankment material

5.2. IN-SITU UNIT WEIGHT DURING EMBANKMENT CONSTRUCTION

The in-situ unit weight of the #8 coarse aggregate and embankment material were determined using the sand cone test (Figure 5.9) according to the ASTM D1556/ D1556M during embankment construction (without compaction), which was used to simulate the worst case field condition.

Sand cone tests were conducted twice to determine the in-situ unit weight of the ***#8 coarse aggregate***. The average measured in-situ unit weight (γ_t) of the #8 coarse aggregate were determined to be 94.8 pcf (14.9 kN/m^3). The average measured moisture content of the #8 material removed from the embankment was 1.15%. From this a dry unit weight (γ_{dry}) of 93.8 pcf (14.7 kN/m^3) was determined. This material was placed by raining down the #8 coarse aggregate as recommended by PennDOT from a height of 16 inches in lab. *On average this achieved 89% of the maximum proctor density.*

Sand cone tests were also conducted twice to determine the in-situ unit weight of the ***embankment material***. The average measured in-situ unit weight (γ_t) of the embankment material were determined to be 102.2 pcf (16.0 kN/m^3). The average measured moisture content of the embankment material removed was 2.15%. From this a dry unit weight (γ_{dry}) of 100.0 pcf (15.7

kN/m^3) was determined. This material was placed by raining down the embankment material as recommended by PennDOT from a height of 16 inches in lab. *On average this achieved 90% of the maximum proctor density.*

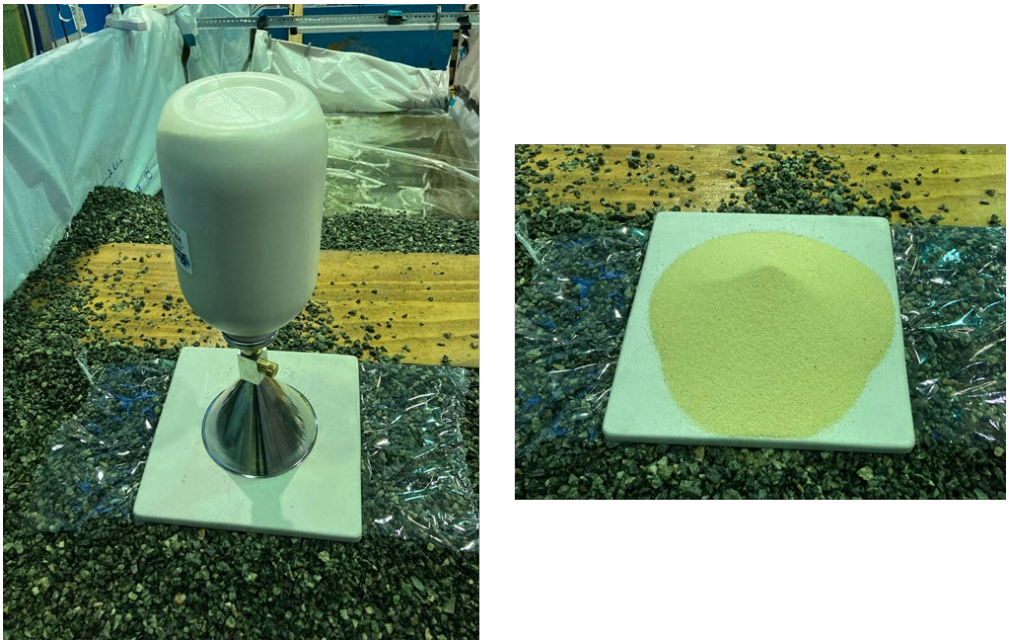

Figure 5.9 Sand cone test determining the unit weight of #8 coarse aggregate

HYDRAULIC CONDUCTIVITY

Hydraulic conductivity of embankment material and #8 coarse aggregate were both determined using falling head permeability test (Holtz et al., 1981) (Figure 5.10). Falling Head Permeability Test is a common lab practice used in determining the permeability of soils. Falling Head Permeability Test allows the water head to decrease as water flow through the soil sample to determine the coefficient of permeability (k) of the soil based on the Darcy's law.

The permeability of the sample can be calculated as:

$$k = [2.3aL/(A\Delta t)] \times \log(\frac{h_1}{h_2}) \qquad (2.1)$$

Where,

- k is the coefficient of permeability of the soil
- L is the height of soil sample
- A is the cross section of the standpipe, a is the sample cross section (A=a in this study)
- h_1 and h_2 are the measured upper and lower water level in the standpipe

- Δt is the recorded time for the water flowing through the sample dropping from h_1 to h_2

The hydraulic conductivity of embankment material was measured as 0.54 cm/sec (0.21 in./sec), the hydraulic conductivity of #2A coarse aggregate was determined as 0.0067 cm/sec (0.0026 in./sec), the hydraulic conductivity of #8 coarse aggregate was determined as 14.0 cm/sec (5.5 in./sec), and the hydraulic conductivity of #57 coarse aggregate was determined as 14.93 cm/sec (5.88 in./sec). When the hydraulic conductivity of soil is larger than 10^{-4} cm/sec, the soil can be defined with good drainage (Holtz et al., 1981). When the hydraulic conductivity of soil is from 10^{-3} to 1.0 cm/sec, the soil mainly consists of clean sands, or clean sand and gravel mixtures, which matches the properties of the embankment material. When the hydraulic conductivity of soil is from 1 to 10^2 cm/sec, the soil mainly consists of clean gravel, which matches the properties of the #8 and #57 coarse aggregate (Holtz et al., 1981). Given that the mean grain size (D_{50}) of embankment material, #8 and #57 coarse aggregates are larger than 0.5 mm (Figure 5.2), the erodibility of the soil is mainly determined by the D_{50}, which is that soils with larger mean grain size have greater erosion resistance (Equation 1 and Equation 2) (Briaud et al., 2008). As illustrated, finer granular materials will have a lower hydraulic conductivity, which will increase likely head differential between the upstream and downstream sections of the embankment during extreme weather events. This larger differential combined with the greater amount of fines in these materials make them more susceptible to erosion mechanisms. Thus, use of #8 and #57 coarse aggregates is appropriate for the structural backfill.

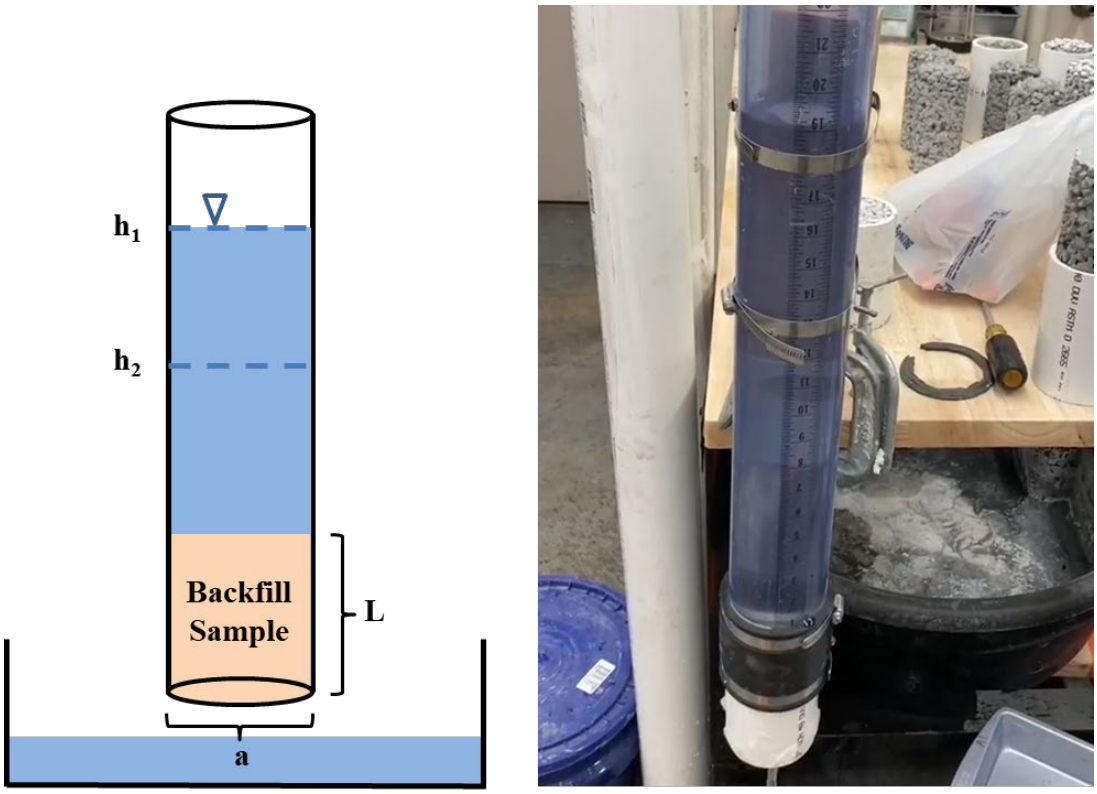

Figure 5.10 Hydraulic conductivity of #8 coarse aggregate and embankment material determined using falling head permeability test

6. STRUCTURAL BACKFILL DISCUSSION

This report provides an overview of the state of the practice for structural backfills in the U.S. The properties of soil and the design of the reinforced structural backfill configurations behind the bridge abutment recommended by PennDOT consist of: (1) a standard coarse aggregate (typically AASHTO #57, or #1) is used for the structural backfill behind the bridge abutment; AASHTO #8 coarse aggregates are recommended for Geosynthetic-Reinforced Backfill; (2) R-4 rock lining is recommended to protect the surface of the slope; (3) Geosynthetics, including Geogrid and Geotextile are used to reinforce and wrap the #8 Coarse Aggregates; (4) Embankment material (originally from the site) can be used away from the structural backfill. The erosion related soil properties (gradation, maximum dry density, in-situ unit weight, and hydraulic conductivity) of the backfill materials (#8, #57 and #2A coarse aggregate, R-2 Rock lining, and embankment material) recommended by PennDOT and used in the experimental program are summarized in this report.

7. STRUCTURAL BACKFILL EXPERIMENTAL PROGRAM

An experimental program was conducted to examine the performance of structural backfill used behind bridge abutments when subjected to flooding events. A standard section cut of a PennDOT bridge embankment is shown in Figure 1.1. As illustrated, the region typically consists of a granular *Structural Backfill* material behind the abutment. Away from the abutment the region transitions to *Embankment Material*. The goal of the research program is to develop recommendations which minimize the likelihood of damage to the structural backfill under extreme rain events. To achieve this goal the research program examined setups with and without a bridge opening to understand the mechanics of failure and effectiveness of reinforcement strategies. This report provides an overview of the experiments and recommendations on reinforcement strategies.

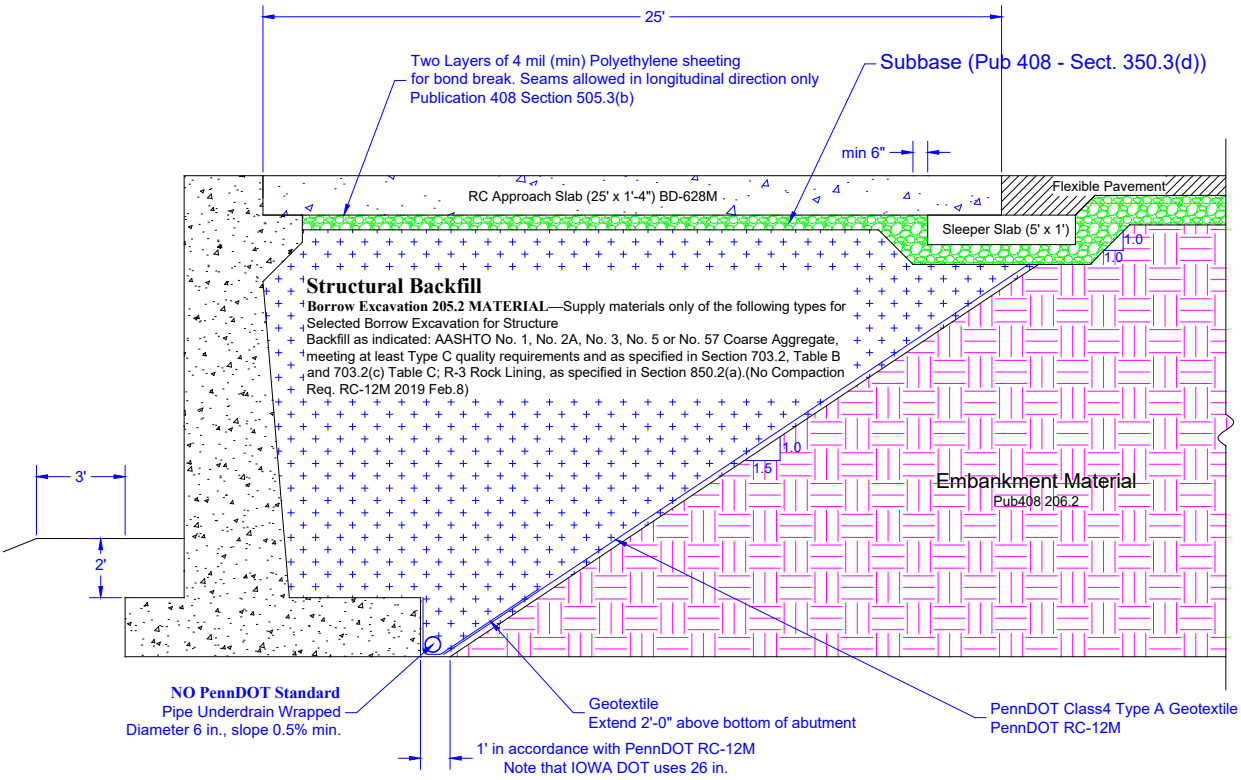

Figure 1.1: Standard backfill detail(PennDOT, 2019, 2020)

7.1. MATERIALS

The materials used in this experimental program are discussed in detail in Task 1.1 report (Gao et al., 2021). For completeness the general descriptions of the materials used in this report are summarized in this section.

Structural Backfill – Material used adjacent to structural components (e.g., abutments) to replace excavated earth allowing for restoration of the strength of the surrounding earth ensuring a sturdy structure. Designed to prevent deformations of the bridge approach which often occurs when using in-situ soils.

Embankment Material – Material used to replace excavated earth a distance away from the structural component. With respect to the experimental program, embankment material is also defined relative to PennDOT Publication 408 Section 206.2 and can consist of Soil, Granular Material, Rock, Shale, and Random Materials. An Embankment Material is used for the initial tests to examine the performance of this lower quality material on the embankment erosion resistance. For the research program, the embankment material consisted of a gravel material with a mean particle diameter of 3.7 mm.

Geosynthetics – Synthetic materials used in civil engineering applications to stabilize terrain, typically made of polymeric materials. Includes geotextiles, geogrid, etc.

Geotextiles – Textile material fabricated from synthetic materials rather than traditional materials such as cotton or wool. These synthetic materials are more resistant to biodegradation, Figure 1.2a.

Geogrid – Polymeric fibers formed into an open grid structure with ribs running in transverse and longitudinal directions. Allows for high flow of liquid across the plane and provides reinforcement of the soil, Figure 1.2b.

a) 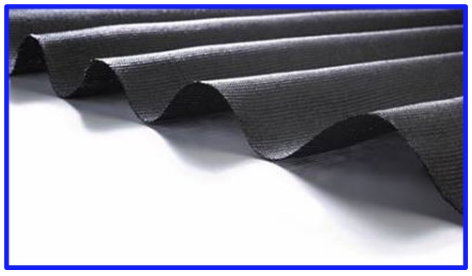 b) 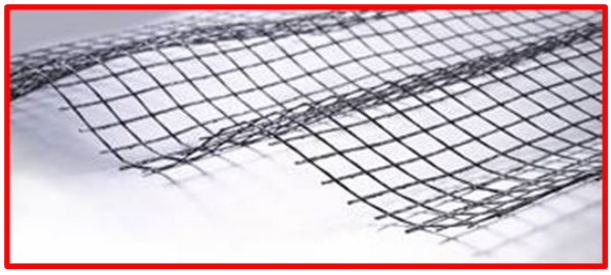

Figure 1.2: Geosynthetics (a) Geotextile, (b) Geogrid

[https://gagneandson.com/products/landscape/accessories/fabrics-grids-adhesives/]

7.2. Experimental Scale

7.2.1. Hydraulic Scaling

The use of model studies is important and needed to predict the behavior in the prototype (Houghtalen et al., 2016). If the hydraulic phenomena are governed by the viscous forces, the Reynolds Law (Inertia force/viscous force) needs to be satisfied, which means that the Reynolds number of the model and prototype should be kept the same. If the hydraulic phenomena are

governed by gravity forces, the Froude Law ((Inertia force/gravity force)$^{1/2}$) needs to be satisfied, which means that the Froude number of the model and prototype should be kept the same.

In hydraulic studies involving open channel flows, the Froude criteria is primary because it is impossible to simultaneously satisfy both the Reynolds and Froude criteria. For long river or canal reaches, a resistance equation such as the Manning or Chezy is used instead of the Reynolds criteria. For short reaches such as flow over a spillway (or an embankment), the Reynolds criteria is not used. Rather, the assumption is made that drag (resistance) forces are comparable in model and prototype if both model and prototype are turbulent flows. This idea emanates from relationships like drag coefficient vs Reynolds number or friction factor vs Reynolds number (Moody diagram) in which the dependent variable (drag coefficient or friction factor are independent of Reynolds number. Hence, the scaling of the hydraulic variables is obtained from the Froude criteria alone.

In this study, the flow rate, and flow velocity need to be scaled to facilitate testing in the laboratory. Note that, for the hydraulic modeling, the sediment size is not mentioned, and will be discussed in a later section.

Considering the limited dimensions of the water tank, and the flow capacity in the lab, the width of the embankment was initially designed as 5 ft, the maximum discharge available in the laboratory tank is close to 4 CFS. Assume that the embankment is overtopped and the water level is 0.5 ft above the embankment, the Reynolds number on top of the embankment can be calculated following the equations below:

$$V = \frac{Q}{L \times H}$$

Where,

Q = discharge= $4 ft^3/s$

V = velocity (ft/s)

L = width of embankment =5 ft

H = head above the embankment =0.5 ft

$$V = \frac{Q}{L \times H} = \frac{4 ft^3/s}{5\ ft \times 0.5\ ft} = 1.6 ft/s$$

$$R_e = \frac{V \times D}{\upsilon}$$

Where,

Re = Reynolds number

υ = kinematic viscosity of water at 20℃ (68℉) = $10^{-5}\frac{ft^2}{s}$

D = H = head on spillway = 0.5 ft

$$R_e = \frac{V \times D}{\upsilon} = \frac{1.6ft/s \times 0.5\ ft}{10^{-5}\frac{ft^2}{s}} = 80{,}000 \qquad Turbulent$$

The Reynolds number in the model is calculated as 80,000, which is turbulent. At such a high Reynolds number, the viscous or drag forces are independent of the Reynolds number.

A scale ratio of 5:1 (Prototype:Model) is chosen in this study. The scale ratio of discharge and flow velocity are then calculated based on the Froude Law:

$$V_R = \sqrt{L_R}$$

$$Q_R = {L_R}^{5/2}$$

Where,

L_R = scale ratio of length = 5

V_R = scale ratio of velocity

Q_R = scale ratio of discharge

$$V_R = \sqrt{L_R} = \sqrt{5} = 2.236$$

$$Q_R = {L_R}^{5/2} = 5^{5/2} = 56$$

For example, assume that the width of the embankment in the model is 5 ft, and the flow velocity is measured as 3 ft/s in the lab, which is sufficient to cause erosion of the sediment chosen for the laboratory embankment. Then the prototype (full-scale) characteristics can be determined:

$$L_P = L_R \times L_M = 5 \times 5\ ft = 25\ ft$$

$$V_P = V_R \times V_M = 2.236 \times 3\ ft/s = 6.708\ ft/s$$

$$Q_P = Q_R \times Q_M = 56 \times 4ft^3/s = 224ft^3/s$$

Where,

L_P = the length in the prototype

V_P = the velocity in the prototype

V_M = the velocity in the model

Q_P = the discharge in the prototype

Q_M = the discharge in the model

7.2.2. Structural Backfill Scale

The gradation of #8 coarse aggregates, embankment material and #57 coarse aggregates are illustrated in Figure 5.2 in *Task1.1 Evaluation of Backfill Properties*. The measured mean grain size (D_{50}) of #8 coarse aggregates are 6.9 mm, the D_{50} of embankment material is measured as 3.7 mm, and the D_{50} of #57 coarse aggregates is measured as 11 mm. The modeling of the general flow with a free surface (discussed in the section 1.2.1) and the flow through porous media (the aggregate material) are very different phenomena because the flow through the embankment is where viscous forces dominate and the Reynolds numbers are small, even likely to fall into the laminar or transition range. The sizes of the structural backfill materials in the model need to be scaled to achieve the similar phenomena, such as piping, slumping and slope failures observed in the prototype. Since the flows and seepage forces through and in the model is smaller than in the prototype, smaller aggregate size was used in the model. Preliminary tests were conducted using embankment material to simulate the #57 coarse aggregates in the prototype (scale ratio of the embankment material/#57 coarse aggregate is 3.0/1 (Prototype/Model)). Piping and surface instability were observed due to the significant loss of fine particles prior to overtopping (Tests 1-3 described in the later section). However, the failure mode (piping and surface instability) when embankment material was used as the backfill material in the model could be different than those expected when #57 coarse aggregates are used as backfill material in the prototype because fine particles are not part of the gradation of #57 coarse aggregates shown in Figure 5.2 and 5.3 in Task1.1 *Evaluation of Backfill Properties*. Hence, #8 coarse aggregates, which contain less fine particles were adopted as the backfill material in the model to simulate the #57 coarse aggregates in the prototype. The scale ratio of the #8 coarse aggregate to the #57 coarse aggregate is 1.6/1 (Prototype/Model). R-2 Rock lining were applied in this study in the model to simulate the R-4 Rock lining as the prototype. The measured mean grain size (D_{50}) of R-2 Rock lining is 40 mm. The average D_{50} of R-4 Rock lining is 176.2 mm. The scale ratio of the R-2 Rock lining/R-2 Rock lining is 4.4/1 (Prototype/Model). Test results (Test 1-21) shows that piping, slumping, and slope failures were achieved in the model as they were expected in the prototype using the chosen smaller aggregate size.

7.2.3. Scale of Geosynthetics Placement

Details of the full-scale (prototype) Geosynthetics placement based on the PennDOT RC-Drawings-14M (PennDOT, 2019) and PennDOT Publication 408/2020 (PennDOT, 2020) are shown in Figure 1.3. The geometry of the embankment is scaled as 5:1 (Prototype: Model) in the lab study. The height of the embankment is fixed at 2 ft in the model (10 ft in the prototype) due to the dimension limitations in the lab. The maximum spacing between two Geogrid layers is18 in. in the prototype. The maximum spacing between two Geogrid layers in the model is supposed to be 3.6 in. based on the scale ratio of 5:1. However, considering that there are also three Geotextile layers between two Geogrid layers, and the spacing between each Geotextile layer is only 1.2 in., which is small and impractical, the placement of the geosynthetic is adjusted. The maximum spacing between Geogrid layers is set as 12 in. in the model (18 in. in the prototype). Two layers of Geotextile, instead of three layers between Geogrid layers are designed with a 6 in. spacing in the model (6 in. in the prototype) between each Geotextile layers. The minimum embedded length of Geotextile wraps is designed as 2 ft in the model (4 ft in the prototype) into the next reinforcement layer.

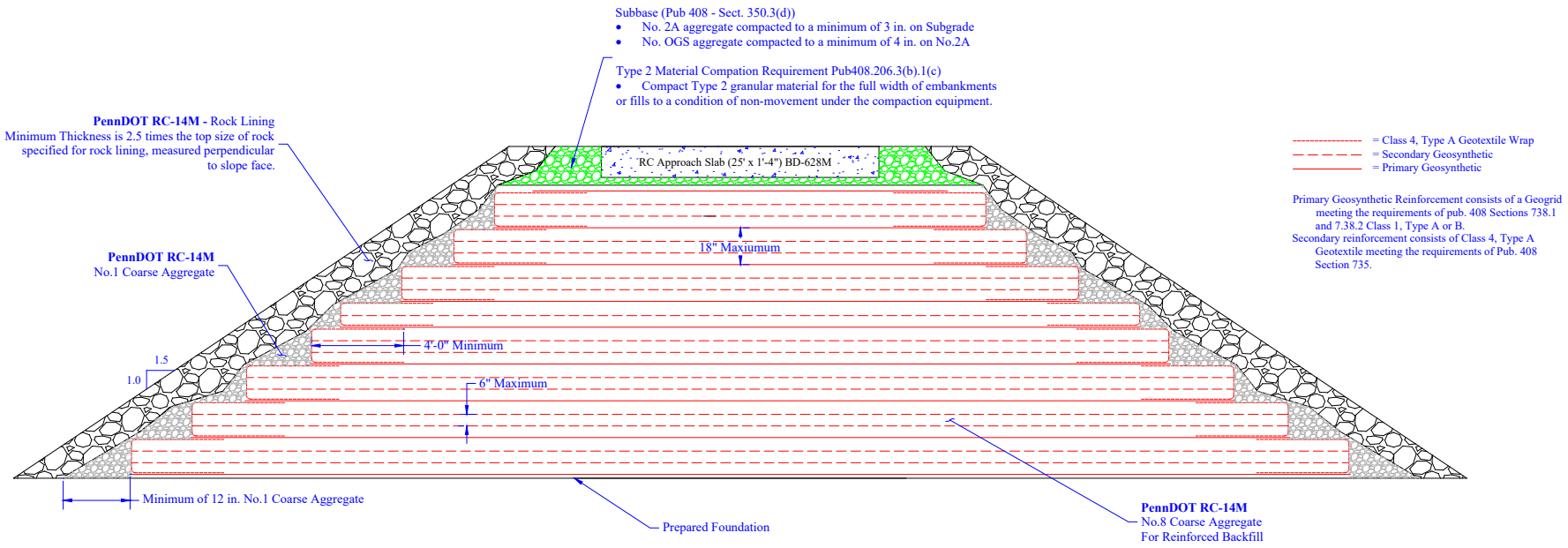

Figure 1.3: Reinforced abutment design based on PennDOT Publication 408/2020 and PennDOT RC-Drawings-14M

7.3. EMBANKMENT CONFIGURATION

Two water tanks were utilized to investigate the resistance of the backfill material under extreme flood events. The erosion of typical embankment material was tested in the "1st floor water tank" with Dimensions (L:W:H) of 25:10:2 ft (Figure 1.4a). The erosion of structural backfill was evaluated in the "balcony water tank" with Dimensions (L:W:H) of 26:16:3 ft (Figure 1.4b). In both systems, water is pumped into the tank from a head box with the flow rate of up to 3.5 ft^3/s. The test sections of the tank are covered with plastic sheets to minimize leakage. Baffle boards are used in some tests on the downstream end of the tank to control the downstream water head. Videos are taken using GoPros located upstream, downstream, and at the top of the embankment to record the experiment. The experimental setups are designed to evaluate the erosion behavior of the embankment. Experimental setup No.1 is shown in Figure 1.5. The embankment with the dimension of 8.5 ft long, 2 ft height and 5 ft wide is constructed in the experimental Setup No.1. The wooden approach slab was fixed to the side walls at the top of the embankment. The approach was filled with stones to prevent buoyancy. Experimental Setup No.2 includes a wingwall and bridge opening as shown in Figure 1.6. Experimental Setup No.2 focuses on evaluation of the erosion behavior at the edge of the wingwall.

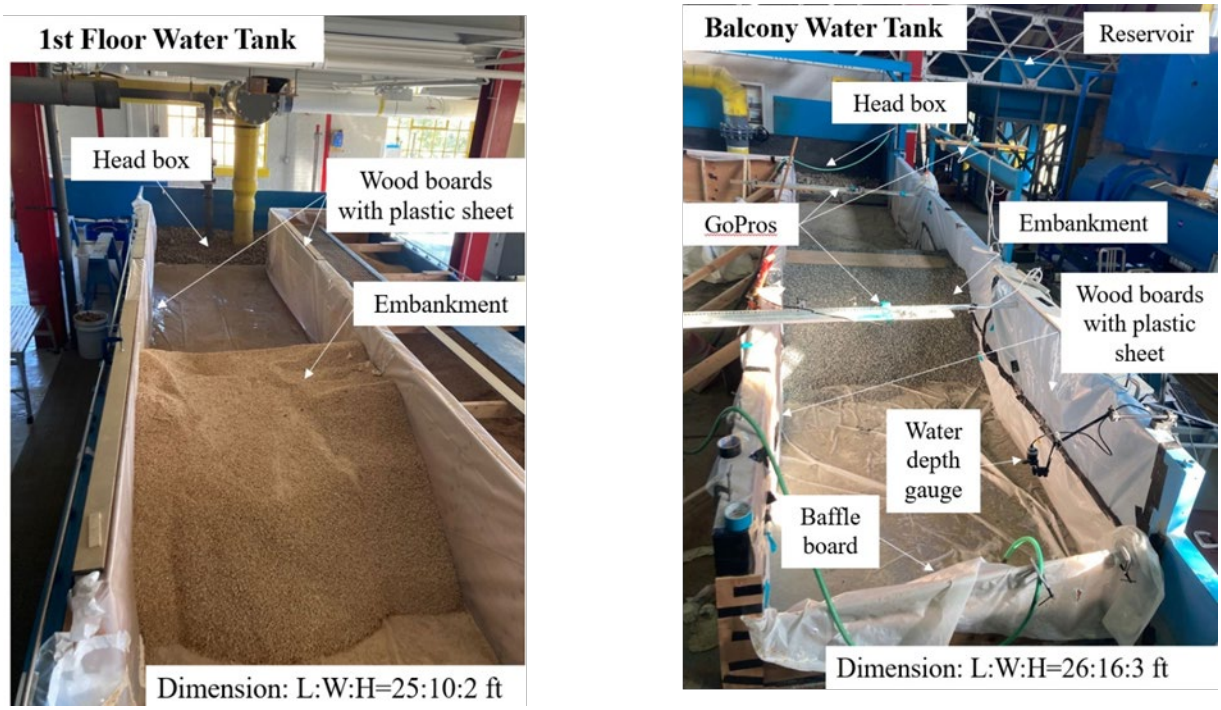

(a) (b)

Figure 1.4: Water tank design (a): 1st floor water tank; (b) balcony water tank

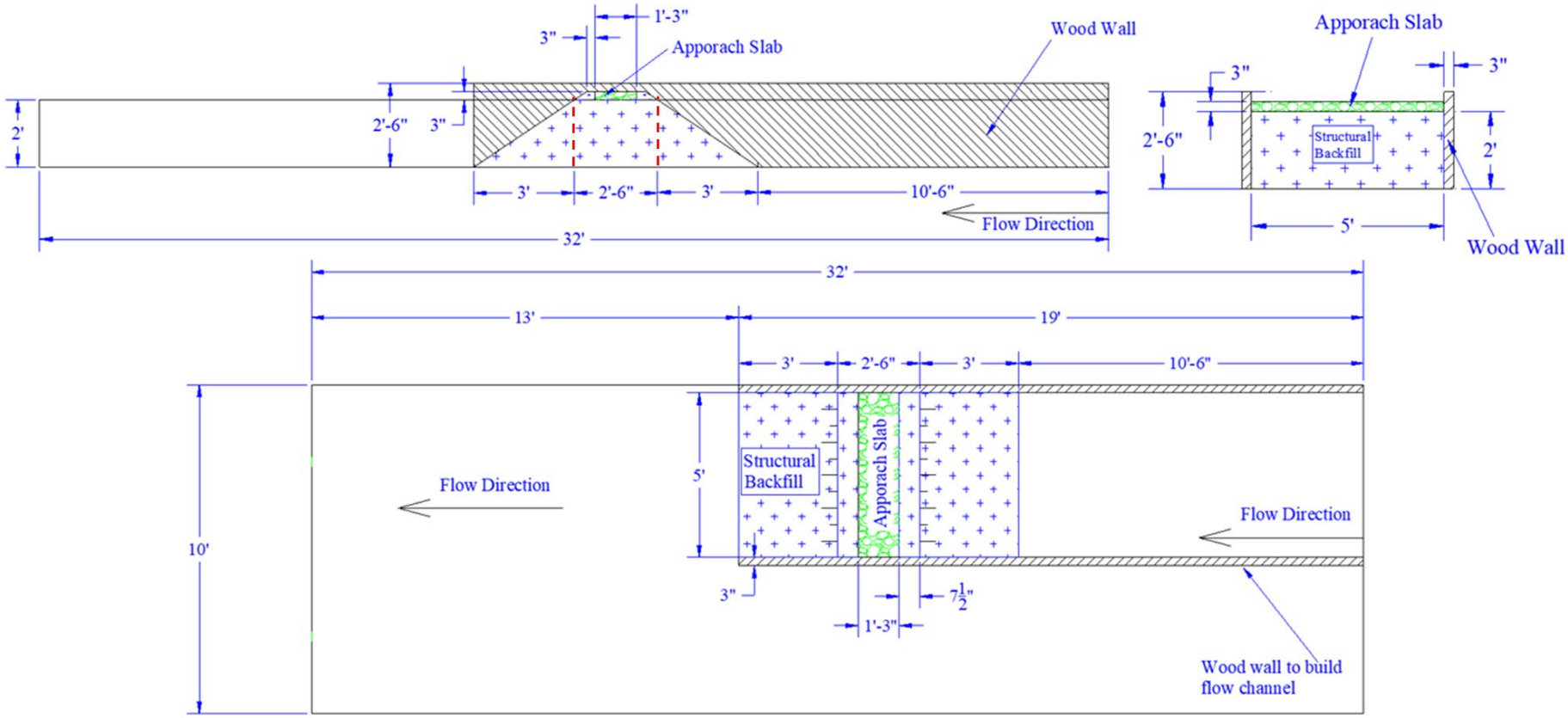

Figure 1.5: Experimental setup No.1

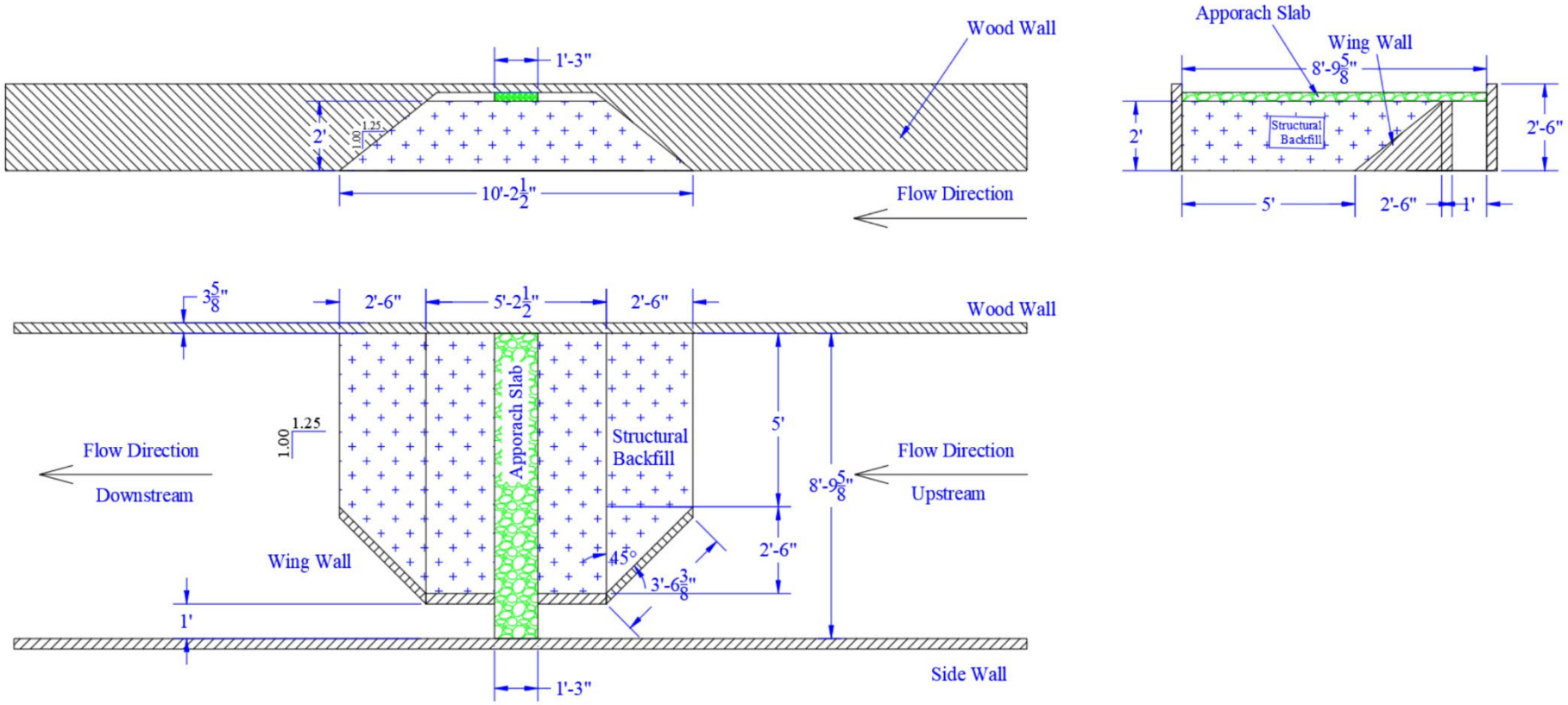

Figure 1.6: Experimental setup No.2 with wingwall and bridge opening

7.4. STRUCTURAL BACKFILL TEST MATRIX

The erosion of the backfill around the bridge abutment was investigated in the water tanks through twenty-one experiments. The erosion behavior of different backfill materials: embankment material and structural backfill (#8 coarse aggregate) was tested. Geosynthetics, including Geotextile and Geogrid, and Rock lining were applied to reinforce the embankment. The input flow rate and the water head difference between the downstream and upstream side were controlled during the tests. The details of the water tank tests are summarized in the Table 1.1.

Table 1.1 Water Tank Test Matrix

Test	Test configuration	Slope	Piping before overtopping			Failure before overtopping			Failure at overtopping			Failure after overtopping			
			Observations	Water head difference (in)	Flow rate (CFS)	Observations	Water head difference (in)	Flow rate (CFS)	Observations	Water head difference (in)	Flow rate (CFS)	Observations	Water head difference (in)	Flow rate (CFS)	Flow velocity (ft/s)
1	Embankment material (Preliminary test, no tangible data)	1/1.5	Yes, and localized surface instability	N/A	N/A	Global failure	N/A	N/A	N/A	N/A	N/A	N/A	N/A	N/A	N/A
2	Embankment material (Preliminary test, no tangible data)	1/1.5	Yes, and localized surface instability	N/A	N/A	Global failure	N/A	N/A	N/A	N/A	N/A	N/A	N/A	N/A	N/A
3	Embankment material	1/1.5	Yes, and localized surface instability	3	0.1	Global failure	6.25	0.415	N/A	N/A	N/A	N/A	N/A	N/A	N/A
4	Structural backfill (#8)	1/1.5	Yes	10	0.38	Slope failure	15	0.63	Global failure	18	0.76	N/A	N/A	N/A	N/A
5	Structural backfill (#8)	1/1.5	Yes	9	0.59	Slope failure	10	0.59	Global failure	10	0.59	N/A	N/A	N/A	N/A
6	Structural backfill (#8)	1/1.5	Yes	4	0.4	No	1	0.627	Surface erosion	2	2.5	Global failure	6	2.5	1
7	Structural backfill (#8)	1/1.5	Yes	10	0.49	Slope failure	12.5	0.55	Global failure	13	0.62	N/A	N/A	N/A	N/A
8	Structural backfill (#8)	1/1.5	Yes	8.5	0.41	Global failure	20	0.714	N/A	N/A	N/A	N/A	N/A	N/A	N/A
9	Structural backfill (#8) with Rock lining (R2)	1/1.5	No	N/A	N/A	No	5	0.313	No	5	2.29	Global failure	8	2.29	1
10	Structural backfill (#8) with Rock lining (R2)	1/1.5	No	N/A	N/A	No	22	0.94	Slope failure	22.5	0.94	Global failure	22.5	1.4	1.8

11	Structural backfill (#8) with heavily reinforced geosynthetics	1/1.5	Yes	10	0.37	Slope failure	16	0.37	Slope failure	24.5	0.6	Surface failure, reinforced part stay	27	3.5	3.1
12	Structural backfill (#8) with heavily reinforced geosynthetics, and Rock lining (R2)	1/1.25	No	N/A	N/A	No	22	0.45	Slope failure	25.5	0.838	Surface failure, reinforced part stay	28.5	3.6	3.2
13	Structural backfill (#8) with heavily reinforced geosynthetics, and Rock lining (R2)	1/1.25	No	N/A	N/A	No	7.5	0.33	No	4	1.85	Surface failure, reinforced part stay	25	3.5	2
14	Structural backfill (#8) with poorly reinforced geosynthetics, and Rock lining	1/1.25	No	N/A	N/A	Slope failure	21	0.622	Slope failure	21	1.1	Global failure, geotextile unwrapped	21	2	2.0
15	Structural backfill (#8) with geosynthetics (with overlap), and Rock lining (R2)	1/1.25	No	N/A	N/A	No	21	0.7	Slope failure	22	1.65	Surface failure, reinforced part stay	22.5	3.2	2.8
16	Continuing of Test 15, no approach slab, no downstream surface backfill	1/1.25	N/A	N/A	N/A	N/A	N/A	N/A	N/A	N/A	N/A	Reinforced part stay	22.5	3.3	N/A
17	Structural backfill (#8) with geosynthetics (no overlap), and Rock lining (R2), larger embankment	1/1.25	No	N/A	N/A	No	23	0.581	Slope failure	25	1.832	Surface failure, corner erosion, reinforced part stay	25.5	3.3	1.1
18	Continuing of Test 17, no approach slab, no downstream surface backfill	1/1.25	N/A	N/A	N/A	N/A	N/A	N/A	N/A	N/A	N/A	Global failure, geotextile unwrapped	25.5	3.3	N/A
19	Structural backfill (#8) with geosynthetics (no overlap), and Rock lining	1/1.25	No	N/A	N/A	No	18	2.7	N/A	N/A	N/A	N/A	N/A	N/A	N/A

	(R2), larger embankment with wingwalls, with bridge opening														
20	Structural backfill (#8) with geosynthetics (no overlap), and Rock lining (R2), larger embankment with wingwalls, block bridge opening	1/1.25	No	N/A	N/A	No	24	2.7	Slope failure	24.5	2.7	Global failure, geotextile unwrapped at the wingwall corner	24.5	2.7	1
21	Structural backfill (#8) with geosynthetics (with overlap), and Rock lining (R2), larger embankment with wingwalls, block bridge opening	1/1.25	No	N/A	N/A	No	25	1.67	Slope failure	25.5	1.67	Surface failure, reinforced part stay	27	3.76	1.2

7.5. SUMMARY OF EMBANKMENT/ABUTMENT TESTS

A series of experiments were conducted to examine the erosion resistance of conventional structural backfill embankments. The baseline unreinforced embankments and the geosynthetic reinforced embankments were based on standard and preliminary drawings provided by Pennsylvania Department of Transportation. Twenty-one water tank tests were conducted to evaluate the erosion behavior around the bridge abutment. The observations are summarized below:

1: Piping and localized soil instability, and significant (large) slope failure were observed at a small water head difference (around 3 in. in the model, 15 in. in the prototype) between upstream and downstream embankment when using uncompacted embankment material as the backfill material. Global failure, which is defined as the continuous significant slope failure under the constant flood occurred before overtopping.

2: Changing the backfill from uncompacted embankment material to an uncompacted standard #8 coarse aggregate (structural backfill) minimized localized soil instability and mitigated erosion caused by piping at a small water head differential. Piping was observed when the water head difference reached 4 to 10 in. in the model (20 to 50 in. in the prototype). Slope failure initiated when the water head difference was 10 to 15 in. in the model (50 to 75 inches in the prototype) before overtopping. Global failure occurred at the start of overtopping.

3: Water head difference is a key factor determining the failure mode of the embankment. If the water head difference was kept at around 1 in. in the model (5 in. in the prototype) during the test, no failure occurred prior to overtopping. The failure mode after overtopping consisted of surface erosion when the water head difference was less than 2 in. in the model (10 in. in the prototype). Global failure was initiated after overtopping when the water head difference was increased to 6 in. in the model (30 in. in the prototype).

4: Piping and large slope failure before overtopping are unlikely to occur when using rock lining on the slope in accordance with PennDOT recommendations. After overtopping surface erosion results in failure of the slope even when using a rock lining protection.

5: Geosynthetics, including the Geogrid and Geotextile are effective in preventing the global failure if the reinforced core part of the embankment is wrapped adequately. This can be accomplished by: (1) using Geotextile to wrap around the #8 coarse aggregate and embedding the Geotextile wrapping with a minimum of 2 ft in the model (4 ft in the prototype) into the next

reinforcement layer; (2) placing the Geogrid in continuous strips perpendicular to the slope face, the maximum allowable vertical spacing of primary geosynthetics is 12 in. in the model (18in. in the prototype); (3) placing one layer in the model (two layers in the prototype) of Geotextile evenly spaced between layers of primary reinforcement; (4) placing the upstream Geotextile over the downstream Geotextile to ensure encasement of the structural backfill. Vertical spacing between Geotextile layers, and between Geotextile and Geosynthetic layers above or below, is both 6 in. in the model and the prototype.

6: The eddies caused by the water flowing through the bridge opening and wingwall did not initiate scour on the surface of the embankment.

7: In all cases, failure only happened on the downstream side, no failure was observed on the upstream side.

7.6. RECOMMENDED STRUCTURAL BACKFILL CONFIGURATION

1. The use of #8 structural backfill covered with R-2 rock lining was shown to provide good performance and resistance to erosion in the experimental program. However, the embankment is still likely to fail after overtopping due to surface erosion of the rock lining and subsequent loss of the contained #8 structural backfill on the downstream face. Considering the scale used in the experimental program, similar performance at prototype scale would likely be achieved using #57 structural backfill and R-4 rock lining.

2. The combination uses of the Geosynthetics, including Geogrid and Geotextile are recommended to protect the core part of the embankment. When erosion of the bridge approach slab or roadway pavement is possible, overlap the geotextile with the upstream edge placed on top of downstream edge with an overlap of at least 4ft (full scale) as shown in Figure 1.7. When pavement erosion is unlikely, the roadway and underlying layers will likely prevent unwrapping of the top layer of geotextile. For these cases, overlapping of the geotextile may not be necessary. For such a case, geotextile from both the downstream and upstream edges should be extended and meet in the middle of the embankment as shown in Figure 1.8. For cases where overtopping occurs, the rock lining will likely be lost during an overtopping situation and will require replacement after the event.

3. To be conservative, it is recommended that all reinforced areas adjacent to structures be constructed with an overlap detail. The drawing in the model is shown in Figure 1.9 (a) and the updated PennDOT drawing in full-scale (prototype) is shown in Figure 1.9 (b). The full-scale detail has a recommended 4 ft overlap of the outer upstream geotextile over the downstream edge. In addition, it is recommended that the downstream edge of the top outer layer of geotextile be extended at least 4 ft under the roadway surface. The overlap of the upstream edge of the geotextile for the top layer can be started at the downstream edge of the roadway.

4. If there are wingwalls next to the bridge abutment, the backfill at the corner of the wingwall should be wrapped in both the longitudinal and lateral direction as shown in Figure 1.10(a) to (d) to ensure containment of the structural backfill within the geotextile.

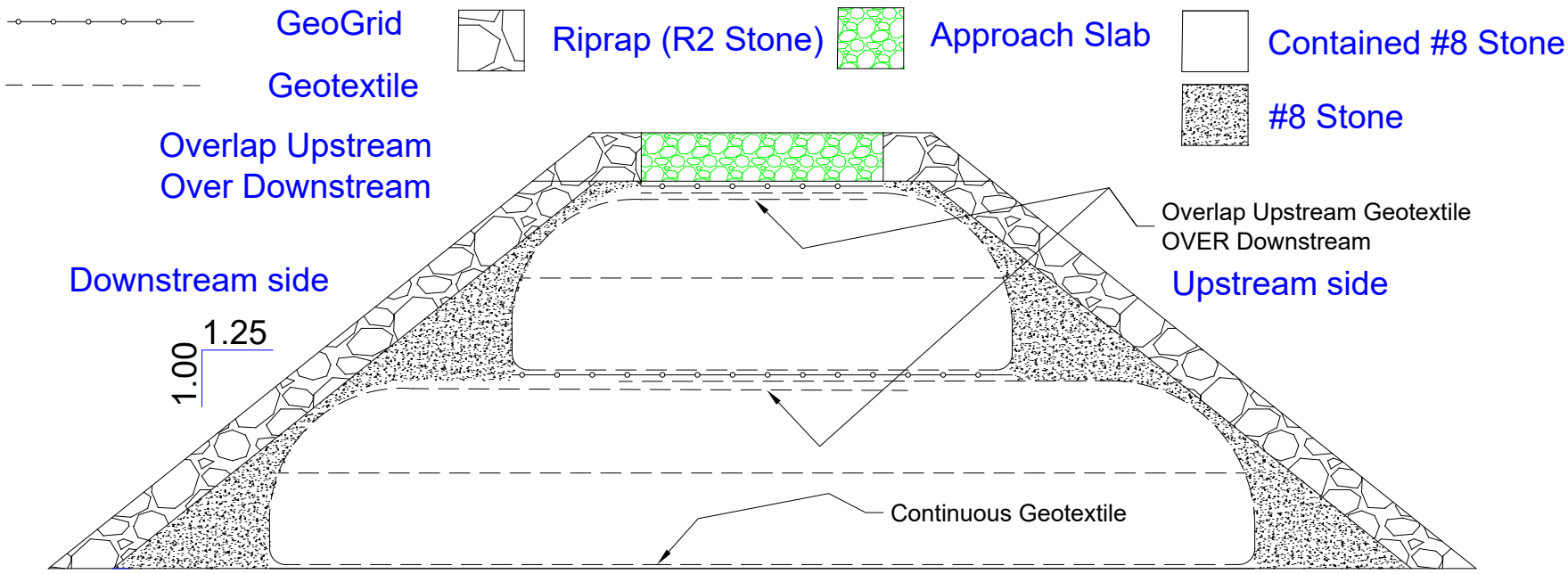

Figure 1.7: Lab scale rock lined reinforced structural backfill for cases where road surface erosion possible

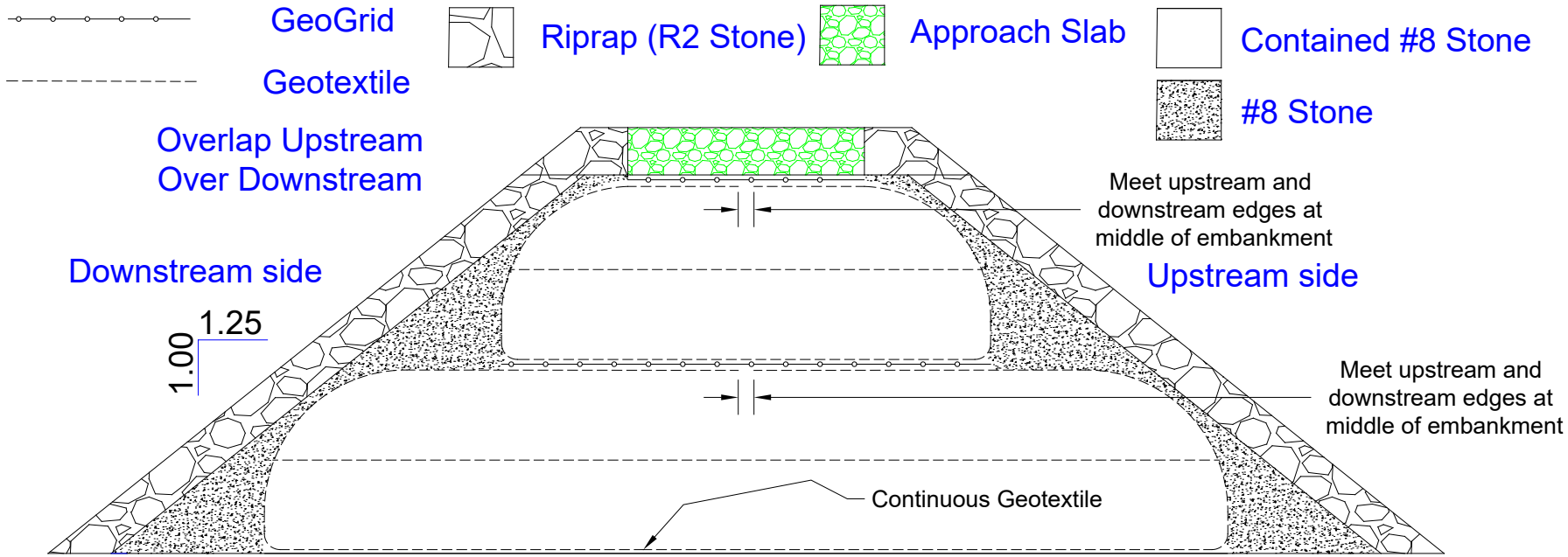

Figure 1.8: Lab scale rock lined reinforced structural backfill for cases where erosion of road surface not expected

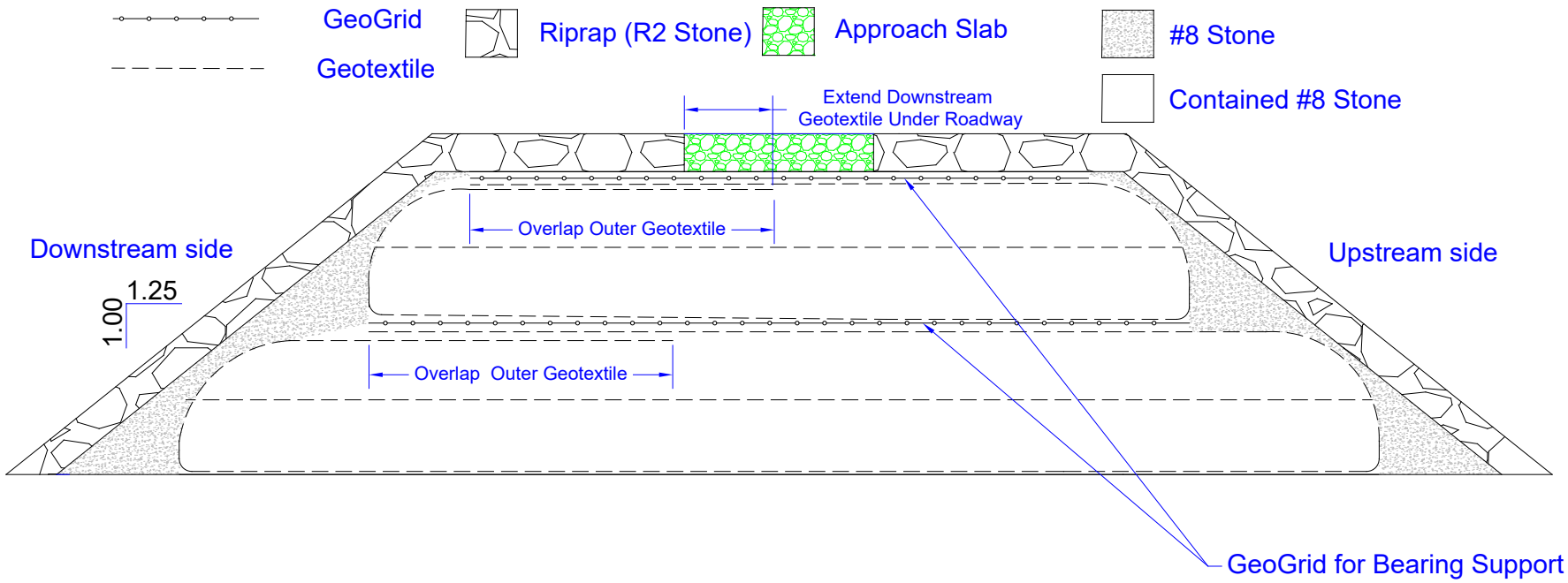
GeoGrid
Geotextile
Riprap (R2 Stone)
Approach Slab
#8 Stone
Contained #8 Stone
Extend Downstream
Geotextile Under Roadway
Overlap Outer Geotextile
Downstream side
Upstream side
1.25
1.00
Overlap Outer Geotextile
GeoGrid for Bearing Support

(a)

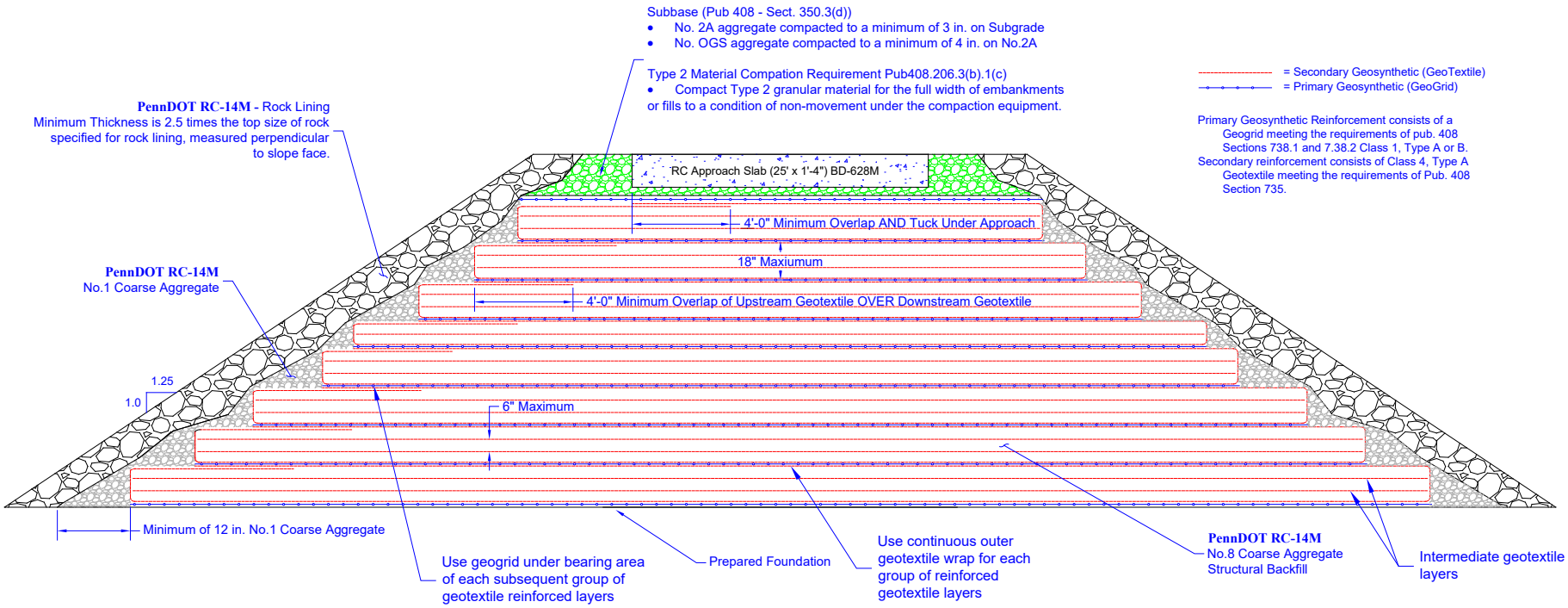

(b)

Figure 1.9 (a) Lab scale rock lined reinforced structural backfill; (b) Recommended PennDOT Detail

(a) (b)

(c) 

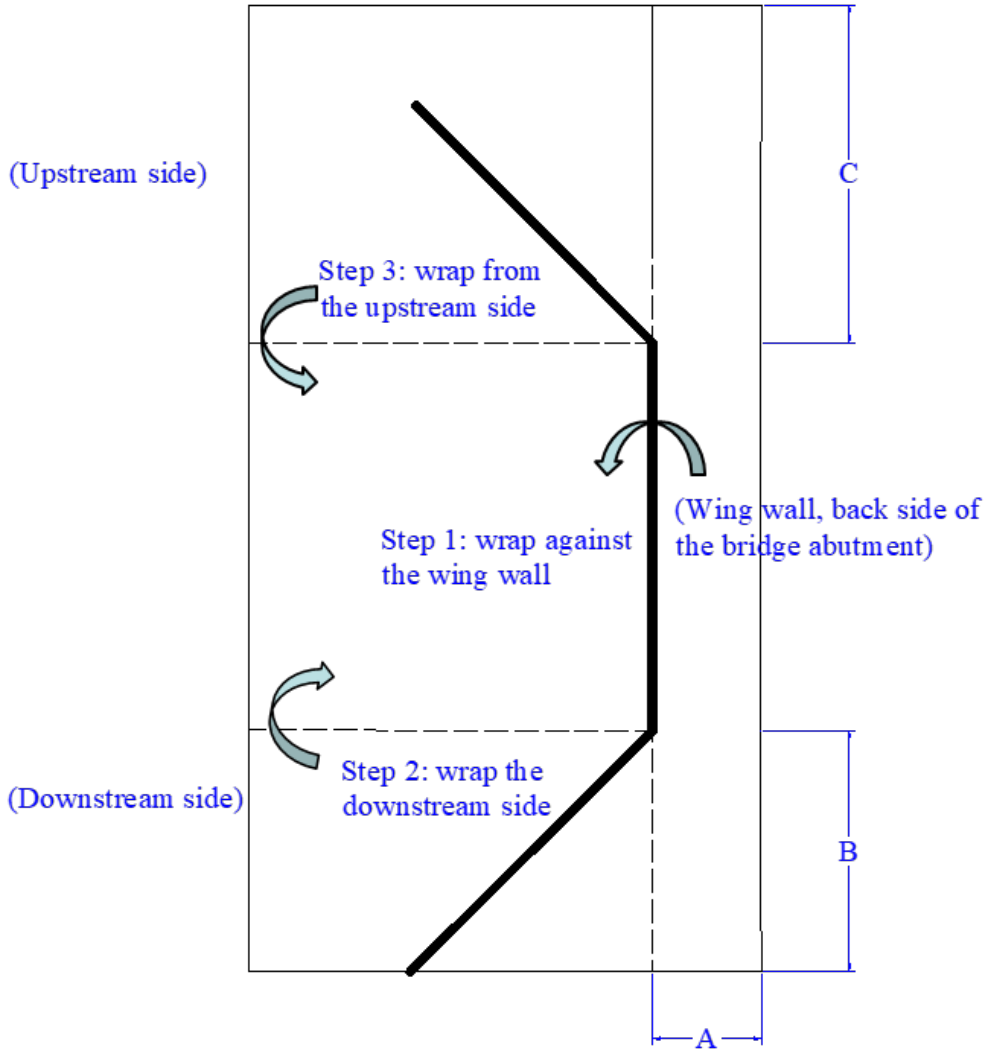

(d)

Figure 1.10: (a) First fold A: wrap against the wing wall (use 4ft wrap), (b) Second fold B: wrap from the downstream side, (c) Third fold C: wrap from the upstream side to cover the downstream wrapping with a 4 ft overlap, and (d) Geotextile wrapping details

7.7. STRUCTURAL BACKFILL FUTURE WORK

During discussions with PennDOT, concerns were raised regarding constructability of the recommended details. To address these concerns an alternate detail is provided. It is important to note that this detail has not been tested as part of the experimental program. It is presented as a possible means of addressing the constructability issue and should be evaluated before implementation in the field. The details are illustrated in Figure 1.11 to Figure 1.11. The potential changes include:

- For large embankment widths utilizing a continuous geotextile wrap for each group of layers will become difficult to implement. For such a situation it may be possible to terminate the bottom portion of the geotextile after a given distance is anchored within the structural backfill. A 10ft width is arbitrarily chosen. For embankments that have widths less than 20 ft the bottom of each geotextile wrap should remain continuous.
- The intermediate geotextile layers within each geotextile group do not appear to be critical for preventing erosion. It is possible that the presence of these intermediate layers will decrease the amount of piping through the embankment; however, this is only speculation. Removal of these intermediate layers would improve constructability.
- The use of Geogrid between two Geotextile layers may cause issues with friction. In conventional situations the Geogrid is in contact with the structural backfill material. As a possible improvement from the tested detail, the Geogrid can be installed within each Geotextile bundle. A 24 in. thickness for the Geotextile bundle with the Geogrid placed at the center is a possible configuration.

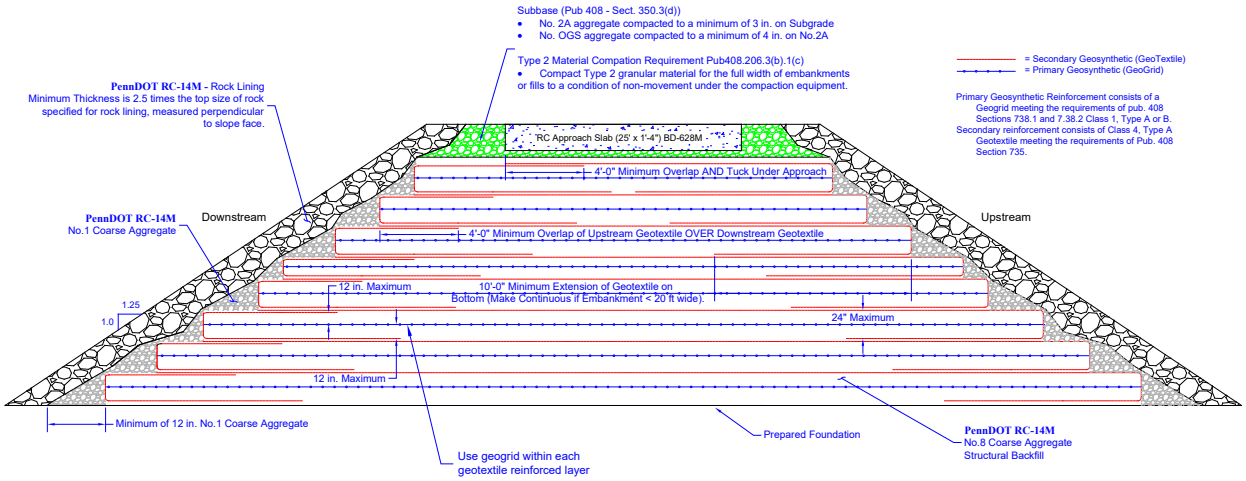

Figure 1.11: Potential reinforced strucutral backfill details

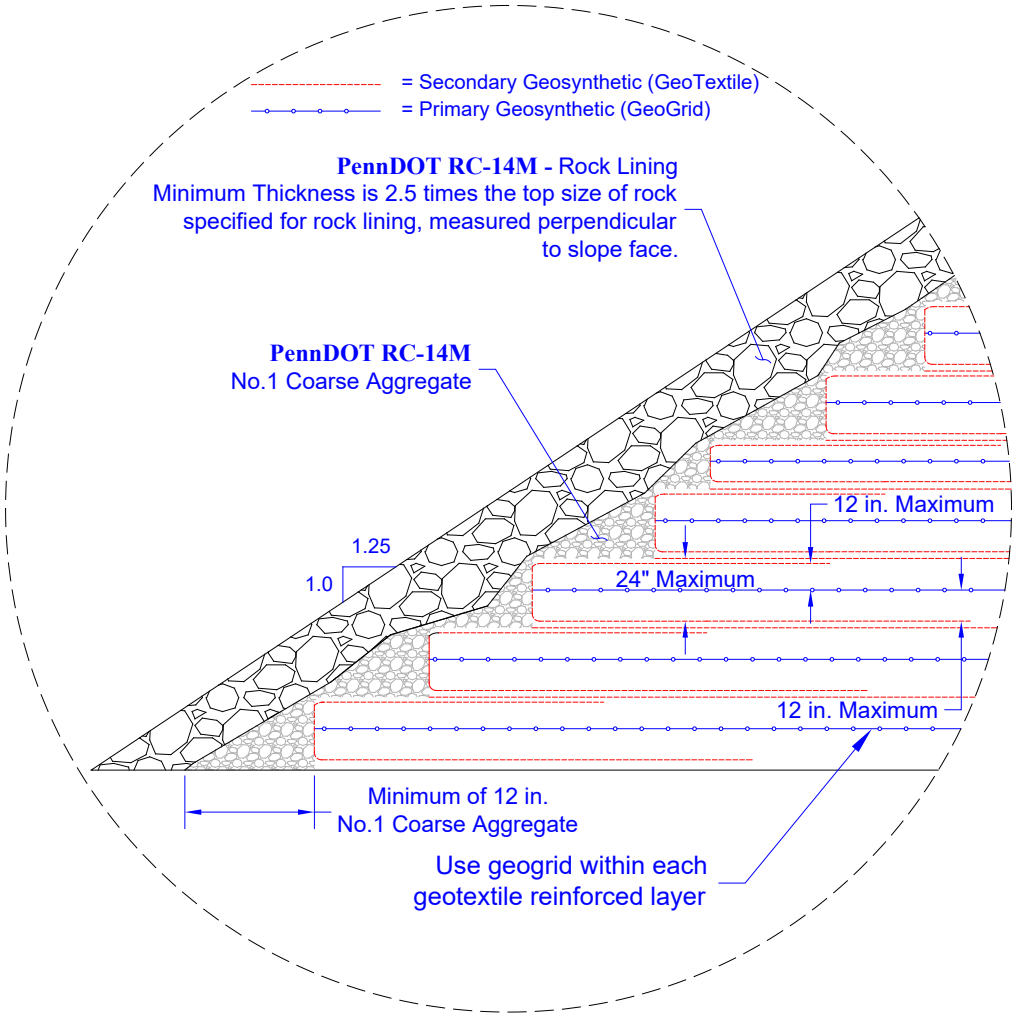

Figure 1.12: Close-up view of potential downstream details

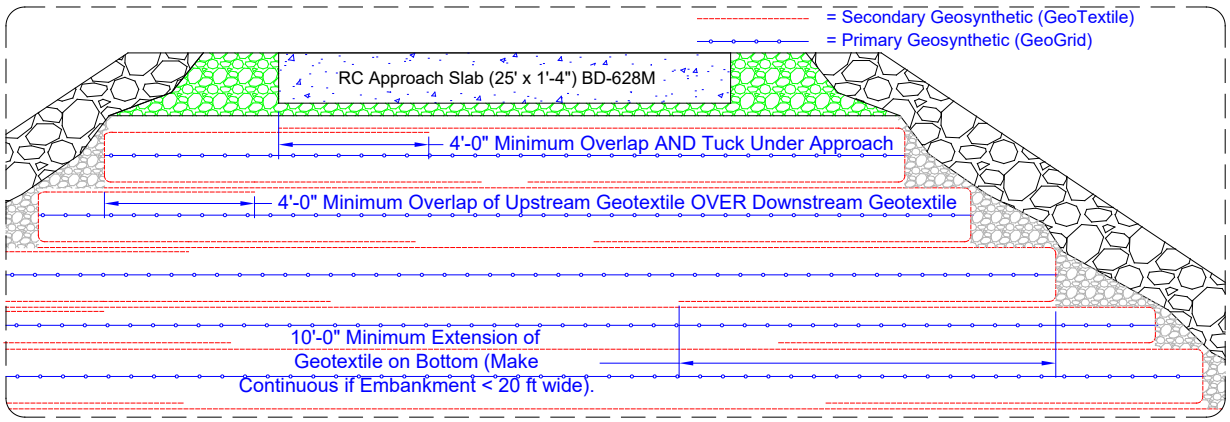

Figure 1.13: Close-up view of potential lapping details

8. STRUCTURAL BACKFILL TEST DETAILS

The results from the twenty-one tests on embankment/abutments are summarized in this section. Each subsection provides a background on the test and a summary of the performance.

8.1. FAILURE MODES

Failure modes observed from Test 1 to Test 21 are summarized below. Details of each test are shown in the later paragraphs.

(1) Piping

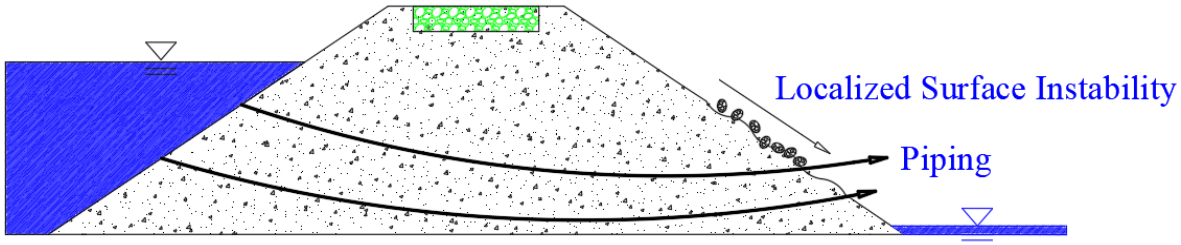

Figure 2.1: Schematic of piping and localized surface instability

(2) Shallow slope failure

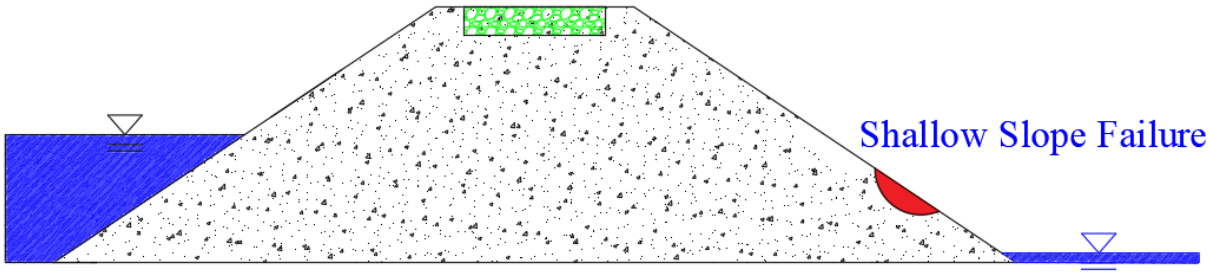

Figure 2.2: Schematic of shallow slope failure

(3) Large slope failure

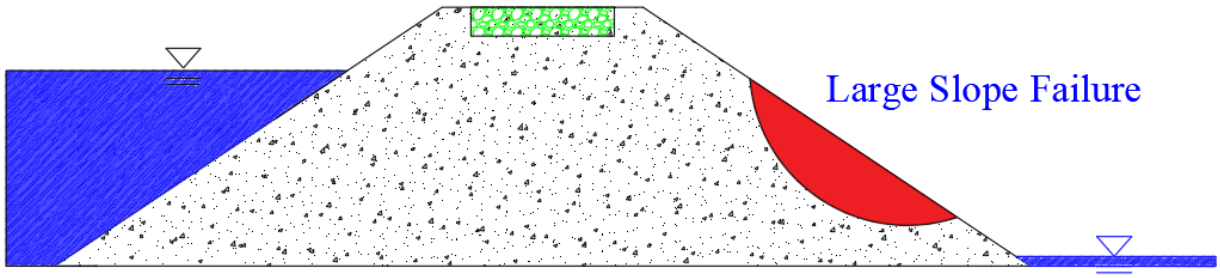

Figure 2.3: Schematic of large slope failure

(4) Surface failure

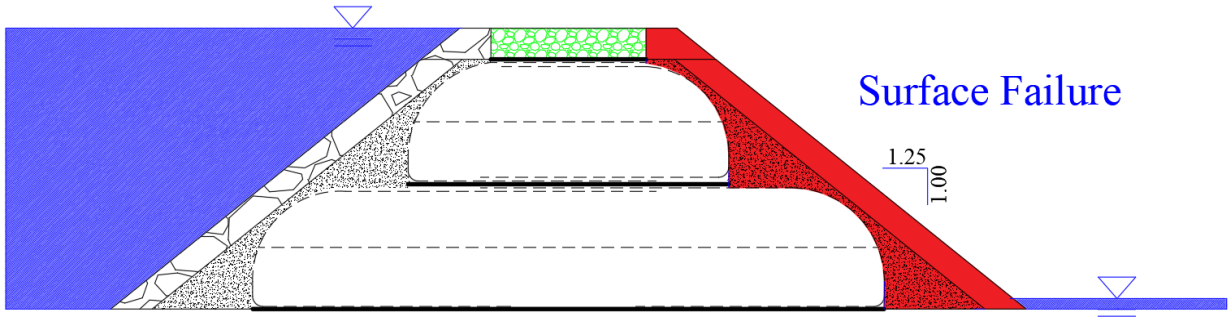

Figure 2.4: Schematic of surface failure for backfill material outside the geosynthetic reinforcement

(5) Surface erosion

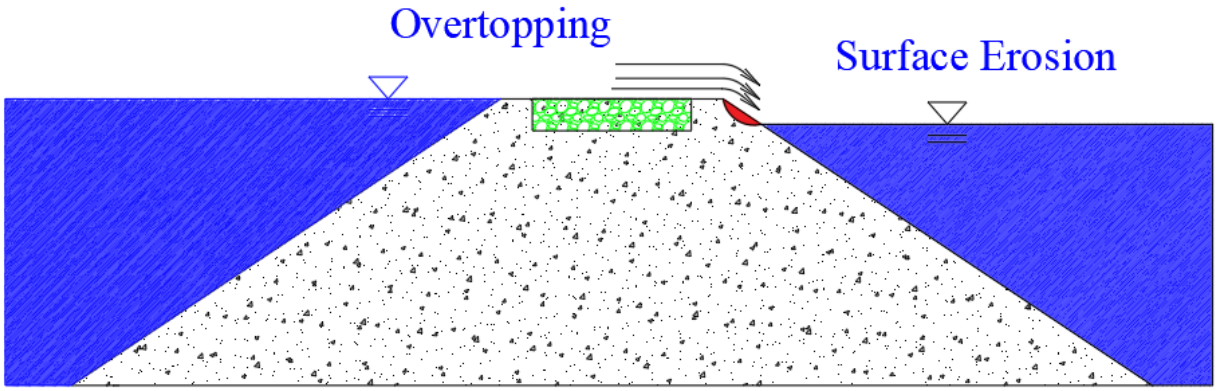

Figure 2.5: Schematic of surface erosion

(6) Global failures

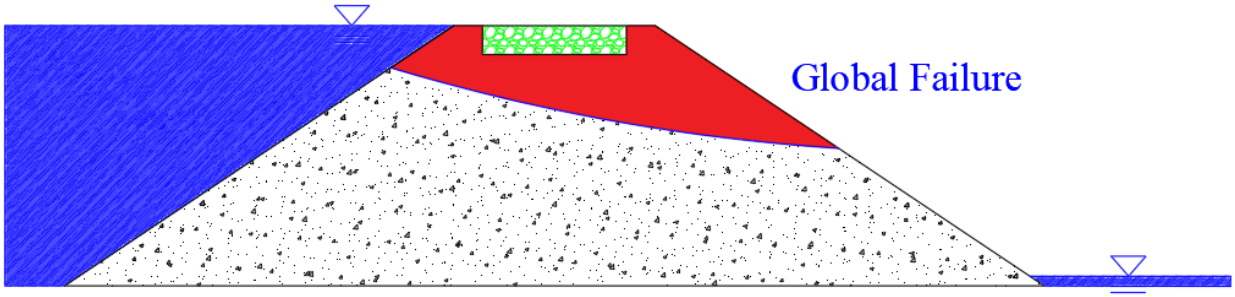

(a)

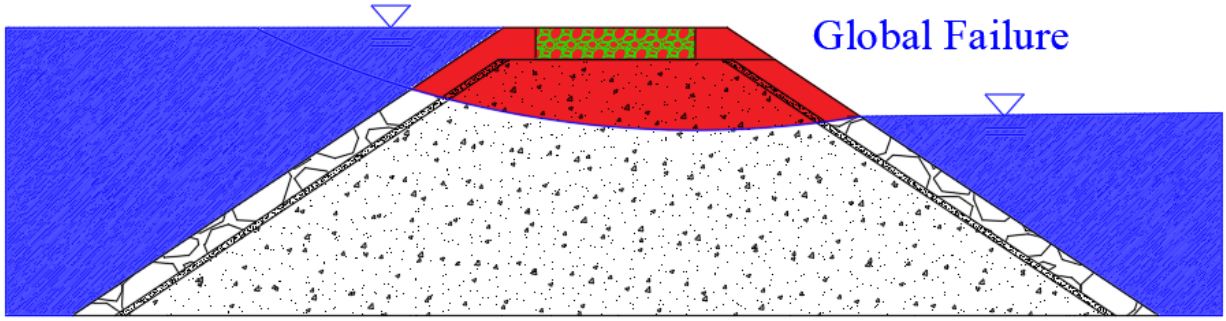

(b)

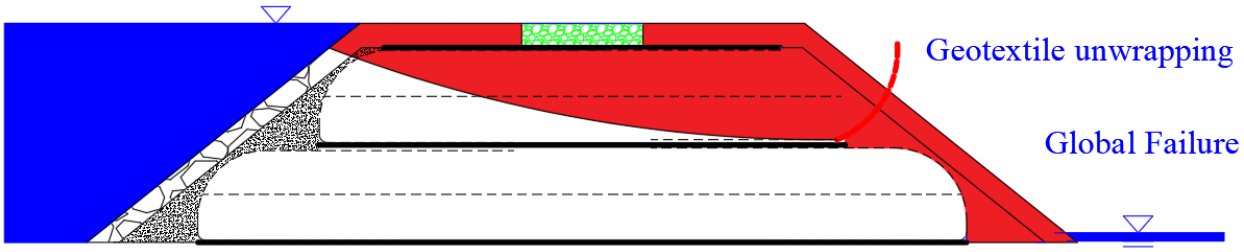

(c)

Figure 2.6: Schematics of (a) global failure at high water head difference, (b) global failure at small water head difference, and (c) global failure when geotextile was unwrapped

8.2. TEST 1 THROUGH 3 – EMBANKMENT MATERIAL ONLY

Preliminary tests were conducted to have a basic understanding of initially how the system would work and to investigate the erosion behavior of embankment material. The tests were conducted in the 1st floor water tank at Fritz lab (Figure 1.4a). The dimension of the water tank is L:W:H = 25 ft:10 ft:2 ft. A wooden frame with the dimension of L:W:H = 19 ft:5 ft:2.5 ft was constructed to create a narrow channel for increased water velocity.

Embankment materials (rather than structural backfill) consisting of a gravel with a mean particle diameter of 3.7 mm (Figure 2.7) were used for construction of the embankment. The embankment material was slowly rained using shovels with no compaction (from PennDOT Pub408, Section 206.3(b)1.c). Shovels were lifted and kept at a constant height of approximately 16 in. above the surface. Surface of the embankment was trimmed and flatten using a brush. The dimension of the embankment is shown in Figure 2.8. A GoPro was set at the downstream side to record the experiment.

The first two preliminary tests (1 and 2) were used to work on the camera setup and flow control. For each of these tests the embankment was lost during the trial, however no tangible data was generated.

In test 3, piping and localized surface instability were observed when the water head difference was at 3 in. when the flow rate was at 0.10 CFS. The continuous slope failure (Figure 2.9a) was then observed and the global failure (Figure 2.9b) was followed when the flow rate was at 0.415 CFS. This occurred prior to overtopping.

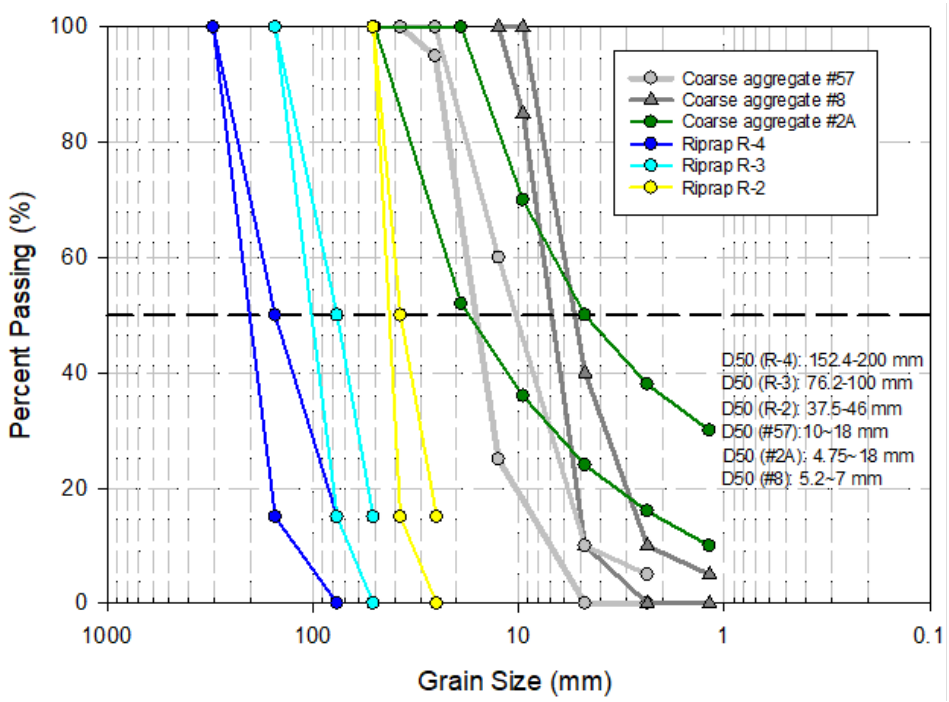

Figure 2.7: Gradation of embankment material at Fritz lab

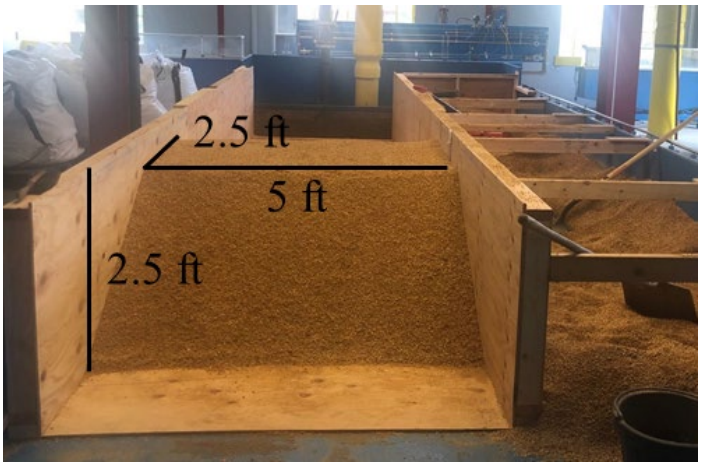

Figure 2.8: Dimension of the embankment

(a) (b)

Figure 2.9: (a) Continuous slope failure, and (b) global failure

8.3. TEST 4 - #8 EMBANKMENT NO REINFORCEMENT LARGE HEAD DIFFERENTIAL FLOW RATE

Test 4 was conducted with the embankment as shown in Experimental Setup No. 1 with the approach slab present in the center (Figure 1.5). The downstream and upstream slopes were 1/1.5. The embankment was comprised of a PennDOT Structural Backfill consisting of #8 coarse aggregates. During the construction, #8 aggregate was gradually and slowly rained using shovels with no compaction. Shovels were lifted and kept at a constant height of approximately 16 in. above the surface. Surface of the embankment was trimmed and flatten using counter brush.

GoPros were setup on the downstream side and at the top of the embankment to record the test. The testing process is illustrated in Figure 2.10. At the beginning of the test, water was pumped into the water tank at the flow rate of 0.38 CFS. At the meantime, downstream water head was kept at around 1 inch. Piping was observed first at the water head difference of 10 inches and followed by the large slope failure at the water head difference of 15 inches. Shortly after, global failure was reached before overtopping at the water head difference of 18 inches.

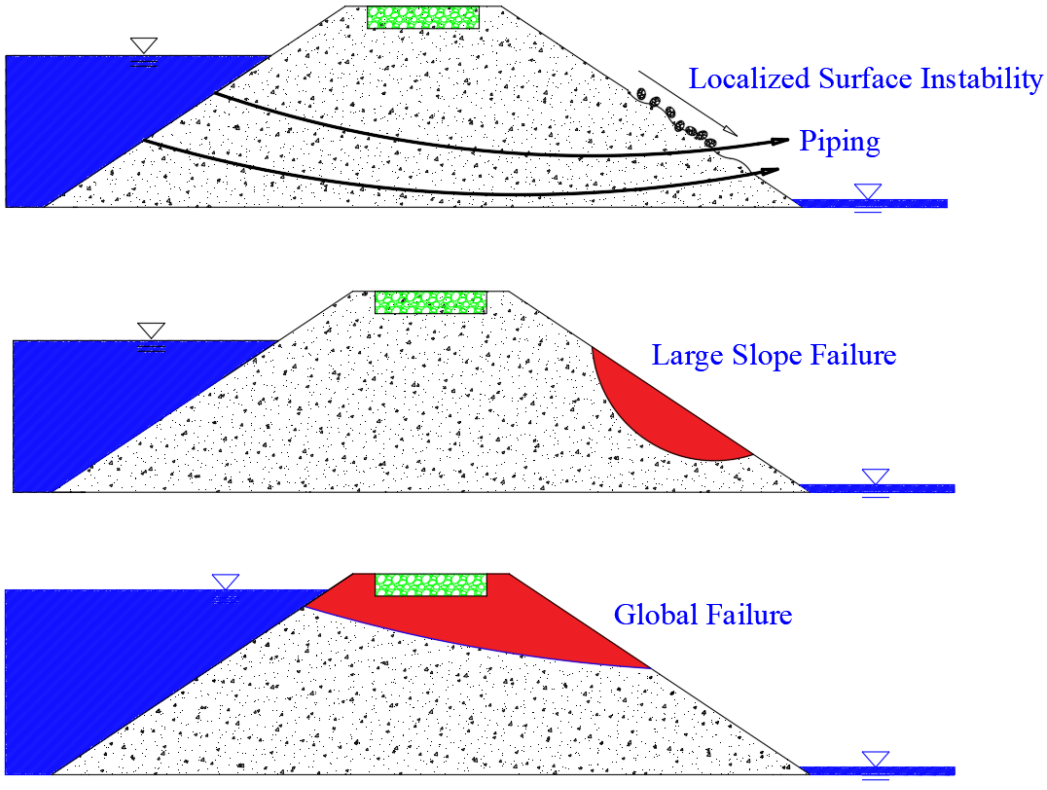

Figure 2.10 Testing process for Test 4

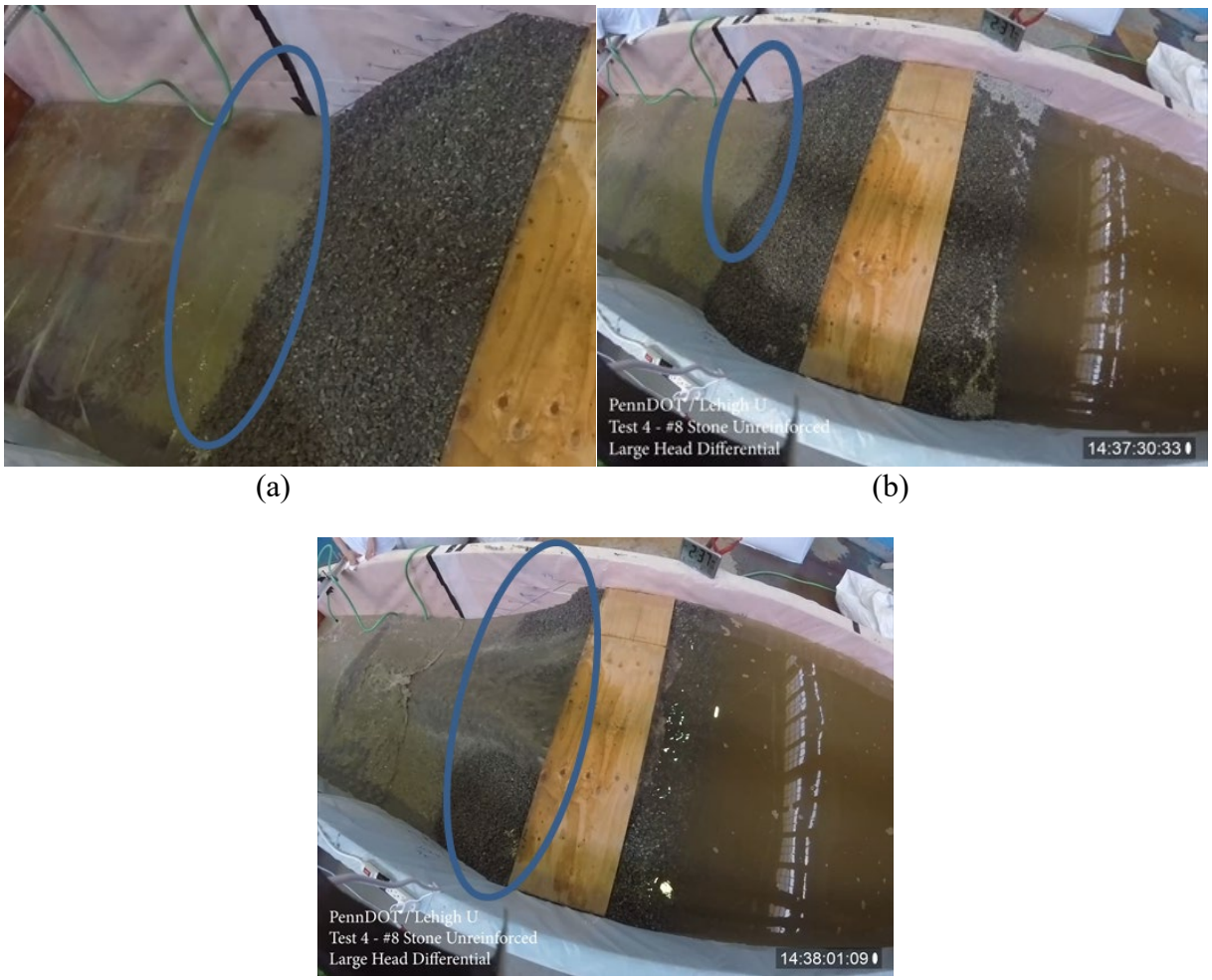

(a) (b)

(c)

Figure 2.11 (a) Piping, (b) slope failure, and (c) global failure from the top view

8.4. TEST 5 - #8 EMBANKMENT NO REINFORCEMENT LOW HEAD DIFFERENTIAL

Test 5 was conducted with the embankment shown in Experimental Setup 1 with the approach slab present in the center (Figure 1.5). The downstream and upstream slopes were 1/1.5. The embankment was comprised of #8 coarse aggregates as the structural backfill. During the construction, the #8 aggregate was gradually and slowly rained using shovels with no compaction. Shovels were lifted and kept at a constant height of approximately 16 in. above the surface. Surface of the embankment was trimmed and flatten using counter brushes.

GoPros were setup on the downstream side and at the top of the embankment to record the test. The testing process is illustrated in Figure 2.12. At the beginning of the test, water was pumped gradually into the water tank at the flow rate of 0.25 CFS. At the meantime, the downstream water head was held by baffle boards covered by the waterproof plastic sheet to keep the medium water head difference (from 3 to 12 inches). Piping was observed first at the water head difference of 9

inches when the flow rate was at 0.59 CFS. Slope failure first occurred at the water head difference of 10 inches when the flow rate was at 0.59 CFS. Shortly after, global failure (Figure 2.13) was reached at the overtopping when the water head difference was at 10 inches.

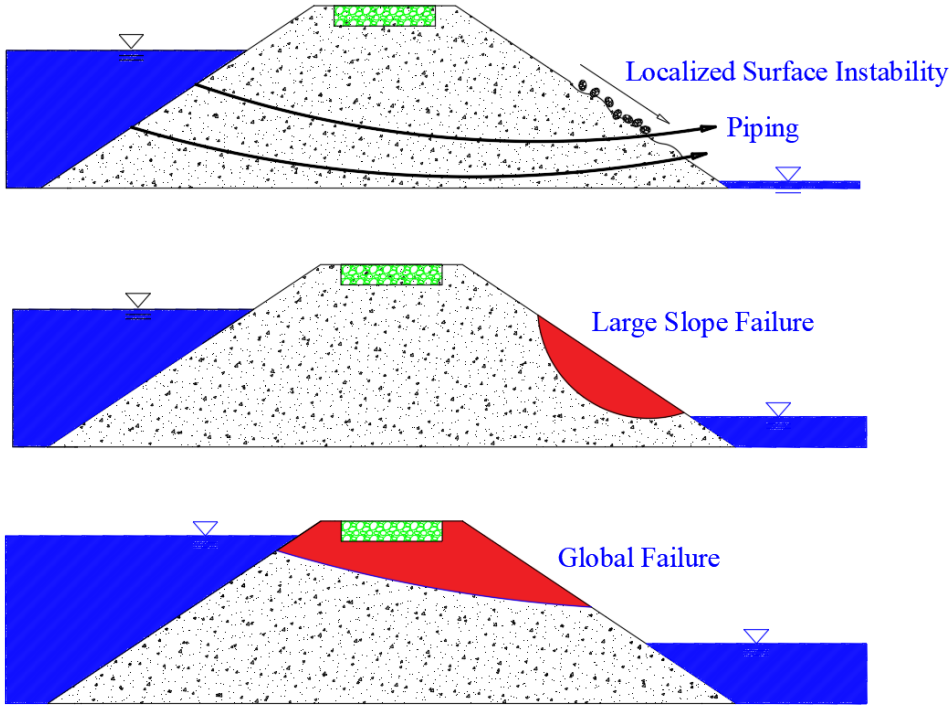

Figure 2.12: Testing process for Test 5

Figure 2.13: Global failure from the top view

8.5. TEST 6 - #8 EMBANKMENT NO REINFORCEMENT SMALL HEAD DIFFERENTIAL LOW VELOCITY

Test 6 was conducted with the embankment shown in Experimental Setup 1 with the approach slab present in the center (Figure 1.5). The downstream and upstream slopes were 1/1.5. The embankment was comprised of #8 coarse aggregates as the structural backfill. During the

construction, #8 aggregate was gradually and slowly rained using shovels with no compaction. Shovels were lifted and kept at a constant height of approximately 16 in. above the surface.

GoPros were setup on the downstream side and at the top of the embankment to record the test. The testing process is illustrated in Figure 2.14. At the beginning of the test, water was pumped into the water tank at a relatively low flow rate (0.383 CFS) to gradually increase the water head on the upstream side. At the meantime, the downstream water head was held by baffle boards covered by the waterproof plastic sheet to keep the water head difference as low as possible. Piping and slope failure were not observed before overtopping. When it reached the overtopping, no failure was observed since there was only 1-inch water head difference between upstream and downstream. The flow rate was then increased up to 0.95 CFS and then surface scour was observed (Figure 2.15a). The flow velocity above the approach slab was measured as 0.65 ft/s. The flow rate was increased up to 2.25 CFS, further scour was observed. The downstream water head was then lowered by removing one of the baffle boards to create a 9 inches water head difference, and then global failure immediately happened (Figure 2.15b).

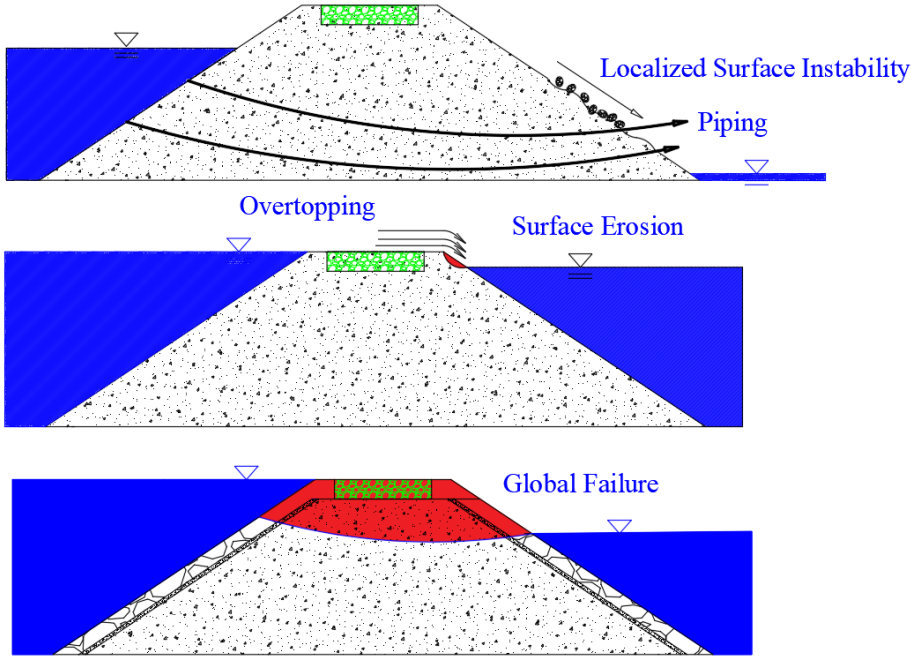

Figure 2.14: Testing process for Test 6

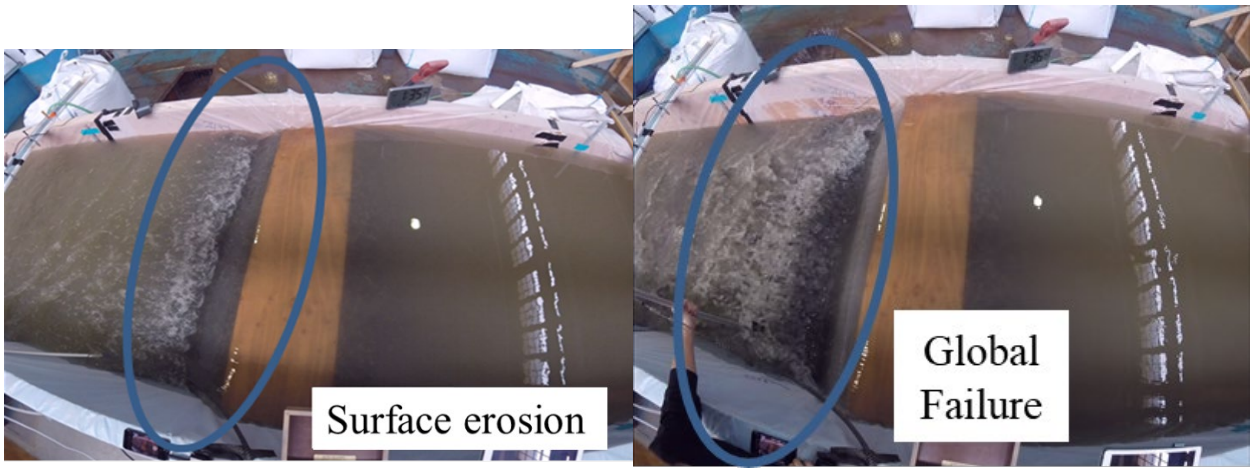

(a) (b)

Figure 2.15: (a) surface erosion at high flood, and (b) global failure when creating a high water head difference

8.6. TEST 7 - #8 EMBANKMENT NO REINFORCEMENT LARGE HEAD DIFFERENTIAL LOW VELOCITY

Test 7 was conducted with the embankment shown in Experimental Setup 1 with the approach slab present in the center (Figure 1.5). The downstream and upstream slopes were 1/1.5. The embankment was comprised of #8 coarse aggregates as the structural backfill. The embankment was incorrectly built with a reduced height of 21 in. tall. During the construction, #8 aggregate was gradually and slowly rained using shovels with no compaction. Shovels were lifted and kept at a constant height of approximately 16 in. above the surface. Surface of the embankment was trimmed and flatten using counter brush.

GoPros were setup on the downstream side and at the top of the embankment to record the test. The testing process is illustrated in Figure 2.16. At the beginning of the test, water was pumped into the water tank at a relatively low flow rate to gradually increase the water head on the upstream side. At the meantime, downstream water head was kept below 10 inches. Starting with no water and then letting it rise to 8 inches while maintaining a relatively low flow rate. Piping was observed when the flow rate was 0.49 CFS and the water height difference was 10 inches. This moment was 13 minutes into the test and the resulting upstream and downstream heights of: 18 and 8 inches. Slope failure was observed with a water height difference of 12.5 inches the upstream being 20.5 inches and the downstream was 8 inches. This happened 14 minutes into the experiment, when the flow rate was 0.53 – 0.55 CFS. Shortly after, global failure was reached it was at the overtopping moment at 14 minutes into the experiment (Figure 2.17 a and b). The water height difference was

a total of 13 inches due to the upstream being 21 inches and the downstream being 8 inches. The flow rate at global failure was 0.55 CFS and the max flow rate for this test was 0.62 CFS.

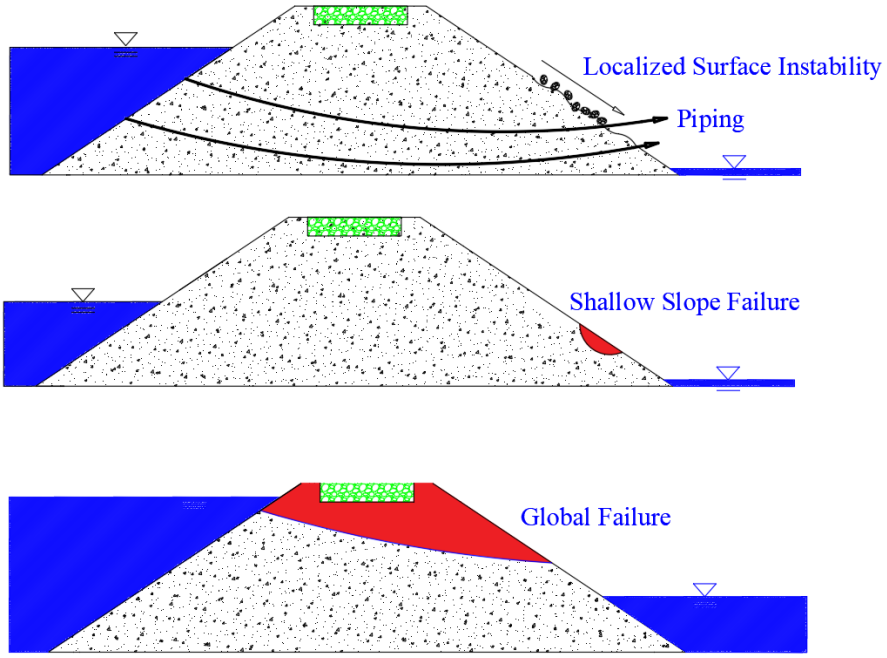

Figure 2.16: Testing process for Test 7

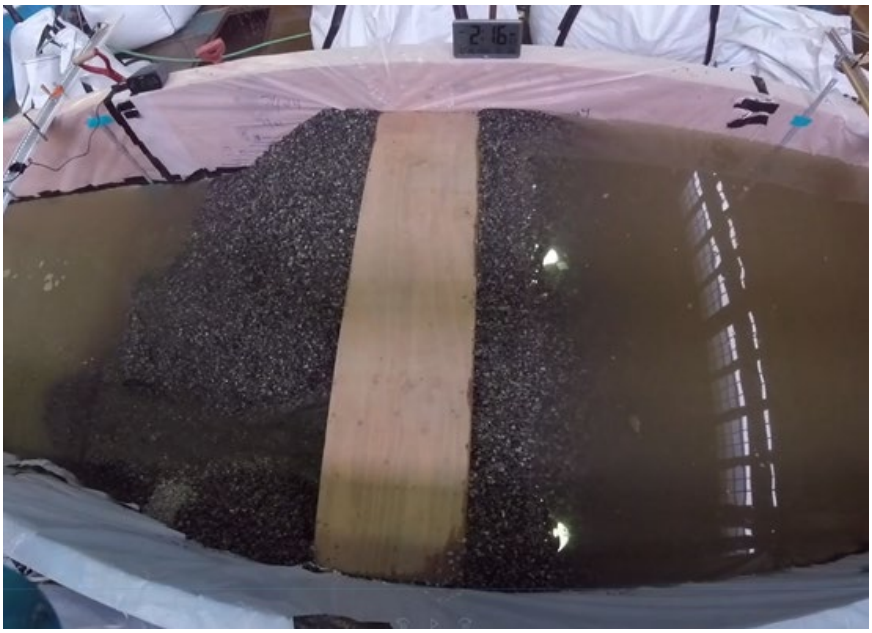

(a)

(b)

Figure 2.17: (a) at the overtopping from the top view, (b) global failure at the overtopping from the downstream view

8.7. TEST 8 - #8 EMBANKMENT NO REINFORCEMENT LARGE HEAD DIFFERENTIAL LOW VELOCITY

Test 8 was conducted with the embankment shown in Experimental Setup 1 with the approach slab present in the center Figure 1.5. The downstream and upstream slopes were 1/1.5. This test was a repeat of Test #7 with the embankment built in accordance with the detailed height of 27 in. The embankment was comprised of #8 coarse aggregates as the structural backfill. During the construction, #8 aggregate was gradually and slowly rained using shovels with no compaction. Shovels were lifted and kept at a constant height of approximately 16 in. above the surface. Surface of the embankment was trimmed and flattened using a brush.

GoPros were setup on the downstream side and at the top of the embankment to record the test. The testing process is illustrated in Figure 2.18. At the beginning of the test, water was pumped into the water tank at a relatively low flow rate (0.313 CFS) to gradually increase the water head on the upstream side. At the meantime, downstream water head was kept at around 1 inch. Piping was observed when the flow rate was 0.41 CFS and the water height difference was 9.5 inches. Slope failure was observed with a water height difference of 16.3 in. when the flow rate was 0.326-0.445 CFS. Shortly after, global failure was reached before the overtopping. The water height difference at failure was 20 inches due to the upstream being 21 inches and the downstream held constant at 1 inch. The flow rate at global failure was at 0.714 CFS.

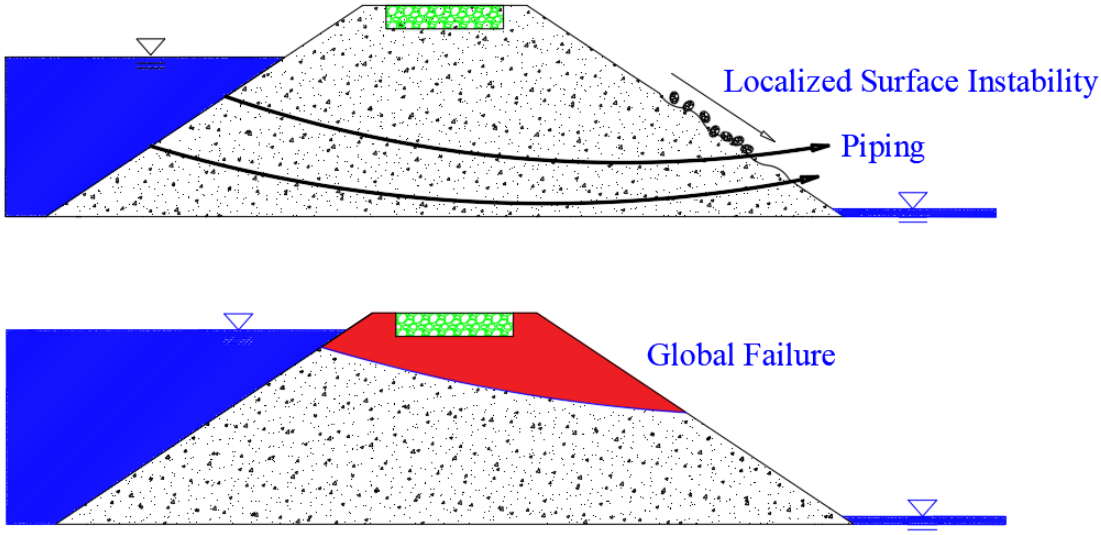

Figure 2.18: Testing process for Test 8

(a) (b)

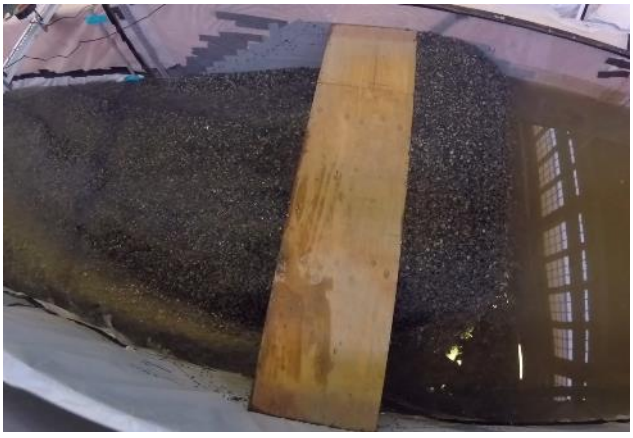

(c)

Figure 2.19: (a) Piping failure, (b) slope failure, and (c) global failure before overtopping from the top view

8.8. TEST 9 - #8 EMBANKMENT NO REINFORCEMENT WITH R-2 ROCK LINING SMALL HEAD DIFFERENTIAL

Test 9 was conducted with the embankment shown in Experimental Setup 1 with the approach slab present in the center (Figure 1.5). The downstream and upstream slopes were 1/1.5. The embankment was comprised of #8 coarse aggregates as the structural backfill. During the construction, #8 aggregate was gradually and slowly rained using shovels with no compaction. Shovels were lifted and kept at a constant height of approximately 16 in. above the surface. R-2 Rock lining were applied by hand and bucket on both upstream and downstream slopes to mitigate the surface erosion caused by seepage and overtopping. #57 coarse aggregates were applied between Rock lining and #8 coarse aggregates as a filter and cushion layer (Figure 2.21a).

GoPros were setup on the downstream side and at the top of the embankment to record the test. The testing process is illustrated in Figure 2.20. At the beginning of the test, water was pumped into the water tank at a relatively low flow rate (0.313 CFS) to gradually increase the water head on the upstream side. At the meantime, the downstream water head was held by baffle boards covered by the waterproof plastic sheet to keep the water head difference as low as possible. Piping and slope failure were not observed before overtopping. When it reached the overtopping, no failure was observed since there was no water head difference between upstream and downstream (Figure 2.21b). The flow rate was then increased up to 2.29 CFS and no failure happened. The flow velocity above the approach slab was measured as 0.88 ft/s. The downstream water head was then lowered by removing one of the baffle boards to create a 5 inches water head difference, and no failure was observed as well (Figure 2.21c). The downstream water head was furthered lowered to create an 8 inches water head difference, which lead to the global failure (Figure 2.21d).

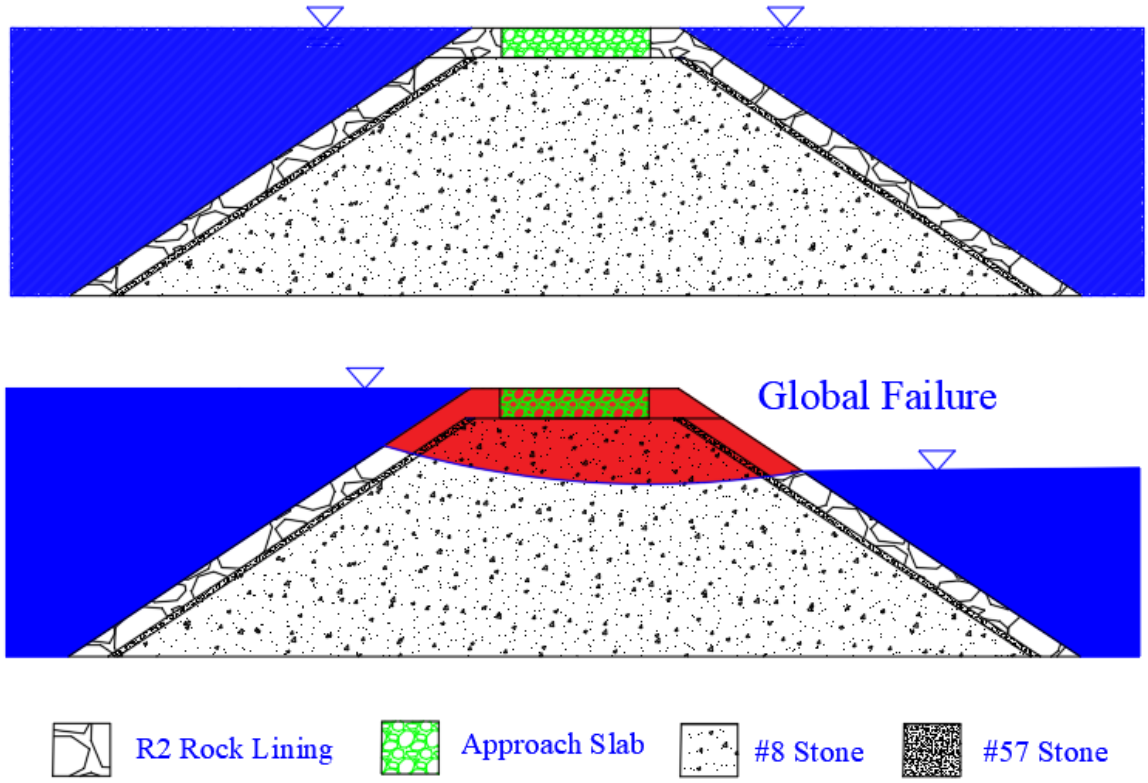

Figure 2.20 Testing process for Test 9

(a) (b)

(c) (d)

Figure 2.21 (a) embankment with R-2 Rock lining, #57 coarse aggregates and #8 coarse aggregates, (b) no failure at the overtopping, (c) no failure under high flood (2.29 CFS) at the water head difference of 5 inches, and (d) global failure at the water head difference of 8 inches from the top view

8.9. TEST 10 - #8 EMBANKMENT WITH R-2 ROCK LINING LARGE HEAD DIFFERENTIAL

Test 10 was conducted with the embankment shown in Experimental Setup 1 with the approach slab present in the center (Figure 1.5). The downstream and upstream slopes were 1/1.5. The embankment was comprised of #8 coarse aggregates as the structural backfill. During the construction, #8 aggregate was gradually and slowly rained using shovels with no compaction. Shovels were lifted and kept at a constant height of approximately 16 in. above the soil surface. R-2 Rock lining were applied by hand and bucket on both upstream and downstream slopes to mitigate the surface erosion caused by seepage and overtopping. The filter layer of #57 coarse aggregates between Rock lining and #8 coarse aggregates was given up because of the construction difficulty in separating the #8 and #57 coarse aggregates after test.

GoPros were setup on the downstream side and at the top of the embankment to record the test. The testing process is illustrated in Figure 2.22. At the beginning of the test, water was pumped into the water tank at a relatively low flow rate (0.265 CFS) to gradually increase the water head on the upstream side. The downstream water head was kept consistently under 2 inches. Piping and slope failure were not observed before overtopping due to the Rock lining reinforced slope (Figure 2.23a). The overtopping moment was met by slope failure at a water height difference of 22.5 inches the upstream being 24.5 inches and the downstream was 2 in. when the flow rate was 0.77-0.94 CFS (Figure 2.23b). Shortly after, global failure was reached when the flow rate was increased to 1.1-1.4 CFS (Figure 2.23c).

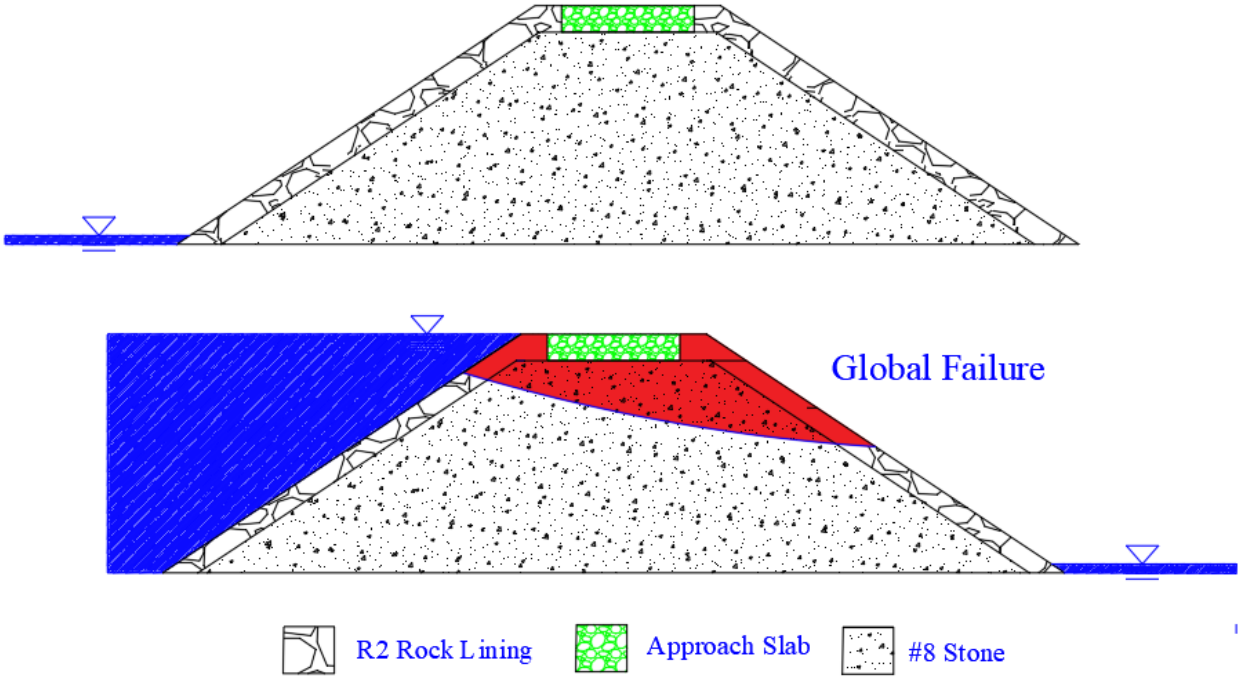

Figure 2.22: Testing process for Test 10

(a) (b)

(c) (d)

Figure 2.23: (a) no failure before the overtopping, (b) slope failure at the overtopping, (c) global failure from the top view, and (d) from downstream view

8.10. TEST 11 – EMBANKMENT WITH EXTRA GEOSYNTHETIC REINFORCEMENT AND #8 LINING

Test 11 was conducted with the embankment shown in Experimental Setup 1 with the approach slab present in the center (Figure 1.5). The downstream and upstream slopes were 1/1.5. The embankment was comprised of #8 coarse aggregates as the structural backfill. The core part of the embankment was heavily reinforced by the Geosynthetics system, including the Geogrid and Geotextile. The embankment was divided into 9 layers in the height direction, and each layer was about 2.75 in. tall. Every backfill layer was wrapped by Geotextile through the bottom to the top with a 1-feet overlap between each layer. Geogrid was applied to wrap every 3 layers of the backfill outside the Geotextile. #8 coarse aggregates were applied outside of the Geosynthetics-reinforced core part of the embankment to achieve the slope of 1/1.5. Details are shown in Figure 2.24.

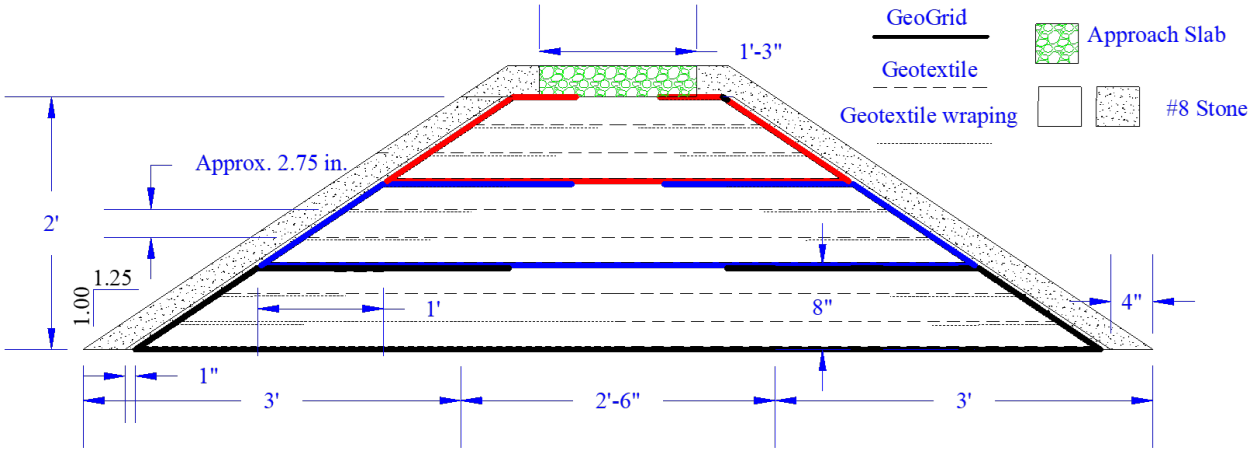

Figure 2.24: Embankment heavily reinforced by Geosynthetics

GoPros were setup on the downstream side and at the top of the embankment to record the test. The testing process is illustrated in Figure 2.50. At the beginning of the test, water was pumped into the water tank at a relatively low flow rate (0.37 CFS) to gradually increase the water head on the upstream side. The downstream water head was held constant at 1 inch. Piping was observed during this experiment at a water height difference of 10 inches and a flow rate of 0.37 CFS. The downstream height was 1 inch and the upstream was 11 inches. Slope failure occurred before overtopping when the water head difference was 16 inches at the flow rate of 0.37 CFS (Figure 2.26a). Further slope failure was observed at the overtopping at a water height difference of 24.5when the flow rate was 0.57-0.60 CFS (Figure 2.26b). The flow rate was increased up to 3.5 CFS, global failure was not reached which is attributed to the reinforcement of the Geosynthetics,

but the entire outside #8 coarse aggregate slope without reinforcement was eroded under the extreme flood (Figure 2.26c). The water height difference was a total of 26.5 inches with the upstream being 27.5 inches and the downstream at 1 inch.

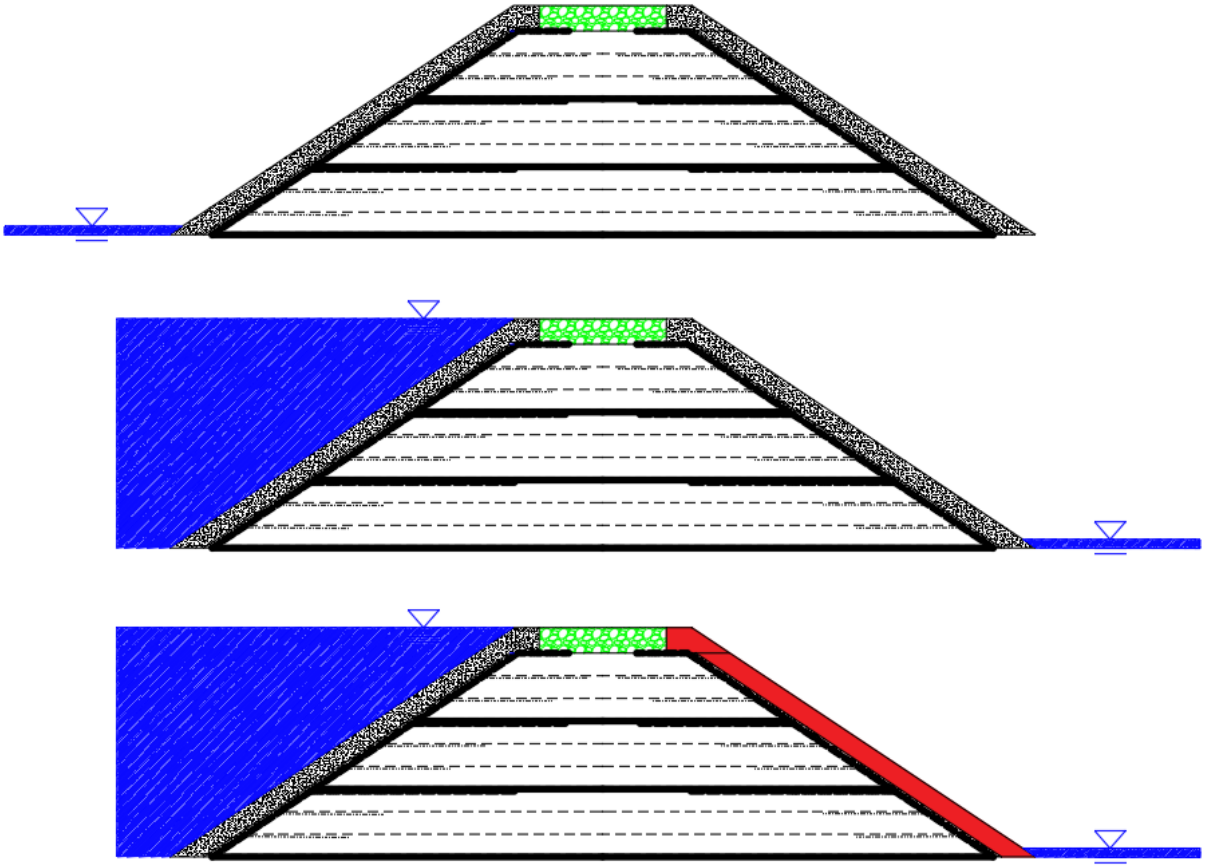

Figure 2.25: Testing process for Test 11

(a) (b)

(c)

Figure 2.26: (a) Surface slope failure initiated, (b) surface slope failure at the overtopping, (c) surface layer of #8 coarse aggregates were fully eroded but core part of the embankment wrapped by Geosynthetics was stable under the extreme flow, and (d) the embankment when the test was over

8.11. TEST 12 – EMBANKMENT WITH HEAVY GEOSYNTHETIC REINFORCEMENT AND R2 ROCK LINING

Test 12 was conducted with the embankment shown in Experimental Setup 1 with the approach slab present in the center (Figure 1.5). The downstream and upstream slopes were 1/1.25. The

embankment was comprised of #8 coarse aggregates as the structural backfill. The core part of the embankment was heavily reinforced by the Geosynthetics system, including the Geogrid and Geotextile. The embankment was divided into 9 layers in the height direction, and each layer was about 2.75 inches' tall. Every backfill layer was wrapped by Geotextile through the bottom to the top with a 1-feet overlap between each layer. Geogrid was applied to wrap every 3 layers of the backfill outside the Geotextile. R-2 Rock lining were applied outside of the Geosynthetics-reinforced core part of the embankment to achieve the slope of 1/1.25. #8 coarse aggregates were applied as a filter and cushion layer between Rock lining layer and the reinforced core part. Details are shown in Figure 2.27.

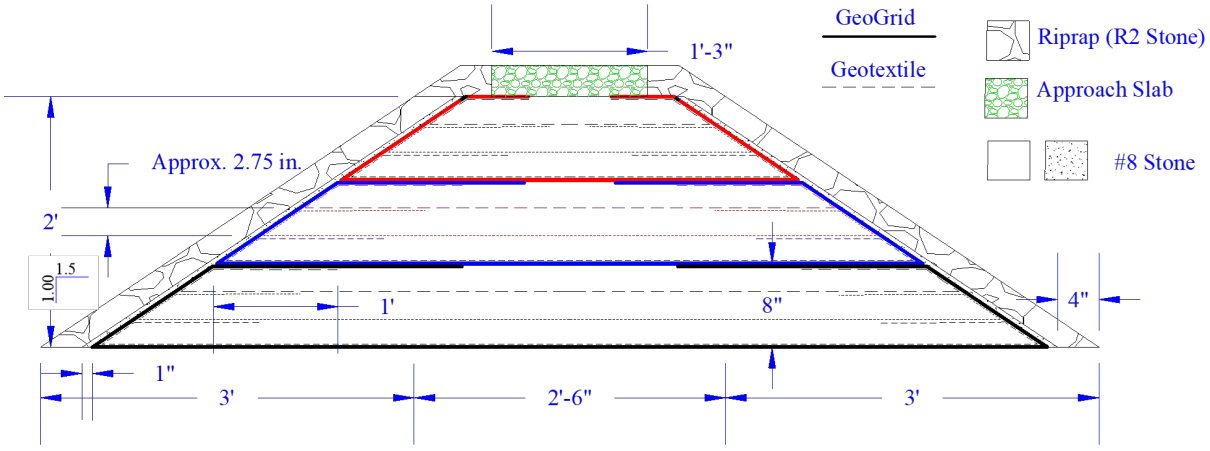

Figure 2.27: Embankment heavily reinforced by Geosynthetics and Rock lining

GoPros were setup on the downstream side and at the top of the embankment to record the test. The testing process is illustrated in Figure 2.28. At the beginning of the test, water was pumped into the water tank at a relatively low flow rate (0.285 CFS) to gradually increase the water head on the upstream side. The downstream water head was held constant at around 1 inch. No piping and slope failure were observed before and at the overtopping. Slope failure was observed after the overtopping at a water height difference of 22 inches when the flow rate was up to 0.838 CFS (Figure 2.26b). The flow rate was increased up to 3.6 CFS, global failure was not reached, which is attributed to the reinforcement of the Geosynthetics, but the entire outside R-2 Rock lining slope was eroded under the extreme flood (Figure 2.26c). The water height difference was a total of 28.5 inches with the upstream being 29.5 inches and the downstream at 1 inch.

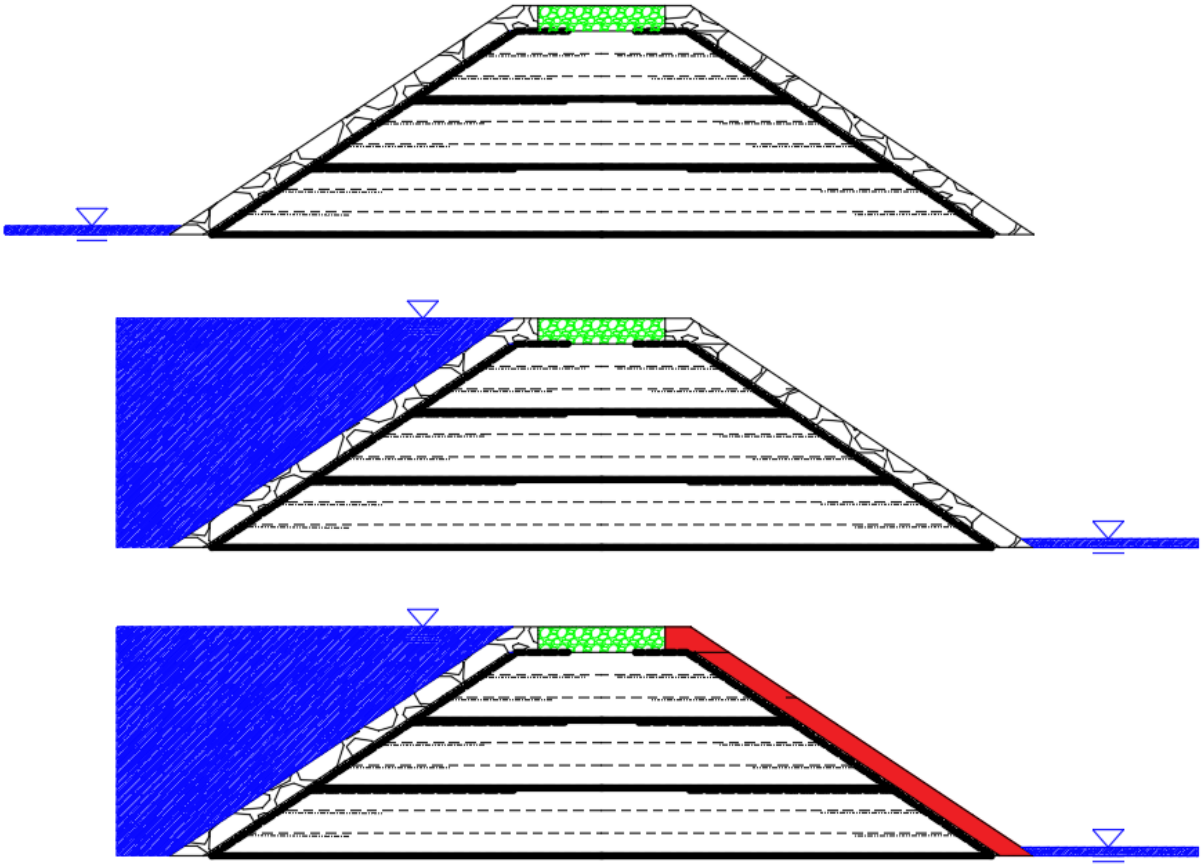

Figure 2.28: Testing process for Test 12

(a) (b)

(c)

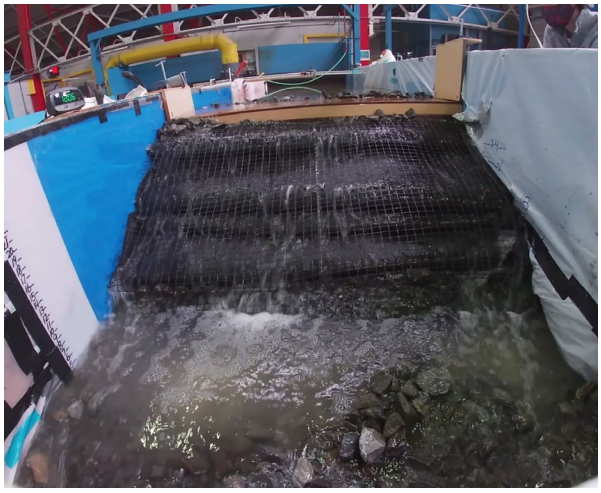

(d)

Figure 2.29: (a) No failure at the overtopping, (b) slope failure after overtopping under high flood, (c) at the maximum flow rate (3.6 CFS), surface Rock lining were eroded, core part of embankment reinforced by Geosynthetics stayed safe, and (d) the embankment when the test was over

8.12. Test 13 - Embankment with Heavy Geosynthetic Reinforcement and R2 Rock Lining, Small Water Head Difference

Test 13 was conducted with the embankment shown in Experimental Setup 1 with the approach slab present in the center (Figure 1.5). The downstream and upstream slopes were 1/1.25. The embankment was comprised of #8 coarse aggregates as the structural backfill. The core part of the embankment was heavily reinforced by the Geosynthetics system, including the Geogrid and Geotextile. The embankment was divided into 9 layers in the height direction, and each layer was about 2.75 inches' tall. Every backfill layer was wrapped by Geotextile through the bottom to the top with a 1-feet overlap between each layer. Geogrid was applied to wrap every 3 layers of the backfill outside the Geotextile. R-2 Rock lining were applied outside of the Geosynthetics-

reinforced core part of the embankment to achieve the slope of 1/1.25. #8 coarse aggregates were applied as a filter and cushion layer between Rock lining layer and the reinforced core part. Details are shown in Figure 2.27.

GoPros were setup on the downstream side and at the top of the embankment to record the test. The testing process is illustrated in Figure 2.30. At the beginning of the test, water was pumped into the water tank at a relatively low flow rate (0.33 CFS) to gradually increase the water head on the upstream side. At the meantime, the downstream water head was held by baffle boards covered by the waterproof plastic sheet to keep the water head difference as low as possible. Piping and slope failure were not observed before overtopping. When it reached the overtopping, no failure was observed since there was no water head difference between upstream and downstream. The flow rate was then increased to 1.85 CFS and the water head difference was increased to 4 inches. Still no failure was observed (Figure 2.31a). After that, the flow rate was increased up to 3.5 CFS, and the water head difference was increased to 25 inches, global failure was not reached, which is attributed to the reinforcement of the Geosynthetics, but the entire outside R-2 Rock lining slope was eroded under the extreme flood (Figure 2.31b).

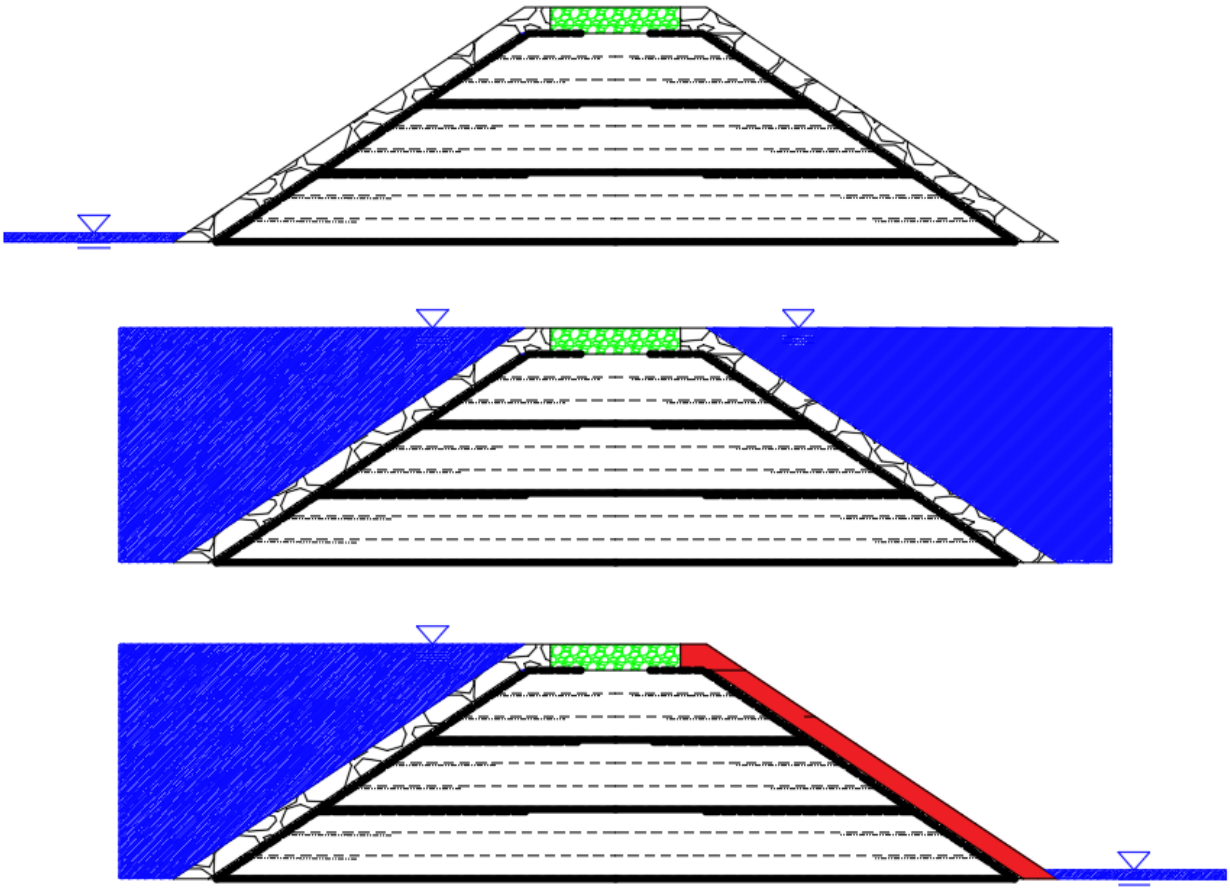

Figure 2.30: Testing process for Test 13

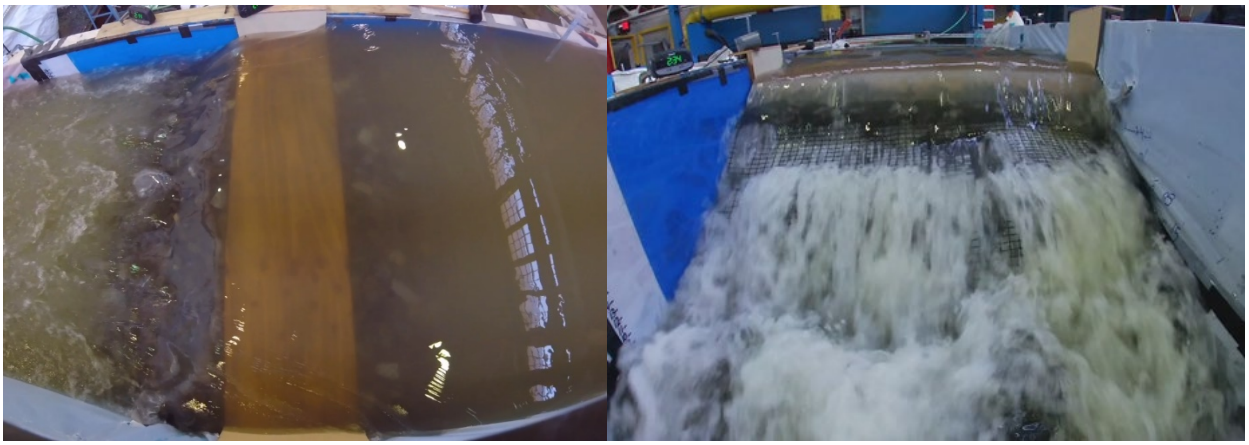

(a) (b)

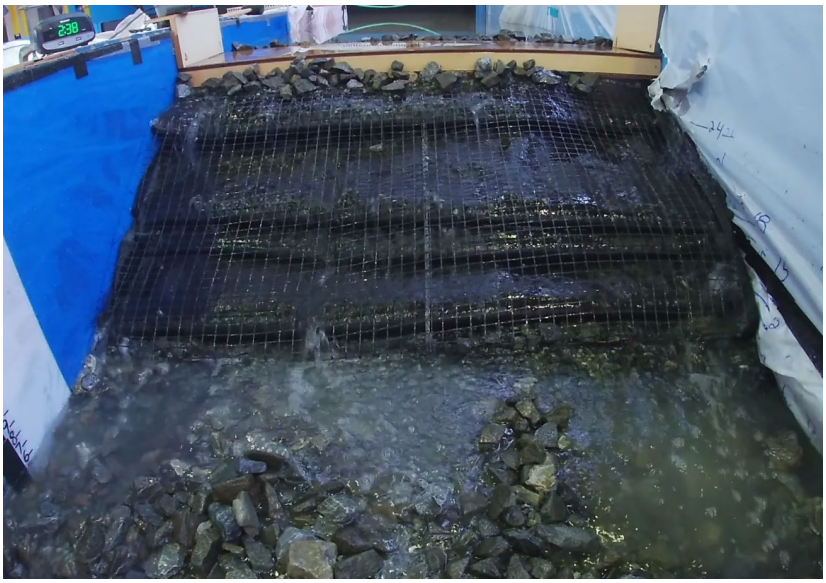

(c)

Figure 2.31: (a) no failure at the small water head difference under high flood, (b) surface Rock lining were eroded at the maximum flow rate (3.5 CFS) when the water head difference is high, core part of embankment reinforced by Geosynthetics stayed safe, and (c) the embankment when the test was over

8.13. Test 14 Embankment with Poorly Placed Geosynthetic Reinforcement and R2 Rock Lining

Test 14 was conducted with the embankment shown in Experimental Setup 1 with the approach slab present in the center (Figure 1.5). The downstream and upstream slopes were 1/1.25. The embankment was comprised of #8 coarse aggregates as the structural backfill. The core part of the embankment was reinforced by the Geosynthetics system, including the Geogrid and Geotextile with a modified wrapping scenario, which is different from the Test 11-13. The embankment was divided into 4 layers in the height direction, and each layer was approximately 6 in. tall.

Two pieces of Geotextile (one whole piece with continuation on the bottom in Test 11-13), one at the downstream side, another at the upstream side were applied together to wrap two layers of the backfills. There was another layer of Geotextile, which was placed at the middle of each backfill layer without wrapping. For the bottom wrapped backfill layer, the Geotextile wrapping length on upstream and downstream sides were both around 2 feet at the top and the bottom of the backfill layer. For the top wrapped backfill layer, the wrapping length below the approach slab was 6.5 in. on both sides, and there was no overlap between upstream and downstream sides. Geogrid was applied every two layers including the layer at the top of the backfill under the approach slab. However, Geogrid was only placed between each backfill layers outside of the Geotextile without wrapping. R-2 Rock lining were applied outside of the Geosynthetics-reinforced core part of the embankment to achieve the slope of 1/1.25. #8 coarse aggregates were applied as a filter and cushion layer between Rock lining layer and the reinforced core part. Details are shown in Figure 2.32.

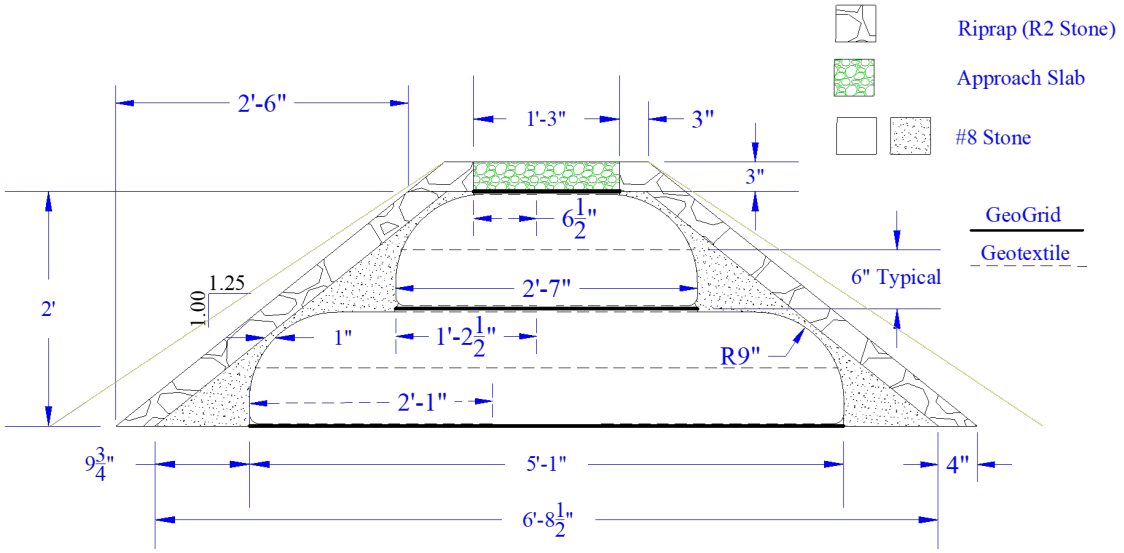

Figure 2.32: Embankment reinforced by Geosynthetics (modified wrapping) and Rock lining

GoPros were setup on the downstream side and at the top of the embankment to record the test. The testing process is illustrated in Figure 2.33. At the beginning of the test, water was pumped into the water tank at a relatively low flow rate (0.489 CFS) to gradually increase the water head on the upstream side. The downstream water head was held constant at around 1 inch. Slope failure was observed before overtopping at the water head difference of 21 inches when the flow rate was at 1.1 CFS (Figure 2.34a). Further slope failure occurred at the overtopping at the water height difference of 21 inches. The flow rate was then increased up to 2 CFS, global failure was reached due to the unwrapping of the top layer Geotextile (Figure 2.34b).

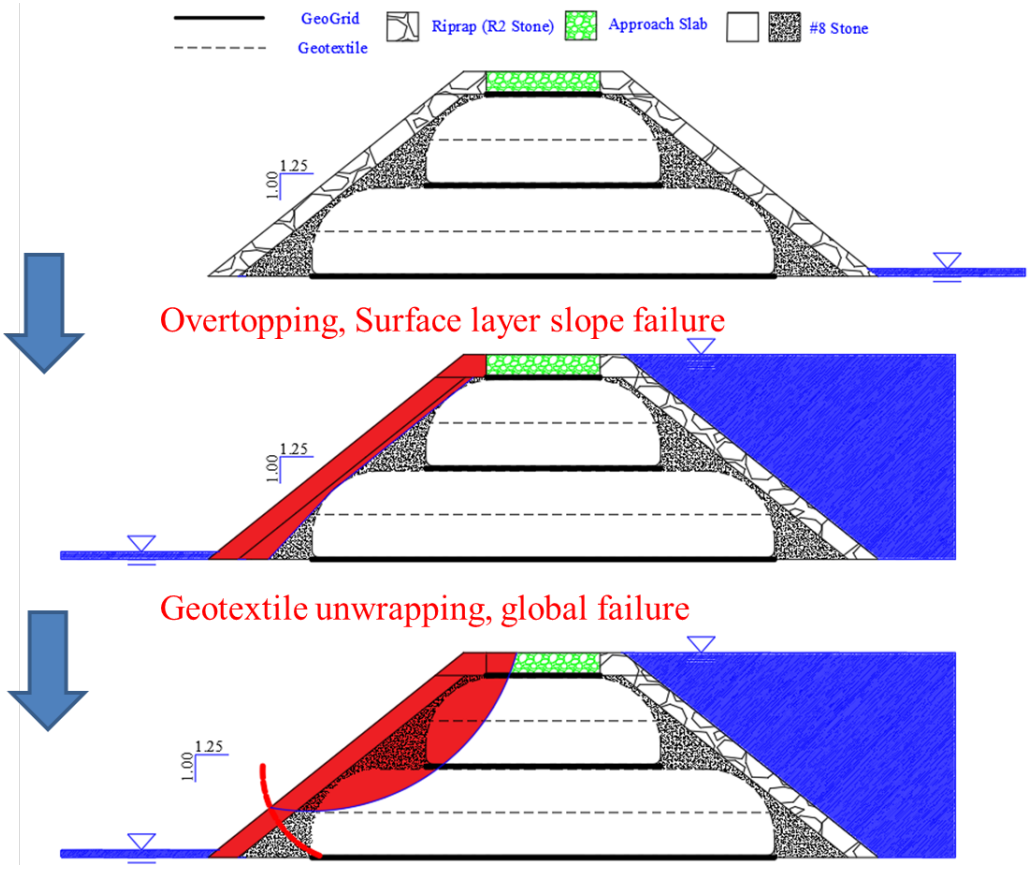

Figure 2.33: Testing process for Test 14

(a) (b)

Figure 2.34: (a) Slope failure before overtopping, (b) top layer Geotextile unwrapping, and (c) the embankment when the test was over

8.14. TEST 15 EMBANKMENT WITH IMPROVED GEOSYNTHETIC REINFORCEMENT WITH OVERLAP AND R2 ROCK LINING

Test 15 was conducted with the embankment shown in Experimental Setup 1 with the approach slab present in the center (Figure 1.5). The downstream and upstream slopes were 1/1.25. The embankment was comprised of #8 coarse aggregates as the structural backfill. The core part of the embankment was reinforced by the Geosynthetics system, including the Geogrid and Geotextile with an improved wrapping scenario based on the experience from Test 14. The embankment was divided into 4 layers in the height direction, and each layer was about 6 inches' tall.

Two pieces of Geotextile (one whole piece with continuation on the bottom in Test 11-13), one at the downstream side, another at the upstream side were applied together to wrap two layers of the backfills. There was another layer of Geotextile, which was placed at the middle of each backfill layer without wrapping. For the bottom wrapped backfill layer, the Geotextile wrapping length on upstream and downstream sides were both around 2 feet at the bottom and top of the backfill layer. For the top of the bottom wrapped backfill layer, the Geotextile at the downstream side was placed below the Geotextile at the upstream side with an overlap. For the top wrapped backfill layer, the wrapping length below the approach slab was around 15 in. on both sides. The Geotextile at the downstream side was placed below the Geotextile at the upstream side with a 15 in. overlap. Geogrid was applied every two layers including the layer at the top of the backfill under the

approach slab. R-2 Rock lining were applied outside of the Geosynthetics-reinforced core part of the embankment to achieve the slope of 1/1.25. #8 coarse aggregates were applied as a filter and cushion layer between Rock lining layer and the reinforced core part. Details are shown in Figure 2.50.

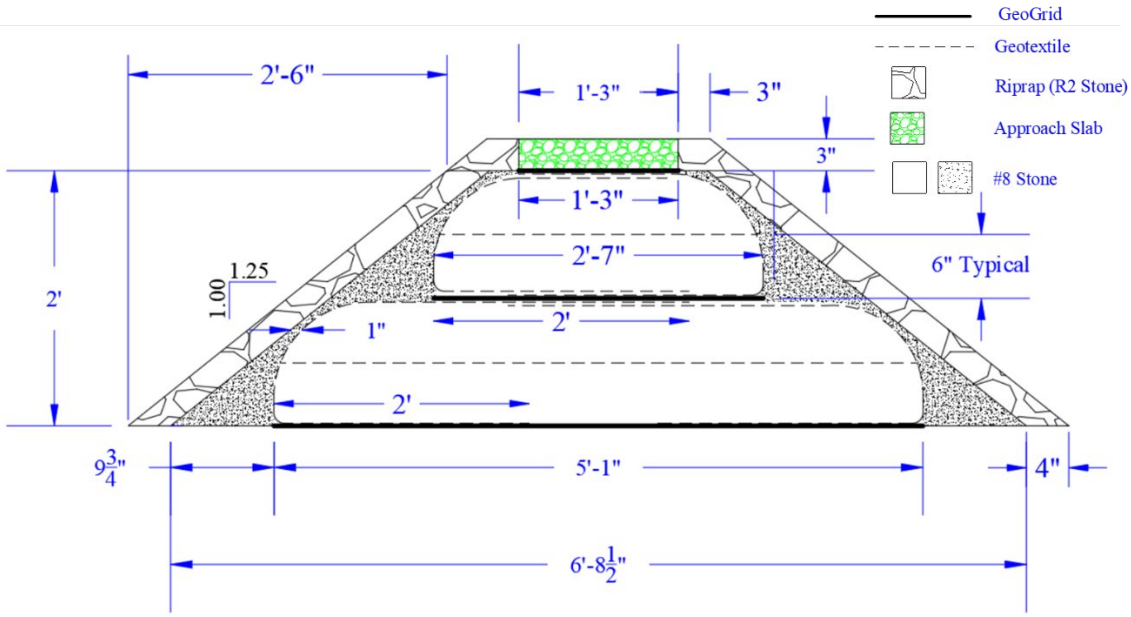

Figure 2.35: Embankment reinforced by Geosynthetics (improved wrapping) and Rock lining

GoPros were setup on the downstream side and at the top of the embankment to record the test. The testing process is illustrated in Figure 2.36. At the beginning of the test, water was pumped into the water tank at a relatively low flow rate (0.283 CFS) to gradually increase the water head on the upstream side. The downstream water head was held constant at around 1~3 inch. No piping and slope failure were observed before and at the overtopping. Slope failure was observed after the overtopping at a water height difference of 22 inches when the flow rate was up to 1.65 CFS (Figure 2.37 a and b). The flow rate was increased up to 3.2 CFS, global failure was not reached, which is attributed to the reinforcement of the Geosynthetics, but the entire outside R-2 Rock lining slope and #8 coarse aggregates cushion layer were eroded under the extreme flood (Figure 2.37c). The water height difference was a total of 22.5 inches.

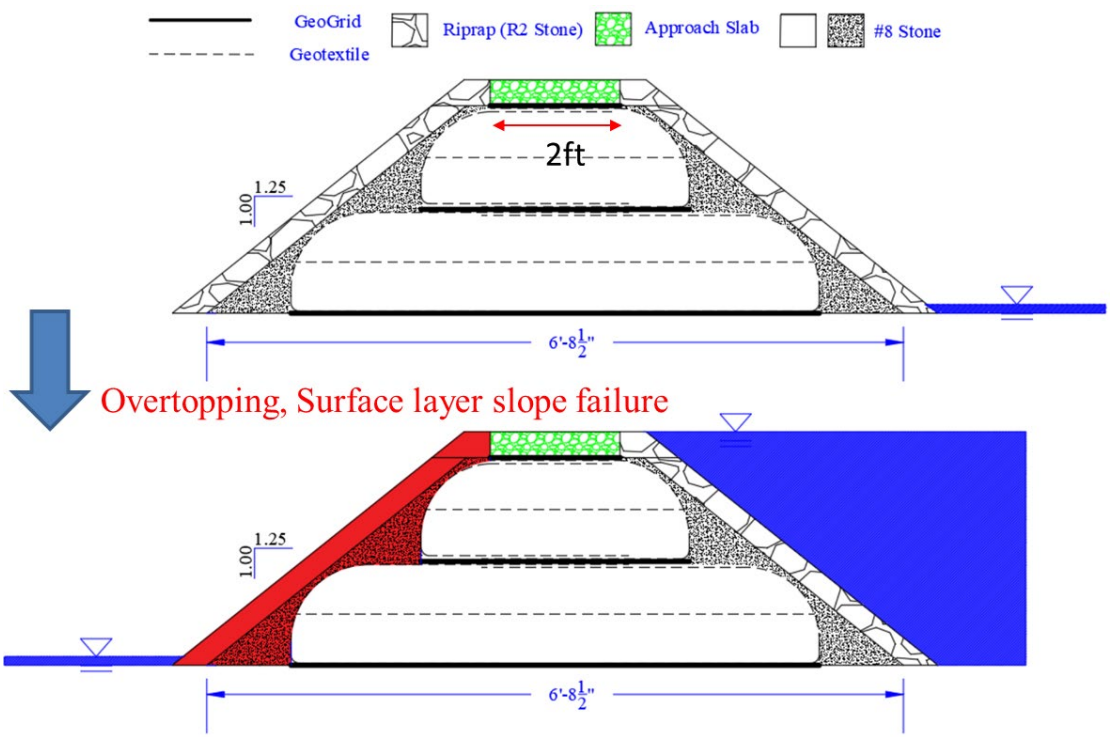

Figure 2.36: Testing process for Test 15

(a) (b)

(c)

Figure 2.37: (a) Slope failure after overtopping, (b) Slope failure under extreme flood, and (c) surface Rock lining and #8 coarse aggregates were eroded at the maximum flow rate (3.2 CFS) when the water head difference is high, core part of embankment reinforced by Geosynthetics stayed safe

8.15. TEST 16 – CONTINUATION OF TEST 15 WITH APPROACH SLAB REMOVED

Test 16 was the continuation of the Test 15. Approach slab was removed after Test 15 to investigate the erosion mechanism of the Geotextile wrapped top layer without the confinement of the approach slab (Figure 2.39a). The testing process is illustrated in Figure 2.38. At the beginning of the test, water was pumped into the water tank at a relatively low flow rate to gradually increase the water head on the upstream side. The downstream water head was held constant at around 1~3 inch. The overtopping was then achieved and the flow rate was increased up to 3.3 CFS. The Geotextile wrapped layers stayed well and no unwrapping was observed (Figure 2.39b).

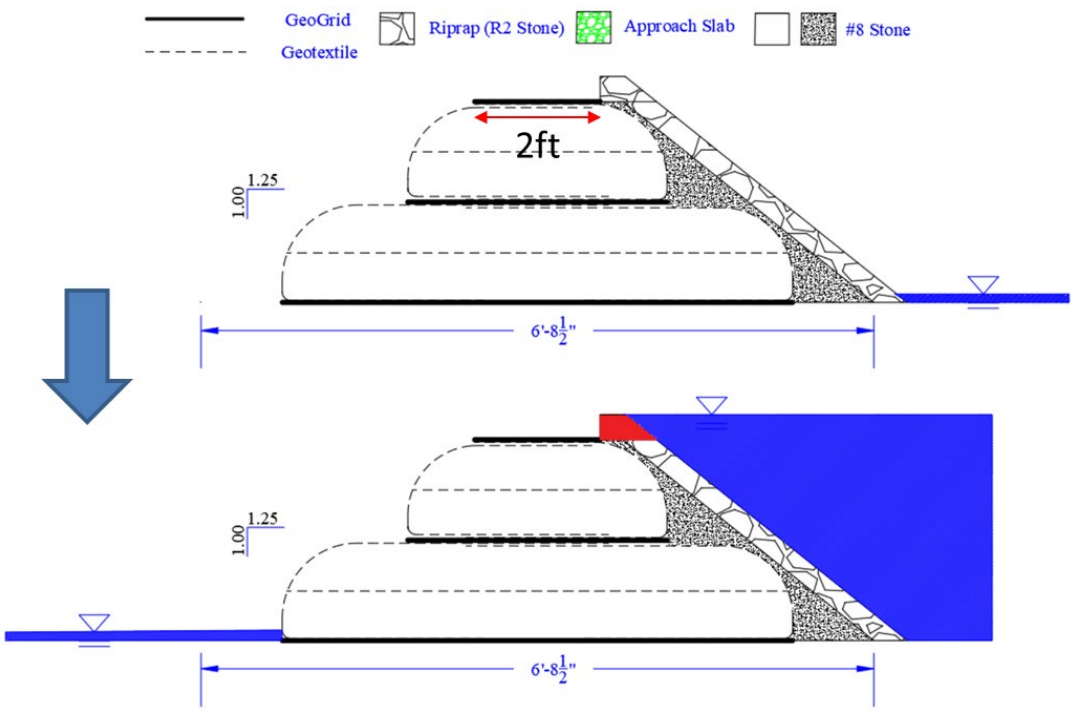

Figure 2.38: Testing process for Test 16

(a) (b)

Figure 2.39: (a) The approach was removed after Test 15, (b) Geosynthetics reinforced core part of the embankment stayed safe under the extreme flood

8.16. TEST 17 - EMBANKMENT WITH IMPROVED GEOSYNTHETIC REINFORCEMENT WITHOUT OVERLAP AND R2 ROCK LINING

Test 17 was conducted with the embankment shown in Experimental Setup 1 with the approach slab present in the center (Figure 1.5). The downstream and upstream slopes were 1/1.25. The embankment was comprised of #8 coarse aggregates as the structural backfill. The core part of the embankment was reinforced by the Geosynthetics system, including the Geogrid and Geotextile with an improved wrapping scenario without overlap at the bottom wrapped layer and the top wrapped layer under the approach slab (Figure 2.40). The length of the embankment was enlarged

to around 10 ft long to achieve the target of no overlap (Figure 2.41). The embankment was divided into 4 layers in the height direction, and each layer was about 6 inches' tall (Figure 2.43a).

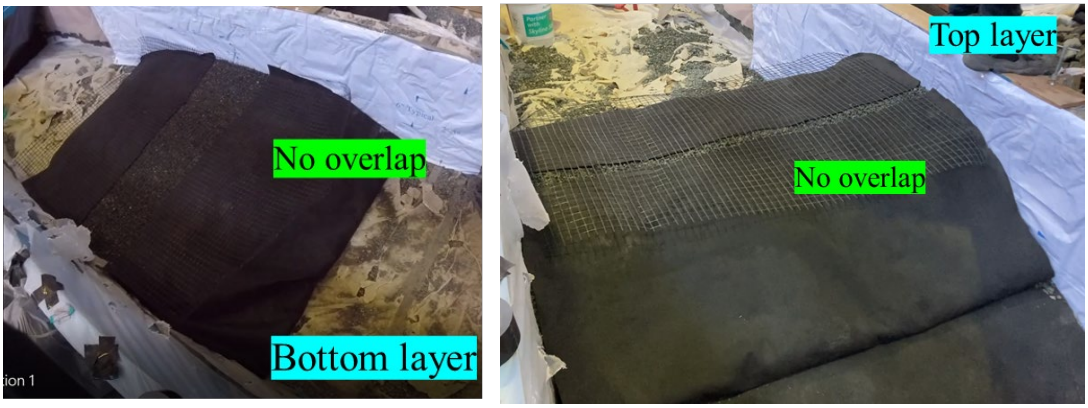

Figure 2.40: No overlap at the bottom and top wrapped layers

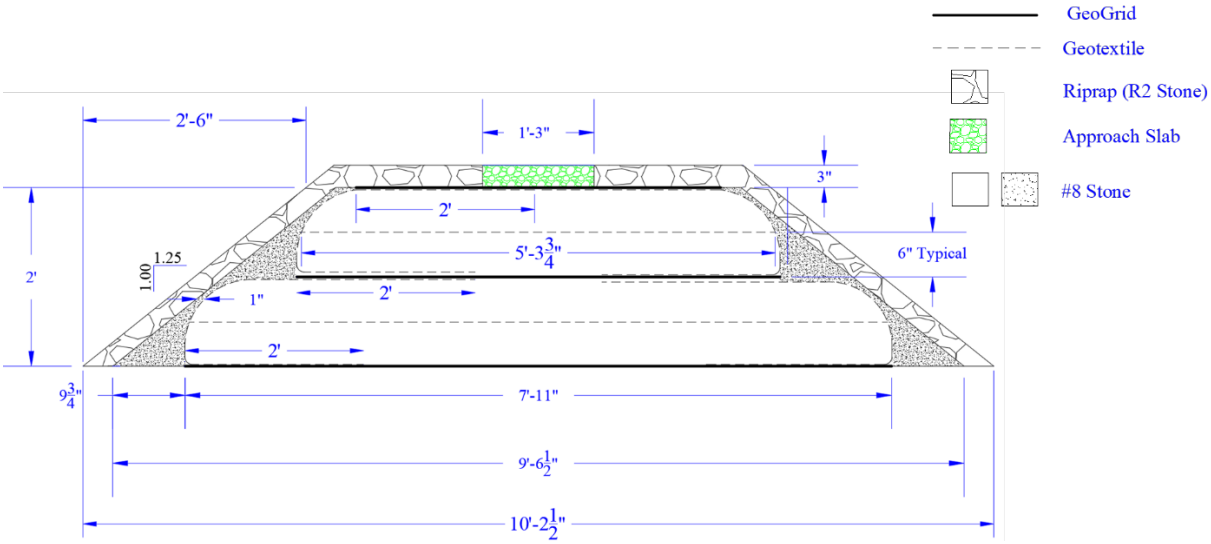

Figure 2.41: Enlarged embankment reinforced by Geosynthetics (improved wrapping without overlap on the top wrapped layer under the approach slab) and Rock lining

Two pieces of Geotextile (one whole piece with continuation on the bottom in Test 11-13), one at the downstream side, another at the upstream side were applied together to wrap two layers of the backfills. There was another layer of Geotextile, which was placed at the middle of each backfill layer without wrapping. For the bottom wrapped backfill layer, the Geotextile wrapping length on upstream and downstream sides were both around 2 feet at the bottom and top of the backfill layer. For the top wrapped backfill layer, the wrapping length below the approach slab was 2 ft on both sides. Geogrid was applied every two layers including the layer at the top of the backfill under the approach slab. R-2 Rock lining were applied outside of the Geosynthetics-reinforced core part of the embankment to achieve the slope of 1/1.25. #8 coarse aggregates were applied as a filter and cushion layer between Rock lining layer and the reinforced core part. Details are shown in Figure 2.41.

GoPros were setup on the downstream side and at the top of the embankment to record the test. The testing process is illustrated in Figure 2.42. At the beginning of the test, water was pumped into the water tank at a relatively low flow rate (0.265 CFS) to gradually increase the water head on the upstream side. The downstream water head was held constant at around 1~3 inch. No piping and slope failure were observed before and at the overtopping. Slope failure was observed after the overtopping at a water height difference of 23 inches when the flow rate was up to 1.832 CFS (Figure 2.43b and c). The flow rate was increased up to 3.3 CFS, global failure was not reached, which is attributed to the reinforcement of the Geosynthetics, but the entire outside R-2 Rock lining slope and #8 coarse aggregates cushion layer were eroded under the extreme flood (Figure 2.43d). The water height difference was a total of 25.5 inches.

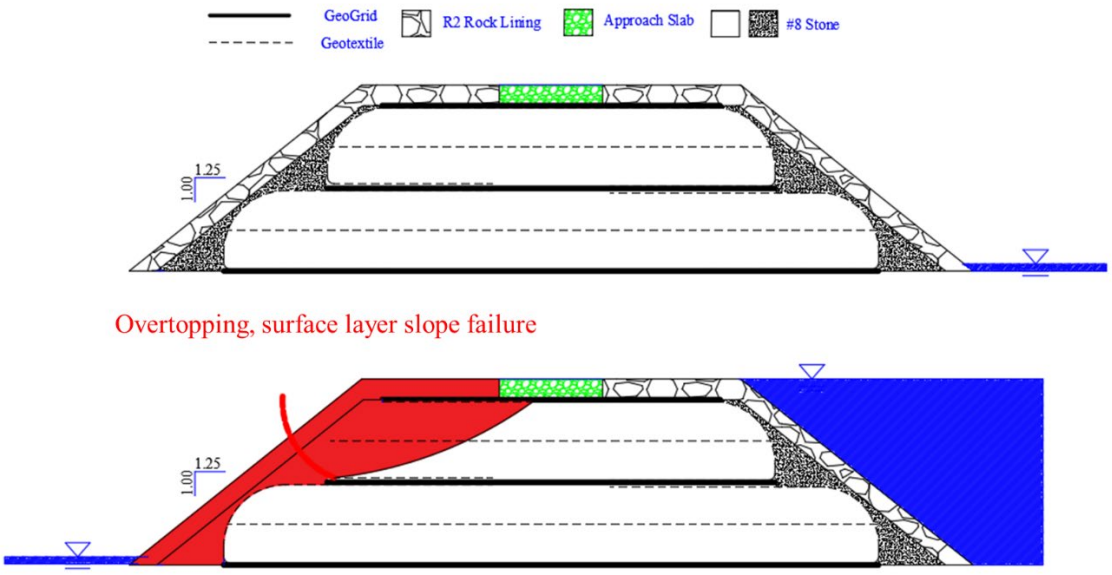

Figure 2.42: Testing process for Test 17

(a) (b)

(c) (d)

Figure 2.43: (a) Enlarged embankment, (b) Slope failure after overtopping, (c) Surface erosion under high flood, and (d) Geosynthetics reinforced core part of the embankment stayed safe under the extreme flood

8.17. TEST 18 – CONTINUATION OF TEST 17 WITH APPROACH SLAB REMOVED

Test 18 was the continuation of the Test 17. Approach slab was removed after Test 17 to investigate the erosion mechanism of the Geotextile wrapped top layer (no overlap) without the confinement of the approach slab (Figure 2.45a). The testing process is illustrated in Figure 2.44. At the beginning of the test, water was pumped into the water tank at a relatively low flow rate to gradually increase the water head on the upstream side. The downstream water head was held constant at around 1~3 inch. The overtopping was then achieved and the flow rate was increased up to 3.3 CFS. Since there was no confinement of the approach slab, the unwrapping of the Geotextile initiated after overtopping (Figure 2.45b). The red dash line in Figure 2.45b represents the unwrapping of the top layer Geotextile under the water flow after overtopping. The red area represents the erosion of the top layer #8 aggregate at the downstream side of the embankment after overtopping since there was no reinforcement after the top layer Geotextile was unwrapped (Figure 2.45c).

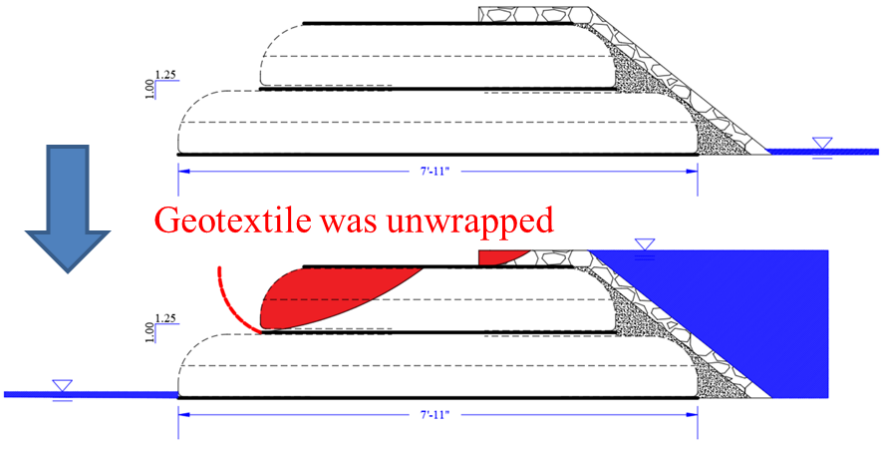

Figure 2.44: Testing process for Test 18

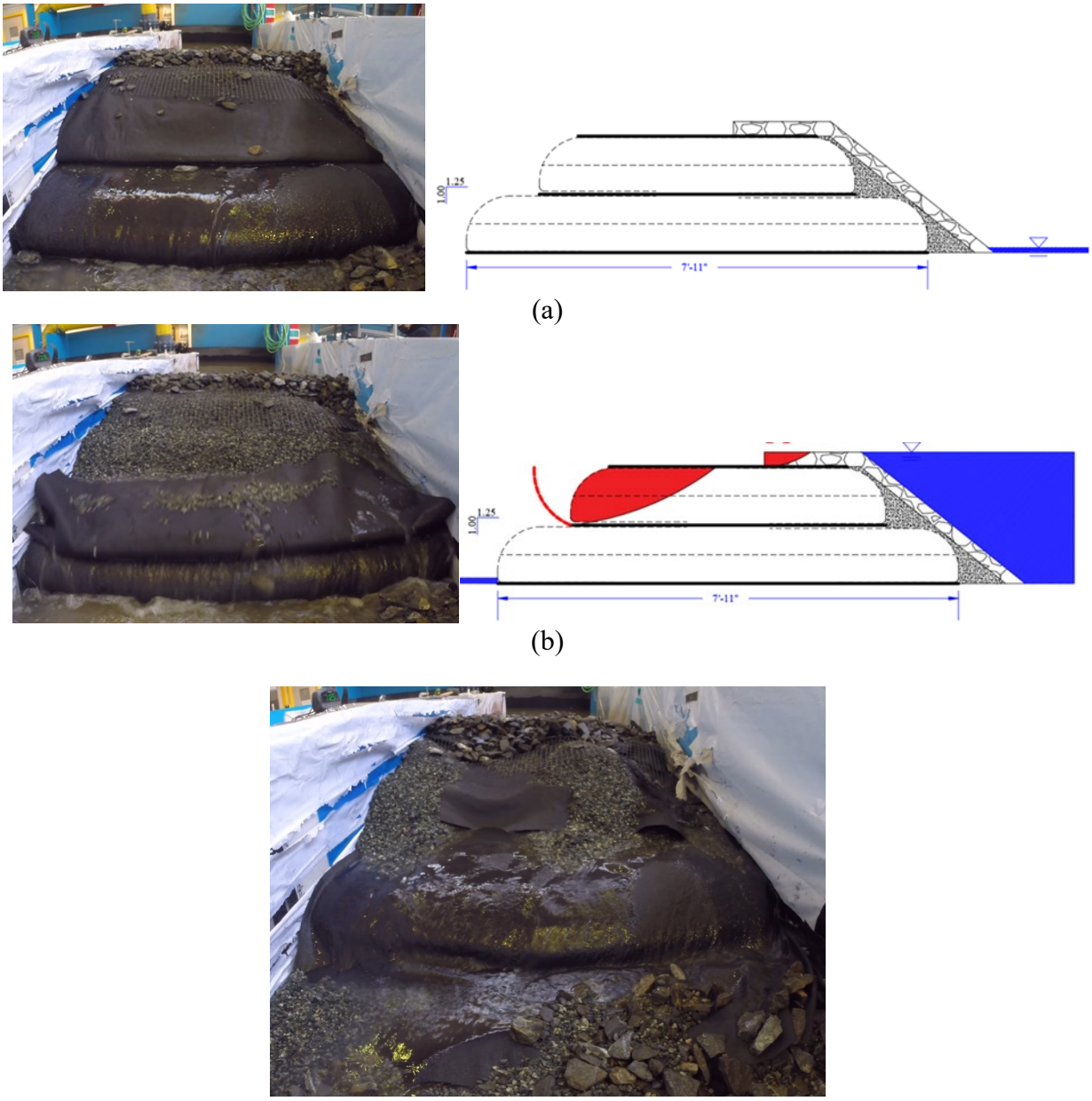

Figure 2.45: (a) The approach was removed after Test 17, (b) top layer Geotextile was unwrapped, and (c) top layer backfill materials were eroded under high flood

8.18. TEST 19 - LARGER EMBANKMENT WITH WING WALL WITH POORLY PLACED GEOSYNTHETIC REINFORCEMENT AND R2 ROCK LINING WITH BRIDGE OPENING

Test 19 was conducted with the larger embankment with the wingwall next to the bridge abutment (Figure 1.6). The bridge opening was left open throughout the experiment. #8 coarse aggregates were used as the structural backfill. The downstream and upstream slopes were 1.25/1. During the construction, #8 aggregate was gradually and slowly rained using shovels with no compaction.

Shovels were lifted and kept at a constant height of approximately 16 in. above the soil surface. Rock lining were applied to protect the slope. The core part of the embankment was reinforced by the Geosynthetics, including the Geogrid and Geotextile with an improved wrapping scenario without overlap at the bottom wrapped layer and the top wrapped layer under the approach slab. Details are shown in Figure 2.46. The backfills at the corner of the wingwall were wrapped with the separate edge wrapping pieces as shown in Figure 2.47.

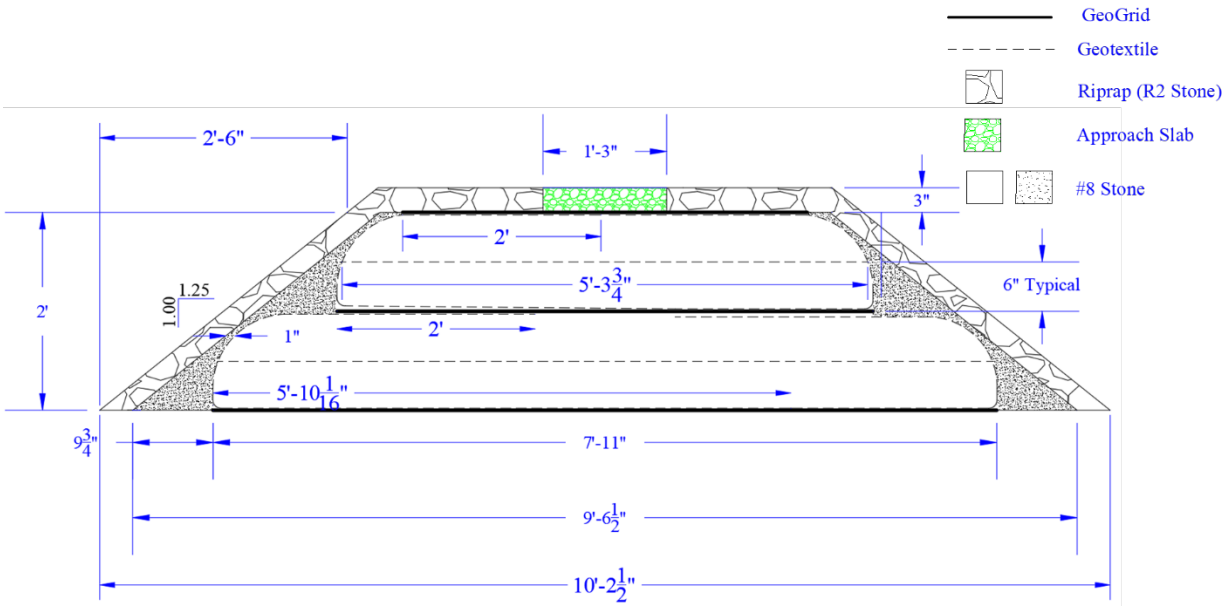

Figure 2.46: Enlarged embankment reinforced by Geosynthetics (improved wrapping without overlap on the top wrapped layer under the approach slab) and Rock lining with wingwalls

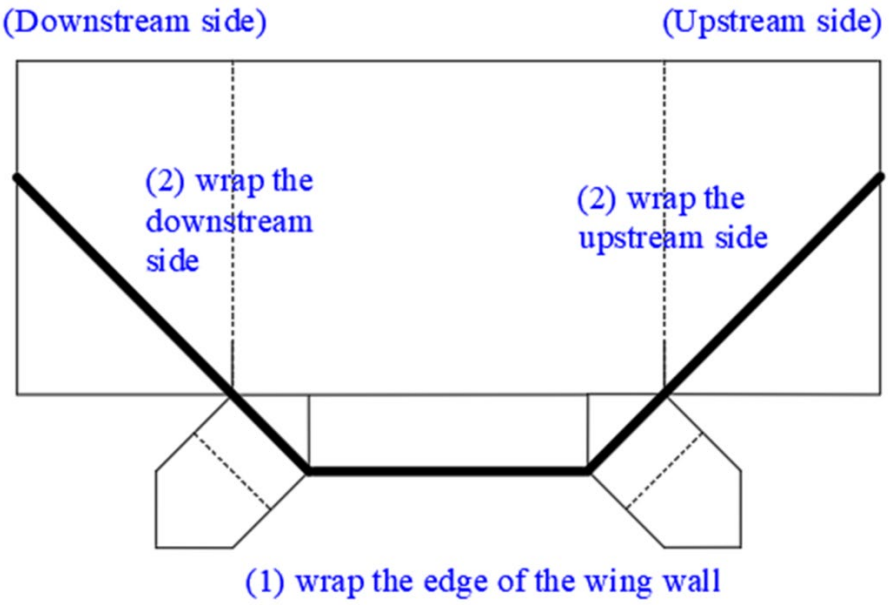

Figure 2.47: Small pieces of Geotextile to wrap the corner of the wingwalls

GoPros were setup on the downstream side and at the top of the embankment to record the test. Most of the water went through the bridge opening at the flow rate of 2.7 CFS during the experiment. The maximum upstream water head was only around 18 inches, and the overtopping was not achieved in Test 19. No failure was observed in Test 19 (a and b)

(a) (b)

Figure 2.48: No failure from (a) top view and (b) downstream view

8.19. Test 20 - Larger Embankment with Wing Wall with Poorly Placed Geosynthetic Reinforcement and R2 Rock Lining with Blocked Bridge Opening

Test 20 was conducted after Test 19, and the baffle boards were used to blocked the bridge opening. GoPros were setup on the downstream side and at the top of the embankment to record the test. At the beginning of the test, water was pumped into the water tank at a relatively low flow rate to gradually increase the water head on the upstream side. At the meantime, downstream water head was kept around 1 inch. When the overtopping was reached on the upstream side, flow rate was gradually increased up to the maximum flow (around 3.76 CFS) and stayed for more than 10 minutes. No failure was found before overtopping. Overtopping was reached at the flow rate of 2.7 CFS. Slope failure occurred at the overtopping (Figure 2.49a) when the water head difference was at 24.5 in. Unwrapping of the geotextile at the corner of the wingwall was then observed (Figure 2.49b), followed by global failure (Figure 2.49c).

(a) (b)

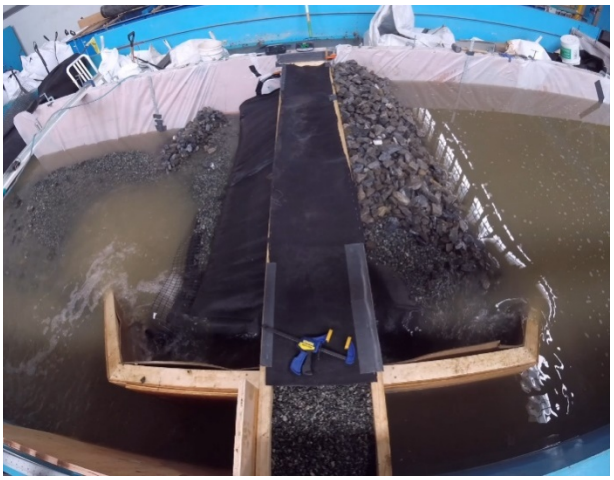

(c)

Figure 2.49: (a) Slope failure at the overtopping, (b) Geotextile at the corner of the wingwall was unwrapped under the high flood, (c) global failure after the Geotextile unwrapping, and (d) the embankment when the test was over

8.20. TEST 21 - LARGER EMBANKMENT WITH WING WALL WITH IMPROVED GEOSYNTHETIC REINFORCEMENT AND R2 ROCK LINING WITH BLOCKED BRIDGE OPENING

Test 21 was conducted with the enlarged embankment with the wingwall next to the bridge abutment (Figure 1.6). The bridge opening was blocked throughout the experiment. #8 coarse aggregates were used as the structural backfill. The downstream and upstream slopes were 1.25/1. During the construction, soils were gradually and slowly rained using shovels with no compaction. Shovels were lifted and kept at a constant height of approximately 16 inches above the soil surface. Rock lining were applied to protect the slope. The core part of the embankment was reinforced by the Geosynthetics, including the Geogrid and Geotextile. Details are shown in Figure 2.50. The backfills at the corner of the wingwall were wrapped on both longitude and latitude direction as shown in Figure 2.51.

GoPros were setup on the downstream side and at the top of the embankment to record the test. At the beginning of the test, water was pumped into the water tank at a relatively low flow rate to gradually increase the water head on the upstream side. At the meantime, downstream water head was kept around 0 inch. When the overtopping was reached on the upstream side, flow rate was gradually increased up to the maximum flow (around 3.76 CFS) and stayed for more than 10 minutes. Piping was not observed and no failure was found before overtopping. Overtopping was reached at the flow rate of 1.67 CFS. Slope failure occurred at the overtopping (Figure 2.53a).Flow rate was then increased up to 3.76 CFS and stayed for 13 mins, no failure happened at the reinforced core part of the embankment (Figure 2.53b). The observations during the Test 21 are summarized in Table 2.1.

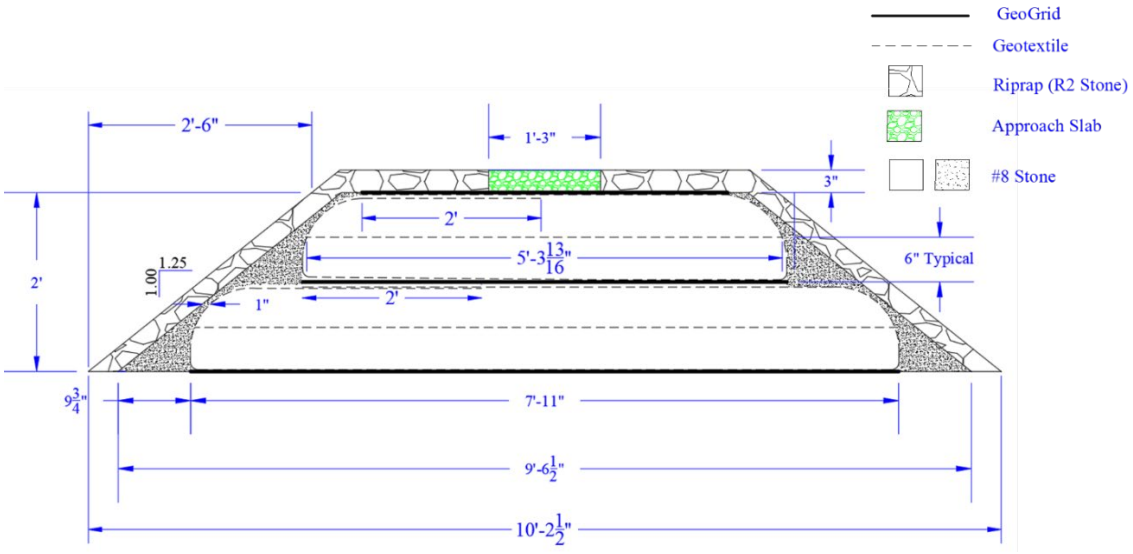

Figure 2.50: Test configurations of Test 20

(a) (b)

(c) 

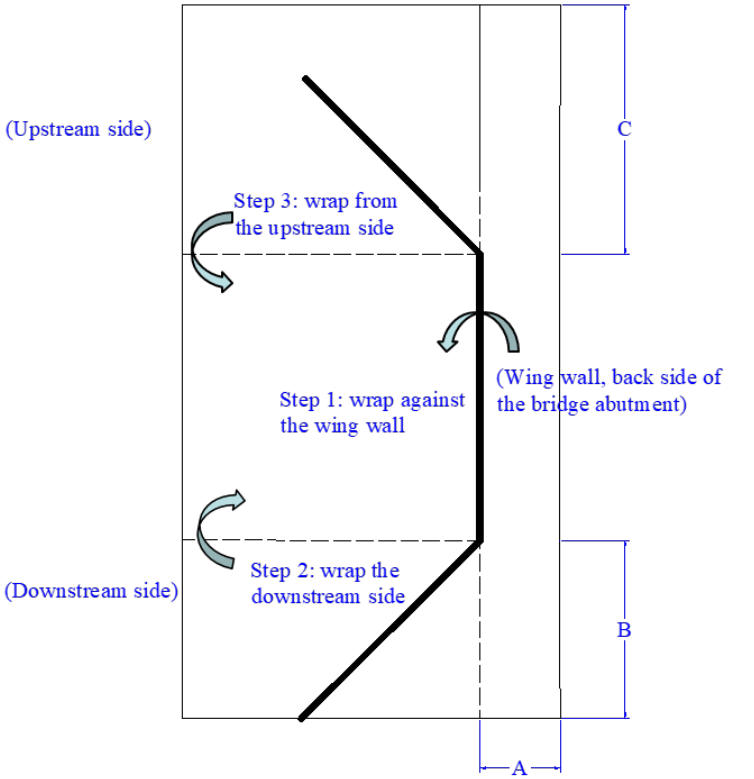

(d)

Figure 2.51: (a) First fold: wrap geotextile against the wingwall with a 2 ft overlap, (b) Second fold: wrap the downstream edge back toward the upstream direction. Ensure that the downstream geotextile covers the backfill a horizontal distance of 4 ft toward the upstream edge. Tuck the excess geotextile near the wingwall under the wrap; (c) Third fold: wrap the upstream edge over downstream geotextile with an overlap of 2 ft.; (d) Geotextile wrapping fold recommendations

(a)

(b)

Figure 2.52: (a) Top view and (b) downstream view of the embankment of Test 21

(a)

(b)

Figure 2.53: (a) Slope failure at the overtopping under high flow; (b) core part of the embankment reinforced by Geosynthetics

Table 2.1: Observations from Test 21

Time	Flow rate (ft^3/s)	Upstream Water Head (in)	Downstream Water Head (in)	Water Head Difference (in)	Downstream Flow Velocity (ft/s)	Flow Velocity Over Approach Slab (ft/s)	Observations
10:04	1.005	7.5	0.2	7.3			No failure
10:17	1.384	18	1	17			No failure
10:22	1.665	24	1	23			No failure
10:24	1.665	28	1	27			Overtopping, downstream slope rock protection failure
10:27	3.76	29	2	27	1.30	1.2	More surface sliding
10:40	3.76	29	2	27	1.30	1.2	Most of the rock lining on the surface were eroded, core part stayed

Erosion of embankments (Fujisawa et al., 2009, 2012; Powledge et al., 1989; Yuan et al., 2014) and earthen dams (Abedini et al., 2012; Fread, 1988; Meyer et al., 1994; Van Tol et al., 2016; Wan & Fell, 2004) has been widely investigated. Seepage erosion (Atkinson et al., 1990; Fell et al., 2003; Jeong et al., 1989; Meyer et al., 1994) and overtopping (Abt & Johnson, 1991; Chanson, 2015; Hanson et al., 2003; McLean & Hansen, 1993) were identified as the main reasons leading to failure of these structures. Failure modes include slope failure (Raj & Sengupta, 2014; Shiotani & Ohtsu, 1999; Wang et al., 2020), toe failure (Abt & Johnson, 1991; Yegian et al., 1994), piping (Foster et al., 2000; Leonards et al., 1991; Richards & Reddy, 2007), and breach erosion (Fread, 1988; Singh et al., 1988; Tingsanchali & Chinnarasri, 2001).

Culverts are normally constructed through a roadway, railway, highway, or trail embankment to facilitate water passage and drainage. As noted by PennDOT publication 584, a culvert, unlike a bridge is composed of structural material around its entire perimeter (PennDOT, 2015). These systems are hydraulically designed to operate with the inlet submerged in a flood condition. Culverts can utilize many cross-sectional shapes including circular (most common), box, arch, and elliptical and can be detailed with different end treatments based on hydraulic and economic needs. End treatments include projected ends, headwalls and wing walls. The culverts are fabricated from concrete, steel, aluminum and plastic and come in both smooth and corrugated surfaces. The erosion characteristics of a typical pipe culvert is examined in this study.

The erosion mechanism of embankments with culverts is similar to that of standard dams and embankments but differs due to the construction details used. Granular materials are conventionally selected as the surrounding backfill around culvert (Moore, 2001). Experimental studies on culverts have indicated that both traditional external and internal erosion of the embankment occurs. In addition, erosion also commonly occurs at the interface of the culvert and surrounding backfill (Xie et al., 2019). When backfilling the material around the culvert interface, it is difficult to completely fill the region under the culvert due to the difference in the curvature of the pipe and the angle of repose of the fill (Figure 1). This creates a channel for seepage which can result in interface erosion. The erosion of the backfill around the culvert can lead to a change in the thrust distribution around the culvert (El Taher & Moore, 2011) which can lead to cracking on the headwall (Najafi & Bhattachar, 2011), development of sinkholes (Stephenson et al., 1999), and structural damage of the culvert (Beben, 2017).

Figure 54: Void created at the culvert interface during the backfilling (https://www.youtube.com/watch?v=1sWxrWmZ_8g)

Backfill around the culvert is usually compacted to mitigate the seepage erosion (Xie et al., 2019). Compaction greatly reduces the rate of erosion, which enhances the seepage erosion resistance (Hanson & Hunt, 2006). To further minimize seepage erosion, flowable backfill is widely used as the backfill material around the culvert for erosion mitigation (Howard & Hitch, 1998; Meade et al., 1994). Flowable backfill typically consists of a low strength mix of aggregate, cement, and water. The water to cement ratio is kept high to allow for high flow and low strengths. The low strength is needed to allow possible future excavation. Flowable backfills are low cost, easy to construct and remove, are stronger than traditional backfill, and non-erodible (Kaneshiro et al., 2001; Lee et al., 1999; Naik & Singh, 1997; Samadi & Herbert, 2003; Wu, 2005).

This report examines the performance of standard PennDOT circular pipe culverts in embankments under flood events. The failure mechanisms are identified and the performance of a flowable backfill strategy is shown.

10. PennDOT Culvert Recommendations

Pennsylvania Department of Transportation recommendations for pipe culverts are outlined in PennDOT Publication 408/2020 (PennDOT, 2020) and illustrated in PennDOT 72M RC-Drawings (PennDOT, 2019). The various configurations specified by PennDOT are summarized in this section. The recommendations summarized include the compaction and material used around the trench and the use of flowable fill material.

10.1. PennDOT Pipe Culvert Standards

The pipe installation procedures and the design details for culverts outlined in PennDOT 72M RC-Drawings-30M (PennDOT, 2019) are reproduced below in Figure 2. Varieties of pipes are used including concrete, metal, and thermoplastic pipes are used. The following procedures are outlined by PennDOT.

The construction details cover the following conditions: (A) pipes lying on top of natural ground, rock, or fill compacted to 97% standard proctor density (SPD); (B) the existing ground is between the top and the bottom of the proposed pipe and the pipe is to be covered with earth fill; (C) the top of pipe is below the level of the natural ground or compacted fill (to minimum 97% SPD) and to be covered with earth fill to heights above the natural ground.

Step 1: Remove the topsoil (compressive layer of organic material) to a width equal to 5 outside diameters of the pipe in all fill conditions: (A), (B), and (C). Also if specified on the contract drawing, undercut for the depth below the bedding as shown by design (make min width 5 diameters of pipe).

Step 2: Construct the embankment to 4'-0" above the top of pipe or to the subgrade elevation, whichever is less. For pipes 72" or greater, the installation is permitted without placing the embankment first. Make the backfill envelope as shown in Figure 2 except provide 2A material on each side of the pipe equal to one outside diameter or span of the pipe. For concrete pipe, the width of uncompacted aggregate for bedding (AASHTO No.8) remains at D_0 +4'-0".

Step 3: Excavate the trench to the width of the outside diameter of the pipe barrel plus 4'-0" and create an appropriate bedding 6" deep.

Step 4: For concrete pipe, if this excavation is through rock, or hard shale, or in areas of undercut, provide 6"+1/2 inch/ft of D_0 +4'-0", below the intended bottom elevation of the

pipe, 16" max. If unsuitable material is found, undercut as directed and backfill with suitable material to bottom of bedding elevation. (Unless otherwise specified).

Step 5: Lay pipe on appropriate bedding.

Step 6: For thermoplastic pipe, place 2A coarse aggregate material, in 5" loose layers, adjacent to the lower haunches to a height of 12" above top of pipe. Compact to non-movement. Test the backfill material and continue embankment in accordance with PennDOT Publication 408/2020, section 601.

Note:

1: permit placement of backfill material in 10" loose layers, when using vibratory compaction equipment in accordance with PennDOT Publication 408/2020, section 601.3(f)3.

2: Compact top 3'-0" of subgrade to 100% in accordance with PennDOT Publication 408/2020, section 206.3. Compact 2A coarse aggregate to non-movement in accordance with PennDOT Publication 408/2020, section 206.3(b)1.c.

3: Use 2A coarse aggregate or suitable material in accordance with PennDOT Publication 408/2020, section 601.3(f)3.

The gradation of 2A coarse aggregate is listed in Table 3.3 in *Task1.1 Evaluation of Backfill Properties* (PennDOT Publication 408/2020 Section 703.2(c), Table c). The requirement of compaction is listed in PennDOT Publication 408/2020, section 206.3(b)1.c: Granular Material, Type 2. Place Type 2 granular material for the full width of the embankment or fill in uniform horizontal layers of not more than a compacted 8 in. depth. Compact material adjacent to structures as indicated on the Standard Drawings. Except for pipe trenches, locations adjacent to structures, and locations where standard, full scale compaction equipment is prohibited, may cause damage, or is not practical due to space or other constraints, compact Type 2 granular material using a smooth drum vibratory roller as specified in Section 108.05(c)3.i. For all other areas except pipe trenches, use dynamic and/or vibratory equipment as specified in Sections 108.05(c)3.d or 108.05(c)4. Reduce lift thickness to 4 in. compacted depth or as directed by the Representative to achieve the equivalent level of compaction as the full-scale compaction equipment. Compact Type 2 granular material for the full width of embankments or fills to a condition of non-movement under the compaction equipment. Compaction acceptance will be determined by the Representative. Non-movement under compaction equipment is defined as creating a stable

condition of the compacted material. A stable condition occurs when there is no rutting, displacement, or shear wave under compaction equipment. A shear wave is bulging of the material surface in front of and behind the compaction equipment. Maintain Type 2 granular material in a surface damp condition, but not wet (no excess moisture) at the time of compaction.

Based on these requirements the following details are used in the experiment: 1) #2A coarse aggregate (Type 2 granular material) are used as the backfill material; 2) An 8 in. thermoplastic pipe are applied as the pipe culvert; 3) APT 131/5214 Backfill Tamper are used as the compactor; 4) Slope of 1:2 are used to simulate an extreme condition; 4) Backfill material are placed in 4 in. lifts that were each compacted to non-movement.

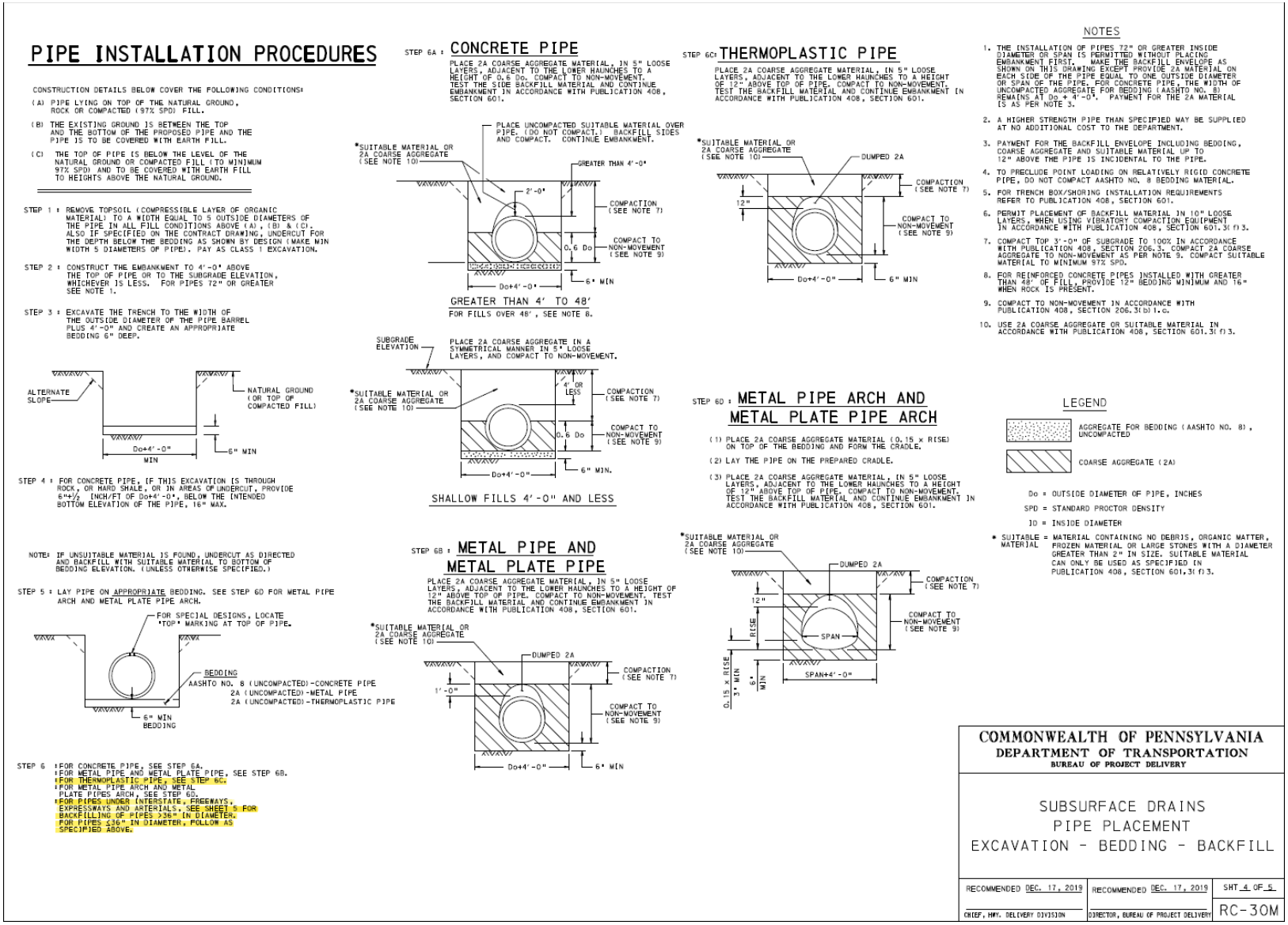

Figure 55: Culvert construction and backfill placement configurations (Pub 72M RC-30M Updates Final)

10.2. FLOWABLE BACKFILL RECOMMENDATIONS

To provide greater resistance to erosion of the pipe, a flowable backfill recommendation has been developed by PennDOT. The flowable backfill is used to envelop the end section of the pipe on both the inlet and outlet. This detail was approved in 2021 and is included in PennDOT 72M RC-Drawings-30M (sheet 5 of 5).

10.3. FLOWABLE BACKFILL MIX DESIGN REQUIREMENTS

Flowable back fill material is defined in PennDOT Publication 408/2020, section 220. Flowable backfill may be a mixture of coarse aggregate, fine aggregate, water and air entraining agents, either cement or supplementary cementitious material, or a combination of both, and may or may not include bottom ash, or other admixtures. There three types of flowable backfill: Flowable Backfill, Type B is for use in regions where future excavation of the backfill may be necessary such as at utility trenches, pipe trenches, bridge abutments, and around box or arch culverts. Type C is for areas where excavation is not anticipated such as replacement of unsuitable soil under foundations, and Type D is for areas where low-density backfill material is needed such as behind retaining walls. **For the application under investigation Type B flowable backfill must be used.**

The flowable backfill mix design requirements for each type is summarized in PennDOT Publication 408/2020, section 220.2(k) and is reproduced as Table 1. Details of the materials allowed are listed in PennDOT Publication 408/2020, section 220.2 (a) to (f), and are reproduced as follows:

(a) Cement. Type I, IP, IS, or II, Section 701. If using Type IP cement, adjust the quantity of fly ash in the design as necessary. If using Type IS cement, adjust the quantity of slag cement in the design as necessary. From a source listed in Bulletin 15.

(b) Fly ash. Type F or C fly ash, Section 724 except as follows:

- *Fly ash—conforming to AASHTO M 295 (or ASTM C 618) Table 1 requirements except maximum loss on ignition is 16%, and excluding the requirements of Table 1A, 2, or 2A. From a source listed in Bulletin 15 or tested and approved before incorporating into the flowable backfill mix.*

(c) Slag Cement. Section 724.3. From a source listed in Bulletin 15.

(d) Fine Aggregate. Type A, B, or C; Section 703.1; except, having a maximum loss of 20% in the Soundness Test, PTM No. 510. The fine aggregate may be natural sand, manufactured sand, or foundry sand meeting Section 703.1. From a source listed in Bulletin 14.

(e) Coarse Aggregate. Type A, B, or C, AASHTO 10, Section 703.2. Except 10% maximum for material finer than the No. 200 sieve. From a source listed in Bulletin 14.

(f) Bottom Ash. From a source listed in Bulletin 14. Coal ash having a maximum loss of 20% in the Soundness Test, PTM No. 510, and conforming to the following dry sieve gradation requirements:

Sieve Size	*% Passing*
1/2-inch	*100*
No. 200	*0-10*

Table 2: Flowable backfill mix design

Properties & Criteria	Type B	Type C	Type D
Mix Design (/CY) Cement (lbs)* Supplementary Cementitious Material (lbs)* Bottom ash (lbs)* or Coarse Aggregate or Fine Aggregate Air Generating Admixture*	50 300 2600	150-200 300 2600	300-700 100-400 **
Slump (inches) AASHTO T 119, ASTM C 136	7 min ****	7 min ****	7 min ****
Density (pcf) AASHTO T 121, ASTM C 136	N/A	N/A	30-70 or as specified ***
Water Absorption of Aggregate AASHTO T 85	--	--	20% max
Compressive Strength (psi) PTM No. 604 28 Days	125 max	800 min	90-400

**Quantities may be varied or alternate designs submitted to adapt mix to conform to density and strength requirements or to adapt to specific site conditions.*

***Requires using a suitable lightweight aggregate or air entraining admixture. Provide a mix design that achieves the specified strength and density requirements.*

****Approximate Value. Use of air entraining agent may reduce these values.*

*****Some applications may require containing flowable backfill by constructing dikes from the mix by using less water to produce a 3-inch minimum slump, if approved by the Representative. Thickening of the mix in other areas is allowed if approved by the Representative.*

As noted in Table 1, a general recommendation on materials and quantities are provided for Type B Flowable fill. The general recommendation is that 50, 300, and 2600 lb/cyd of cement, SCM,

and aggregate like material should be used, respectively. These values are general recommendations with Note 1 stating that these can be varied as needed to achieve density or strength requirements. The amount of water is not prescribed and instead the value must be determined to achieve a maximum 28-day strength of 125 psi. This low strength is chosen to allow for future excavation as needed. A minimum 7 in. slump is also required with allowance for lower slumps with approval of PennDOT.

Flowable backfill mix designs have been developed by numerous ready-mix concrete suppliers in Pennsylvania. A typical mix utilizes Portland Cement, Ground Granulated Blast Furnace Slag (GGBFS), Type A Fine Aggregate with gradation as noted in Table 2, and water. Two PennDOT approved mixes are summarized in Table 3. Note that water to cement ratios of 2.0 to 3.3 are typically used to achieve the low strength limit. These mixes are examined in the following sections.

Table 3: Type A Fine Aggregate Requirements (PennDOT 408 2020)

	Cement Concrete Sand
Sieve Size	**Type A**
9.5 mm (3/8-inch)	100
4.75 mm (No. 4)	95-100
2.36 mm (No. 8)	70-100
1.18 mm (No. 16)	45-85
600 µm (No. 30)	25-65
300 µm (No. 50)	10-30
150 µm (No. 100)	0-10
75 µm (No. 200)	—
Material Finer Than 75 µm (No. 200) Sieve Max. Percent Passing	3
Strength Ratio Min. Percent	95
Soundness Test Max. Loss Percent	10
Fineness Modulus	2.30-3.15

Table 4: PennDOT Approved Flowable Backfill Designs		
Mix	A	B
Portland Type I Cement Sp. Gr.	3.150	3.150
Slag Specific Gravity	2.900	2.900
Fine Aggregate Specific Gravity/Absorption	2.608 / 0.84	2.632 / 0.40
Water/Cement Ratio by Weight	3.299	2.300
Portland Type I Cement (lbs/yd^3)	50	40
Slag Cement (lbs/yd^3)	50	160
Total Cementitious Material (lbs/yd^3)	100	200
Fine Aggregate (lbs/yd^3)	2438	2781
Total Water (lbs/yd^3)	330	460
28 Day Compressive Strength (psi)	70	110

10.4. FLOWABLE BACKFILL PLACEMENT

The new recommendation on flowable backfill alters the standard pipe culvert installation procedure outlined in RC-30M. When flowable backfill is used, Step 6 described in Chapter 2.1 and in Figure 2 is specified. The flowable backfill details provided in the updated PennDOT 72M RC-Drawings-30M (sheet 5 of 5) are reproduced in are shown in Figure 3 and Figure 4. Notes listed in sheet 5 are provided below:

1. *Provide materials and construct as specified in publication 408, sections 601 and 220.*
2. *Payment for the backfill envelope (aggregate, bedding and backfill or flowable backfill material) and suitable material up to 12" above the pipe is incidental to the pipe.*
3. *Flowable backfill will envelop the last section of pipe or end section. Construct dike of flowable backfill material as specified in special provision or provide formwork to contain flowable backfill.*
4. *The flowable backfill detail replaces steps 6a, 6b, 6c and 6d on sheet 4 when flowable backfill is specified.*

★ *If drainage is required to maintain positive flow of water away from the trench, it must be provided by use of properly designed granular or synthetic drains.*

**Suitable = Material containing no debris, organic material matter, frozen material or large stones with a diameter greater than 2 in. in size. Suitable material can only be used as specified in publication 408, section 601.3(f)3.*

As illustrated, flowable backfill is specified for a minimum of 10 ft on both the inlet and outlet of the pipe. Conventional backfill is used between these sections. For larger diameter steel or thermoplastic pipes exceeding 36 in. in diameter additional ground anchors are also required to help resist failure.

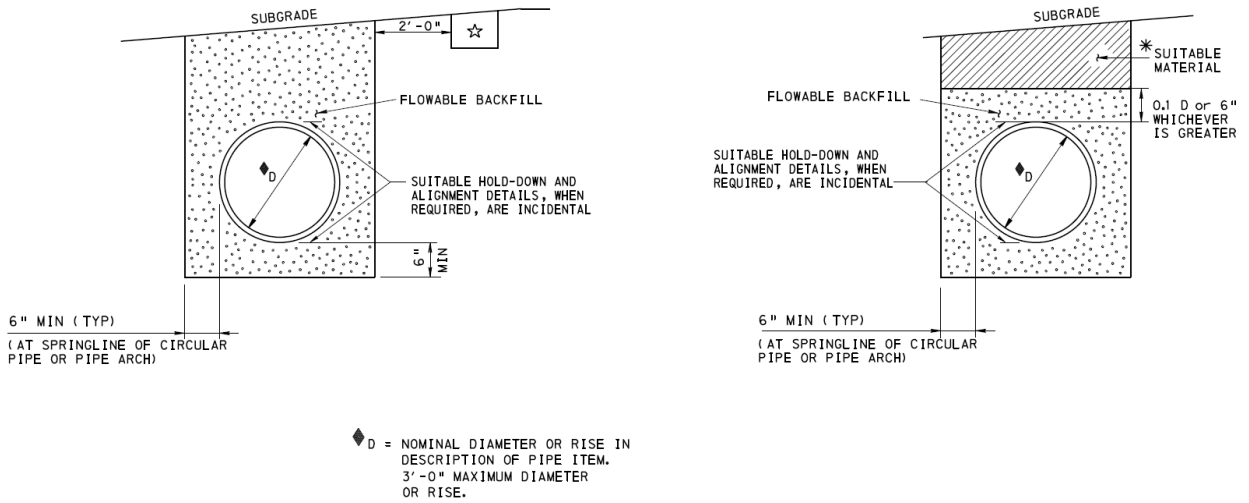

Figure 56: Flowable backfill detail 1 (PennDOT, 2019)

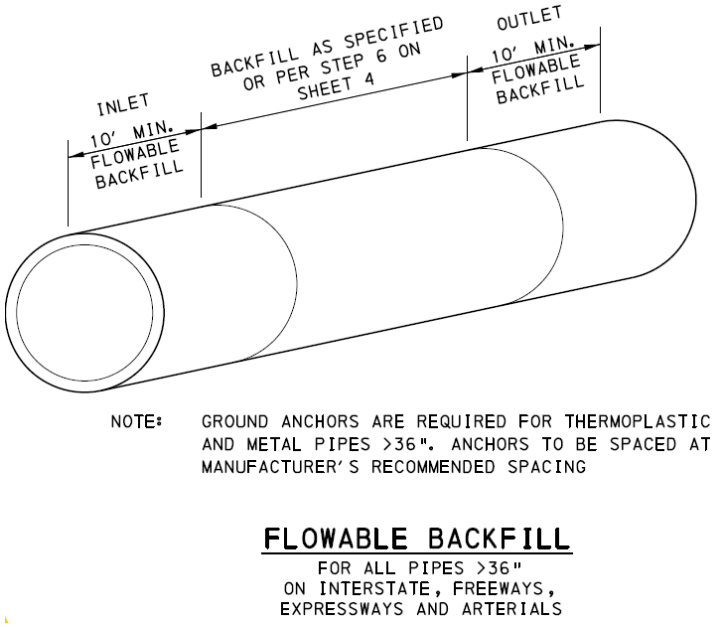

Figure 57: Flowable backfill detail 2 (PennDOT, 2019)

As noted in PennDOT Publication 584 several end treatments are used. The end treatments are typically designed to act as a retaining wall to keep the roadway embankment material out of the culvert. In addition the end conditions can be designed to improve performance of the culvert, ensure public safety during flood events, and control the amount of debris that can accumulate (PennDOT, 2015). The end treatment can consist of a projected end of the pipe, a projected bell inlet, a head wall, or a head wall with wing walls to direct the flow. End walls and end sections for culverts are specified in RC drawings (PennDOT, 2010). The end section details presented in RC-33M are reproduced in Figure 5. As illustrated in the details a 1:3 slope is recommended at the end region. These details would improve the resilience of the culvert against severe rain events. Consequently, the experimental program examines the case of a projected end.

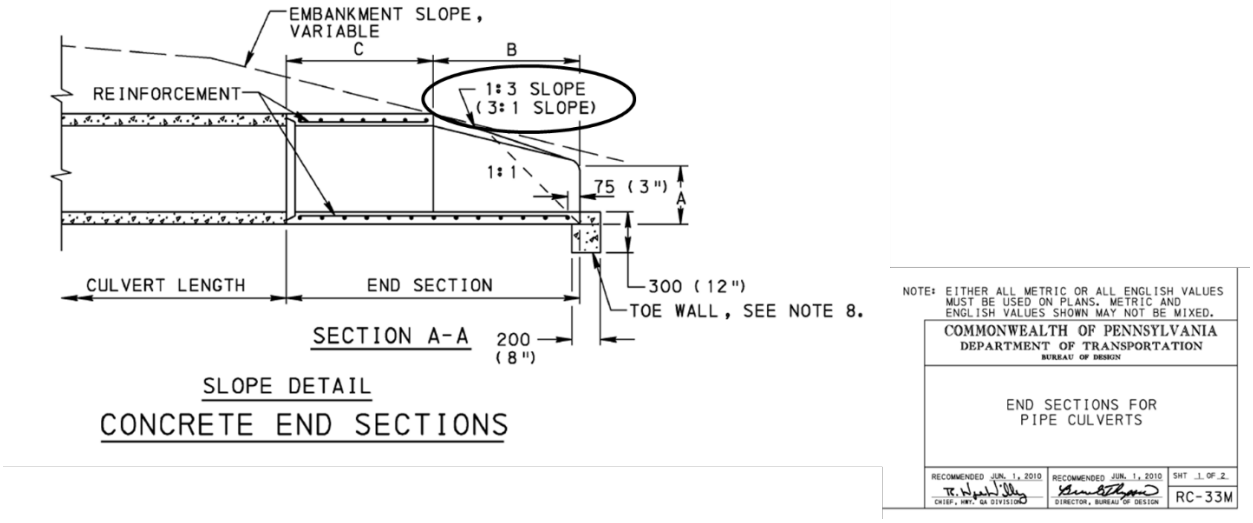

Figure 58: End section for pipe culverts

11. CULVERT EXPERIMENTAL PROGRAM

The culvert was evaluated using the balcony water tank at Lehigh University. The water tank measures (L:W:H) of 26:16:3 ft. The flow rate to the experiment can be maintained at a constant rate (maximum 3.5 ft^3/s) and the rate of flow is controlled by a valve. A temporary wood wall was fabricated 2 ft away from the side wall of the steel tank to create the desired culvert fill width. The assumption was made that the culvert trench would be subject to erosion while the undisturbed soil adjacent to the trench would be resistant to erosion. The walls of the tank were covered with plastic sheets to minimize leakage. Videos were taken using GoPros located upstream, downstream, and at the top of the culvert to record the experiment.

Three experimental setups were developed:

1) Standard compacted embankment culvert
2) Sloped uncompacted embankment culvert
3) Uncompacted embankment with flowable fill

The details of each setup are outlined in the following sections.

11.1. COMPACTED EMBANKMENT FOR CULVERT

The embankment with culvert design was based on the PennDOT Publication 408/2020 (PennDOT, 2020) and PennDOT 72M RC-Drawings-30M (PennDOT, 2019). The laboratory model configuration is shown in Figure 6. The dimension of the pipe culvert and the dimension of the backfill were scaled with a ratio of 1/3, which was limited by the height dimension of the water tank. The size of the aggregates (No. 2A Coarse Aggregate) was not scaled since the water velocity achieved in the lab was beyond the critical velocity of the No. 2A Coarse Aggregate to initiate the erosion, which was discussed in *Task12 - Assessment of Erosion of Abutment Backfill, Chapter 1.1.* The required slope of the end section of the embankment is noted by PennDOT as 1:3 (Figure 5). The test configuration, however, used an embankment slope of 1:2 to simulate an extreme condition. This slope was decided on during an update meeting with PennDOT on 05/26/2021. An 8 in. pipe was used as the model culvert size. The pipe culvert was placed on a 2 in. uncompacted No.2A coarse aggregate bedding placed on the bottom surface of the tank as required for thermoplastic pipes in RC-30M (Figure 2). No.2A coarse aggregate was then dumped to bury the pipe culvert. The No.2A coarse aggregate on the side was compacted using an APT 131/5214 Backfill Tamper, weighing 37.5lbs with a 6 in. butt. The material was placed in 4 in. lifts above the pipe that were each compacted to non-movement. After that, 4 in. of No.2A coarse aggregate

was dumped on the top of the pipe culvert without compaction. The No.2A coarse aggregate above and on the side of the uncompacted layer was compacted in three 4 in. lifts to a condition of non-movement. The dimensions of the aggregate placement were in accordance with the requirements of RC-30M and were conducted at the 1/3 scale factor. The as-built configuration is shown in Figure 6 and an image of the culvert embankment prior to testing is shown in Figure 7.

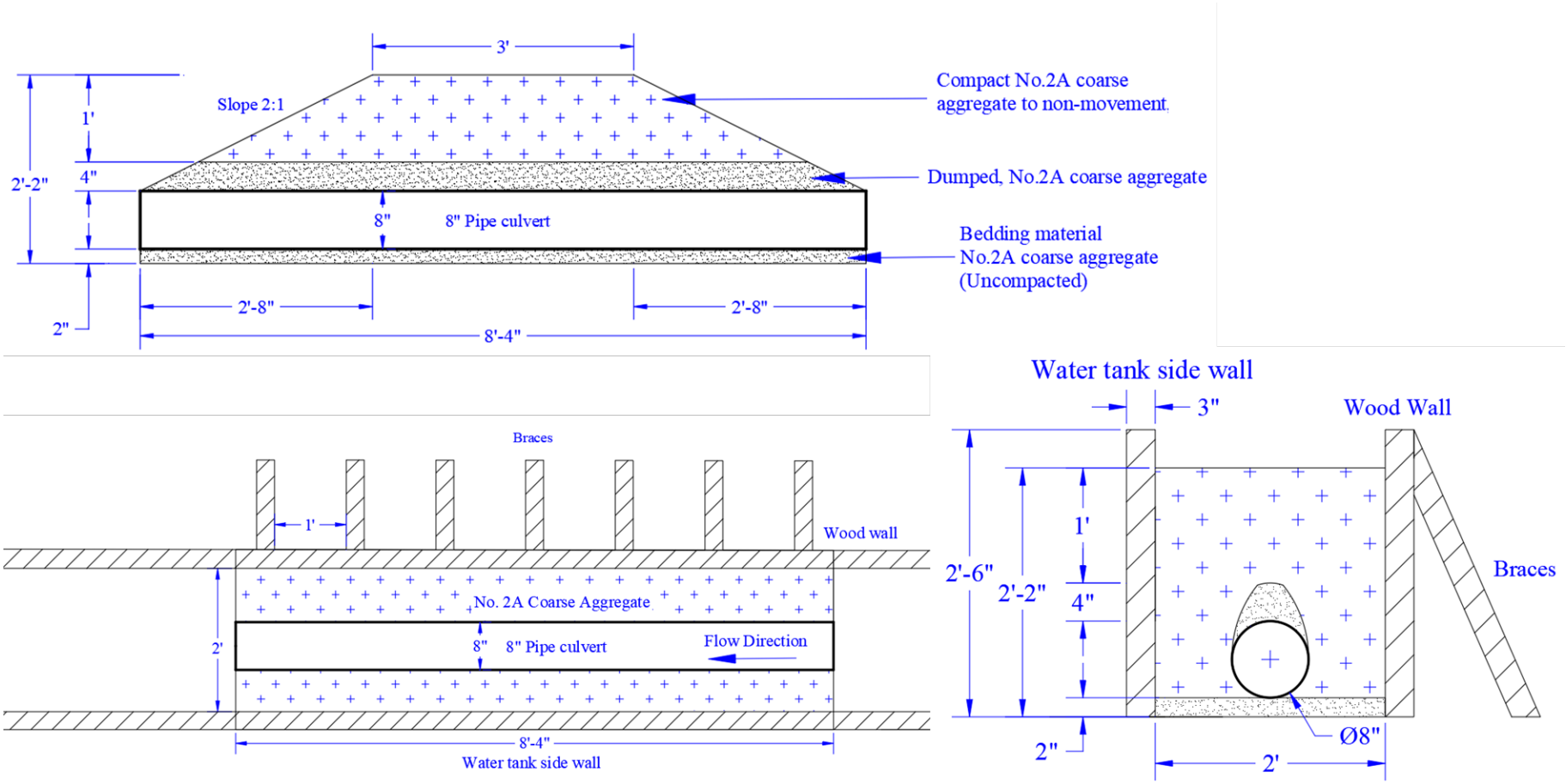

Figure 59: Test configuration of the compacted embankment with culvert

Figure 60: Compacted culvert embankment prior to testing

11.2. Compacted Embankment for 2° Tilting Culvert

In the second setup, the pipe was sloped downward at 2° from the inlet to outlet and the material around the pipe was lightly compacted to non-movement using the cast steel hand tamper. The hand tamper was lifted about 3 to 4 in. and then slammed down to compact the soil. These two conditions were expected to create a condition where the embankment would be more prone to erosion and failure. The tilted culvert setup is shown in Figure 8. The dimension of the pipe culvert, the dimension of the backfill were scaled with a ratio of 1/3. The pipe culvert was tilted with a 2° angle (upstream side higher than downstream side) on an uncompacted No.2A coarse aggregate bedding material at the bottom of the tank. The No.2A coarse aggregate was then dumped to bury the pipe culvert. The No.2A coarse aggregate on the side was compacted using the hand tamper. The material was placed in 4 in. lifts above the pipe that were each compacted to non-movement. After that, a layer of No.2A coarse aggregate was dumped on the top of the pipe culvert without compaction. The No.2A coarse aggregate above and on the side of the uncompacted layer was all compacted for every 4 in. to a condition of non-movement. A photo of the setup prior to testing is shown in Figure 9.

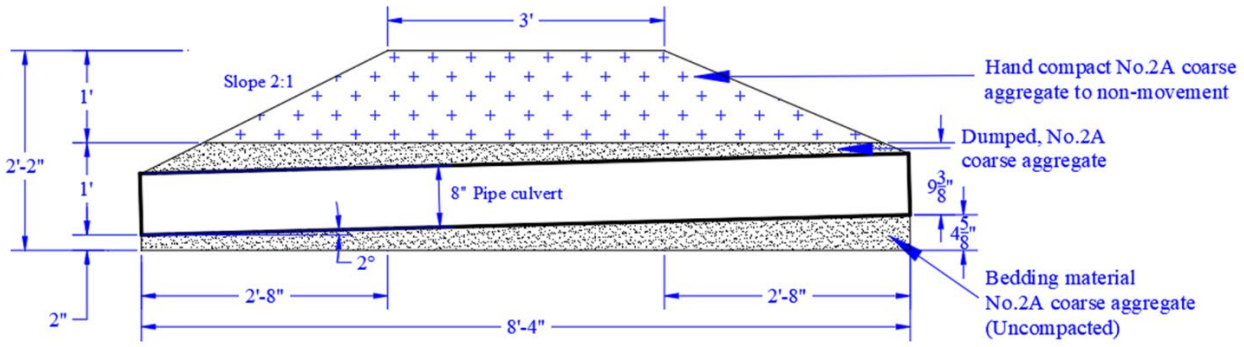

Figure 61: Test configuration of the uncompacted embankment with 2° tilted culvert

Figure 62: Uncompacted embankment with 2° tilted culvert prior to testing

11.3. FLOWABLE FILL EMBANKMENT FOR CULVERT

The final setup examines the performance of flowable fill and its ability to prevent erosion of the pipe culvert embankment. The flowable backfill embankment with culvert was detailed in accordance with PennDOT Publication 408/2020 (PennDOT, 2020) and PennDOT 72M RC-Drawings-30M (PennDOT, 2019). The end sections on the inlet and outlet were constructed with flowable backfill. The middle part of the embankment consisted of the compacted #2A coarse aggregate. The laboratory model details are shown in Figure 10. The dimension of the pipe culvert, the dimension of the backfill were constructed at a 1/3 scale. Wood forms were placed before pouring the flowable backfill. Wood forms (Form 1 to Form 3) shown in Figure 10 were used to form the flowable fill. The bottom half of Forms 1 were installed and a 2 in. layer of No. 2A Coarse

Aggregate was dumped between bottom section of Forms 1. and used to support the pipe culvert. Pipe culvert was placed on the bottom of Forms 1. A steel all-thread bar was run from one end of the embankment to the other through the center of the pipe (from Form 2 to Form 2) and used to keep the pipe straight and the end forms rigidly attached. The top of the forms 1 was then installed. Forms 3 were set and fixed to the side wood wall to provide the appropriate slope on the flowable fill embankment. Gaps between wood forms and water tank were sealed with duct tape. No.2A coarse aggregate was then dumped to bury the pipe culvert between the two upper Form 1 pieces. The No.2A coarse aggregate on the side was compacted in 4 in. lifts to a condition of non-movement using the hand tamper. Once the aggregate reached the top of the pipe, an additional 4 in. of No.2A coarse aggregate was dumped on the top of the pipe culvert without compaction. The No.2A coarse aggregate above and on the side of the uncompacted layer was compacted in three 4 in. lifts to a condition of non-movement as shown in Figure 12. Flowable backfill was placed between Form 3 and Form 1. Form 3 was removed after 1 day of curing as shown in Figure 11. Forms 1 were kept in place and acted as a collar for the embankment.

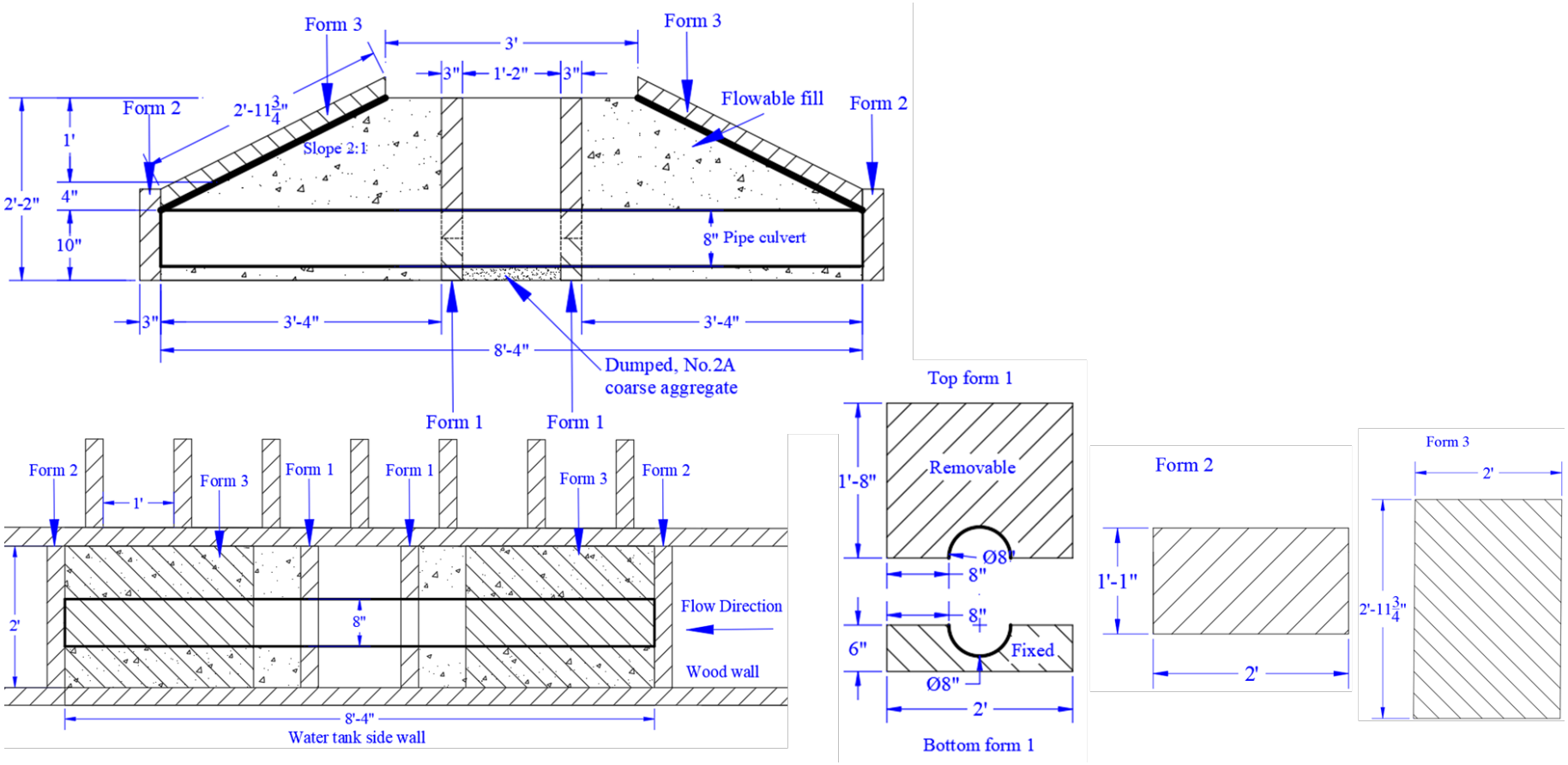

Figure 63 Test configuration of the flowable backfill embankment for culvert with forms

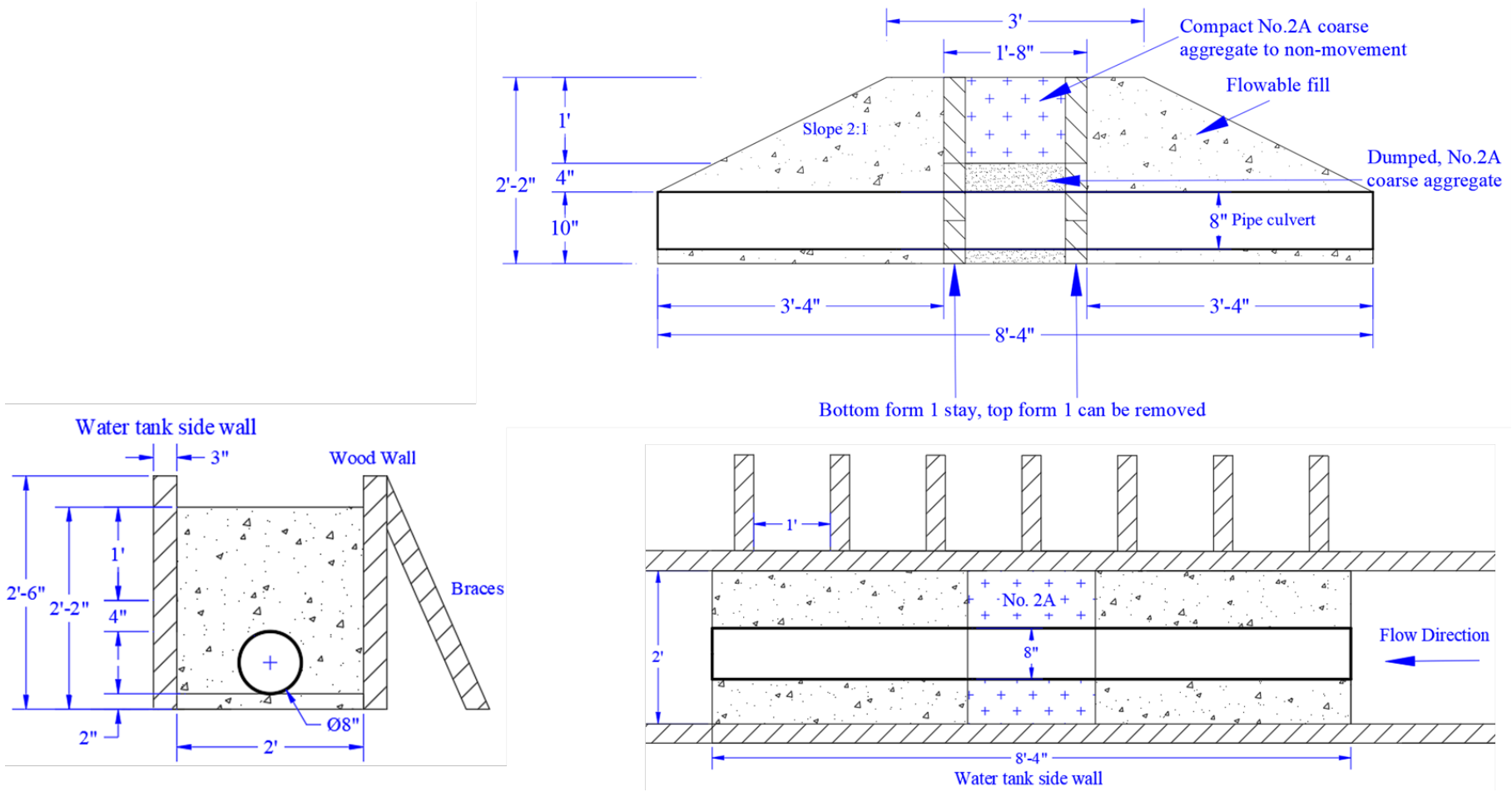

Figure 64: Test configuration of the flowable backfill embankment for culvert with forms removed

Figure 65: Construction of flowable backfill

12. CULVERT STUDY MATERIALS

The materials used in the overall research program are presented in this section. Note that some of the material results presented describe materials used in Task 1.1 and 1.2 of the program that were only recently tested and are included in this report for completeness.

12.1. RELATIVE DENSITY MEASUREMENT

Vibrating table tests were conducted to determine the relative density of the aggregates (embankment material and #8 coarse aggregate from task 1.2, and #2A coarse aggregate used in task 1.3) based on the ASTM D4253 and ASTM D4254 (ASTM, 2006a, 2006b). A mold of 0.1 ft^3 volume (6 in. tall x 6 in. diameter) was used for the vibrating table tests. The specific gravity (Gs) was then determined based on the ASTM C127 (ASTM, 2015a). The specific gravity of embankment material was determined as 2.68, the specific gravity of #8 coarse aggregate was determined as 2.66, and the specific gravity of #2A coarse aggregate was determined as 2.70. The properties of the embankment material, #8 coarse aggregate, and #2A coarse aggregate measured during the vibrating table tests are summarized in Table 4.

Table 5: Aggregate properties based on vibrating table test

	Embankment material	**#8 coarse aggregate**	**#2A coarse aggregate**
$\rho_{dmin,n}$ (g/cm^3)	1.54	1.47	1.55
γ_{dmin} (kN/m^3)	15.13	14.42	15.25
e_{max}	0.74	0.81	0.74
$\rho_{dmax,n}$ (g/cm^3)	1.80	1.70	2.06
γ_{dmax} (kN/m^3)	17.65	16.66	20.20
e_{min}	0.49	0.57	0.31
Dr (%)	25.26	14.34	30.95

Where,

$\rho_{dmin,n}$ is the minimum index density for given trial,

γ_{dmin} is the minimum -index unit weight,

e_{max} is the maximum-index void ratio,

$\rho_{dmax,n}$ is the maximum index density for given trial,

γ_{dmax} is the maximum-index unit weight,

e_{min} is the minimum-index void ratio,

D_r (%) is the relative density, $D_r\ (\%) = \frac{\gamma_{d\,max}}{\gamma_d} \times (\frac{\gamma_d - \gamma_{d\,min}}{\gamma_{d\,max} - \gamma_{d\,min}})$,

γ_d is the dry unit weight of the soil determined using sand cone test during the lab construction.

Relative density, D_r, is expressed as a percentage of the difference between the maximum index void ratio and any given void ratio of a cohesionless, free-draining soil to the difference between its maximum and minimum index void ratios (ASTM, 2006b). Relative density indicates the compaction level of the cohesionless soil. The maximum void ratio, e_{max}, of the soil, represents the loosest condition of the soil. The minimum void ratio, e_{min}, of the soil, represents the densest condition of the soil. The classification of the soil according to the relative density is shown in Table 5. Hence, the natural existing state of the #8 coarse aggregate (D_r = 14.34%) can be classified as the very loose soil, the embankment material (D_r = 25.26%) and the #2A coarse aggregate (D_r = 30.95%) can be classified as the loose soil. In this study, the #2A coarse is denser than the embankment material and the #8 coarse aggregate, and the hydraulic conductivity of the #2A coarse aggregate is lower than the embankment material and the #8 coarse aggregate (*Task 1.1 Evaluation of Backfill Properties, Chapter 5*). Higher relative density indicates a lower void ratio in the natural existing state of the soil, which leads to a lower hydraulic conductivity of the soil. Lower hydraulic conductivity, which will increase likely head differential between the upstream and downstream sections of the embankment during extreme weather events. This larger differential accelerates the process to reach the overtopping condition, which makes the backfill materials more susceptible to erosion mechanisms.

Table 6: Soil classification according to relative density (Mitchell & Soga, 2005)

Relative Density, D_r [%]	Classification
0 to 20	Very Loose
20 to 40	Loose
40 to 60	Medium Dense
60 to 80	Dense
80 to 100	Very Dense

12.2. AASHTO #2A COARSE AGGREGATE

Coarse Aggregate meeting AASHTO #2A requirements was used as the main material for the culvert test program. The gradation, hydraulic conductivity, and maximum dry density of AASHTO 2A coarse aggregate used in this project were previously investigated and summarized in *Task1.1 Evaluation of Backfill Properties, Chapter 5.*

12.3. FLOWABLE FILL MIX DESIGN

Preliminary tests were conducted to determine the mix design of the flowable backfill in lab based on the mix design from PennDOT Publication 408/2020, section 220.2k (Table 1). The absorption

of the coarse aggregate was determined based on the ASTM C127 – 15 (ASTM, 2015a), and the absorption of the fine aggregate was determined based on the ASTM C128 – 15 (ASTM, 2015a). Materials (cement, slag, aggregate, and water) were weighed and mixed in a standard concrete mixer. The slump of the flowable backfill was then measured followed the ASTM C143 (ASTM, 2015b). The flowable backfill cylinders were prepared and cured in molds for a day. The mold (4x8 Gray Concrete Test Cylinder w/ Flat Lid, from Paragon Products) has the diameter of 4 inches and the height of 8 inches. Compressive strength of the flowable backfill cylinders was tested in accordance with ASTM C39 (ASTM, 2012) using a CONTROLS-Automax Multitest frame.

Mixes were developed based on the PennDOT requirements and sample mix designs previously discussed in section 2.3. Mixes were fabricated using combinations of Type III Portland cement, slag, #8 coarse aggregate, PennDOT type A fine aggregate and water. The #8 coarse aggregate used in trial No.1 was the same material used for task 1.2 testing. The gradation properties of that material were previously reported. The fine aggregate consists of Type A material. The measured properties are summarized in Table 6. The mill certifications on the cement and slag are shown in Table 7 and Table 8.

Table 7: Properties of fine aggregate	
Bulk specific gravity (SSD):	2.622
Bulk specific gravity:	2.608
Absorption:	0.54
Uncompacted voids:	40
Rock compositions and order of abundance:	QS (Quartz sand):1; CH (Chert):2
Sodium sulfate soundness	2%
Alkali-silica reactivity (ASR), ASTM C1293	0.022
ASTM C1293 reactivity class	R0

Three mix designs were examined to develop a viable proportion for the lab experiments. Trial #1 was based on PennDOT Specifications (as noted in Table 1) and utilized #8 coarse aggregates (Figure 13). Trial #2 was based on mix design A summarized in Table 3 and utilized a fine aggregate. Trial #3 was based on mix design B summarized in Table 3 and also utilized the fine aggregate. The three mix designs as well as their measured slump and compressive strengths are summarized in Table 9. Mix No.1 provided adequate slump however the strength after 4 days already exceeded the max allowable 28-day compressive strength of 125 psi. The water to cement ratio was greatly increased and the ratio of Type III cement to slag was adjusted for trial No.2. Trial No.2 resulted in a non-flowable material (Figure 14) and consequently strength cylinders were not taken. Trial No.3 produced adequate slump and low strengths as required by PennDOT

Publication 408/2020, section 220.2k (Table 1). The 4 and 9-day compressive strengths were measured as 79 psi and 83 psi, respectively. The average 28-day compressive strength (two cylinders 130/158 psi) was measured to be 144 psi. This marginally exceeds the maximum allowable 28-day compressive strength of 125 psi. The system however was tested at an age of 5 days which correlates to an approximate compressive strength of 79.8 psi based on linear interpolation of the cylinder test results. Thus, while the pipe tests were conducted within the allowable compressive strength, the mix would need to be redesigned to produce a lower 28-day performance. This can be achieved with a marginal increase in the w/c ratio.

Table 8: Mill certification for Type III cement used

LEHIGH
HEIDELBERGCEMENT Group

Mill Test Certificate Report

Type: III ASTM, III AASHTO

Grind Number: June-21

Test Period: 06/01/21 **to:** 07/01/21

Certification

Lehigh Cement Company, LLC certifies that at time of shipment, the portland cement designated as Type III manufactured at the Evansville, Pennsylvania plant conforms to the standard composition and physical requirements of the current Standard Specification for Portland Cement of ASTM C 150 and AASHTO M85 for Type III portland cement. This certification carries no other express or implied warranties and Lehigh Cement Company LLC, is not responsible for improper use or workmanship of the described cement.

General Information

Supplier: Lehigh Cement Company LLC
Address: 537 Evansville Rd
Fleetwood, PA, 19522
Telephone: 610-926-1024

Source Location: Evansville Plant

Contact: Sales Office

Test Data on ASTM "Standard" Requirements

Chemical Requirements (ASTM C-150, Table 1)

Item	Limit	Results
SiO_2	A	19.78
Al_2O_3	A	4.64
Fe_2O_3	A	3.88
CaO	A	61.39
MgO	6.0 max	3.60
SO_3	D	3.98
Loss on Ignition	3.5 max	1.75
Na_2O	A	0.33
K_2O	A	0.95
Insoluble Residue	1.5 max	0.51
CO_2	A	1.26
Limestone %	5.0 max	4.1
$CaCO_3$ in Limestone	70% min	81.0
Inorganic Process Addition	5.0 Max	-
Potential Compounds:		Adjusted
C_3S	A	50
C_2S	A	18
C_3A	15.0 max	5
C_4AF	A	12

Physical Requirements (ASTM C-150, Table 3)

Item	Limit	Results
Fineness: % Passing 45µm (No. 325)	A	1.9
Blaine Fineness (m^2/Kg)	260 min	561
Autoclave Expansion (%)	0.8 max	0.128
Vicat Setting Time:		
Initial Set (minutes)	45 min	91
Air Content (%)	12 max	8.7
Compressive Strengths MPa:		
1-Day	A	24.0
3-Day	12.0 min	29.8
7-Day	19.0 min	33.9
28-Day	A	39.0
Compressive Strengths psi:		
1-Day	A	3380
3-Day	1740	4420
7-Day	2760	4912
28-Day	A	5657
Mortar Bar Expansion, C-1038, %	max 0.020	0.009

Test Data on ASTM Optional Requirement

Chemical Requirements (ASTM C-150, Table 2)

Item	Limit	Results
Equivalent Alkalies		0.96

Physical Requirements (ASTM C-150, Table 4)

Item	Limit	Result
False Set	min 50	66
Heat of Hydration, 3-day C-1702, cal/g	A	79.4

Additional Data

Item	Limestone	Inorganic Processing Addition - CKD
Amount	4.1	-
SiO_2	13.81	-
Al_2O_3	5.18	-
Fe_2O_3	1.99	-
CaO	45.36	-
SO_3	1.00	-

Base Cement Phase Compostion	Result
C_3S	52
C_2S	18
C_3A	6
C_4AF	12

Notes

Footnotes:
A: No limit applicable
D: If SO3 exceeds 3.0%, C-1038 shall not be more than 0.020%

Table 9: Mill certification for slag used

LEHIGH
HEIDELBERGCEMENT Group

Material Certification Report

Brand Name: **Allcem Slag Cement** **Test Period:** **06/01/21**
Type: **ASTM C989-Grade 120** **to:** **07/01/21**

General Information

Supplier:	Lehigh Cement Company	Source Location:	Evnasville Plant
Address:	537 Evansville Road Fleewood, PA 19522	Contact:	Sales Office

Lehigh Slag Cement meets ASTM C-989 and AASHTO M-302 for Grade 120 Ground Granulated Blast-Furnace Slag
We are not responsible for improper use or workmanship

Test Data on ASTM "Standard" Requirements

Chemical (C989, Table 2)			Physical (C989, Table1)		
Item	**Limit**	**Result**	**Item**	**Limit**	**Result**
			+45 µm (No. 325) Sieve (%)	20 max	0.65
			Blaine Fineness (m^2/g)	-	603
Sulfide S (%)	2.5 max	0.18	Air Content (%)	12 max	9.3
Sulfate Ion - SO_3 (%)	NA	2.5	Slag Activity Index (SAI %)		
			Average of Last 5 Samples:		
			Avg 28 Day Index	115 min	127
			Current Samples:		
			28 Day Index	110 min	132

Test Data on Reference Cement

Chemical			Physical		
Item	**Limit**	**Result**	**Item**	**Limit**	**Result**
Total Alkalies as Na_2O (%)	0.60 - 0.90	0.86	Blaine Fineness (m2/kg)	-	396
C_3S	-	50	Compressive Strength MPa (psi):		
C_2S	-	18	7 Day	-	4111
C_3A	-	6	28 Day	35 (5000) min	5258
C_4AF	-	12			

Optional Test Data

Chemical			Physical		
Item	**Limit**	**Result**	**Item**	**Limit**	**Result**
% Total Alkalies	-	0.57	Specific Gravity	-	2.93
%Cl (Chloride)	-	0.03	Sulfate Expansion, C-1038, %	0.020%	-

Notes

Figure 66: Flowable backfill cylinders using mix trial No.1

Table 10: Trial Flowable Fill Mix Designs			
Trial	1	2	3
Cement Type	Type III Portland	Type III Portland	Type III Portland
Cement [lb/yd^3]	50	50	40
Slag [lb/yd^3]	300	50	160
Aggregate Type	Coarse #8	Fine Type A	Fine Type A
Aggregate Oven Dried [lb/yd^3]	2566	2302	2727
Aggregate SSD [lb/yd^3]	2596	2334	2742
Aggregate MC	1.33%	1.45%	1.96%
Aggregate Absorption	1.17%	0.54%	0.54%
Water Required [lb/yd^3]	170.5	613.8	460
Weight of Agg In-Situ [lb/yd^3]	2600	2348	2781
Water on Aggregate [lb/yd^3]	3.99	13.81	38.73
Total Water to be Added [lb/yd^3]	166.5	600	421.3
Water Cement Ratio	0.49	6.14	2.30
Measured Slump	7.0	0	7.25
Strength Age [days]	4	Not Measured	4 / 9 / 28
Strength [psi]	510 ± 52	Not Measured	79 / 83 / 144±13

Figure 67: Slump for trial mix No.2

Figure 68: Compressive strength measurement of trial No.3 flowable fill

Four experiments were conducted and are summarized in this section. Test 22 examines a baseline embankment with culvert constructed in accordance with PennDOT recommendations. Test 23 examines the same embankment with an obstruction in the culvert. Test 24 examines a lighter compaction level and looks at the implication of a sloping culvert. Test 25 looks at the performance of the flowable fill.

13.1. TEST 22 COMPACTED EMBANKMENT WITH CULVERT - PIPE OPEN

The embankment was constructed as described in Chapter 3.1. The No.2A coarse aggregate was placed as the bedding material (Figure 16), and the pipe culvert was placed on the bedding material (Figure 17). The material above the pipe culvert was compacted to non-movement using the APT 131/5214 Backfill Tamper, 37.5# (6"Butt) (Figure 18). Sand cone tests were conducted during the construction to measure the in-situ density of the No.2A coarse aggregate. The average measured in-situ unit weight (γ_t) of the uncompacted #2A coarse aggregate were determined to be 106.8 pcf (16.8 kN/m^3). The average measured moisture content of the compacted #2A coarse aggregate removed from the embankment was 1.77%. From this a dry unit weight (γ_{dry}) of 104.9 pcf (16.5 kN/m^3) was determined. The average measured in-situ unit weight (γ_t) of the compacted #2A coarse aggregate were determined to be 126.8 pcf (19.9 kN/m^3). The average measured moisture content of the compacted #2A coarse aggregate removed from the embankment was 1.52%. From this a dry unit weight (γ_{dry}) of 124.9 pcf (19.6 kN/m^3) was determined. *On average this achieved 89% of the maximum proctor density.*

Figure 69: Uncompacted bedding material (No.2A coarse aggregate)

Figure 70: Pipe culvert installed on the bedding material

Figure 71: No.2A coarse aggregate compacted to non-movement using a backfill tamper

The experiment started with the pipe culvert open. Scour of the bedding material and the compacted backfill around the pipe was observed when the flow rate was 0.27 CFS before overtopping (Figure 19). The flow rate was gradually increased 2.4 CFS to achieve overtopping (27 mins). Significant surface scour occurred after the embankment was overtopped (Figure 20). Water flow was maintained after overtopping leading to gradual surface erosion of the embankment. Erosion was observed on both upstream and downstream sides (Figure 21).

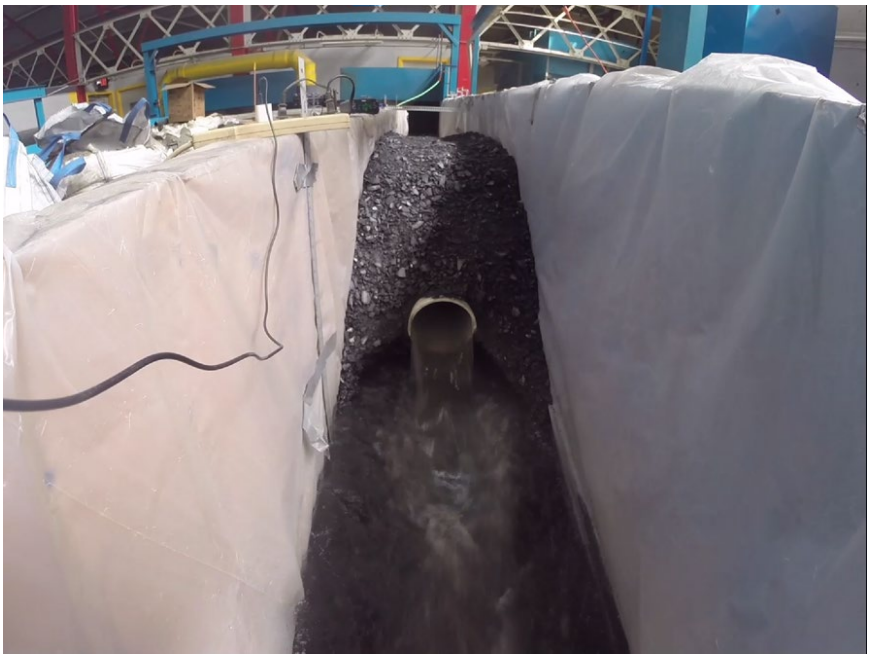

Figure 72: Scour of the backfill material under the pipe culvert

Figure 73: Significant surface scour after overtopping

Figure 74: Erosion of both upstream and downstream sides

13.2. Test 23 Compacted Embankment for Culvert with Pipe Blocked

The embankment after Test 22 was kept using in Test 23. The upstream of the pipe culvert was blocked after Test 22 to examine a greater demand scenario for the embankment. Flow rate was kept as 0.27 CFS throughout the experiment until overtopping (10 mins). Piping and the seepage flow through the embankment were not observed during the experiment (Figure 22). Significant surface scour occurred after the embankment was overtopped as shown in Test 22. The accumulated surface scours on both upstream and downstream sides after Test 22 and 23 were found after overtopping (Figure 23).

Figure 75: Outlet view prior to overtopping indicating no piping through the embankment

Figure 76: Significant surface scour visible after overtopping (image taken post-test)

13.3. TEST 24 COMPACTED EMBANKMENT WITH 2° TILTED CULVERT WITH PIPE BLOCKED

Pipe culvert was tilted placed on the bedding material with the upstream side higher than the downstream side. The No.2A coarse aggregate in the compacted area was hand compacted to non-

movement with the compactor. Sand cone tests were conducted during the construction to measure the in-situ density of the No.2A coarse aggregate. The average measured in-situ unit weight (γ_t) of the uncompacted #2A coarse aggregate were determined to be 105.1 pcf (16.5 kN/m^3). The average measured moisture content of the compacted #2A coarse aggregate removed from the embankment was 2.34%. From this a dry unit weight (γ_{dry}) of 102.7 pcf (16.1 kN/m^3) was determined. The average measured in-situ unit weight (γ_t) of the compacted #2A coarse aggregate were determined to be 124.0 pcf (19.5 kN/m^3). The average measured moisture content of the compacted #2A coarse aggregate removed from the embankment was 2.09%. From this a dry unit weight (γ_{dry}) of 121.5 pcf (19.1 kN/m^3) was determined. *On average this achieved 86% of the maximum proctor density, which was closed to (2% less) what was achieved using the* Backfill Tamper.

The upstream pipe culvert was blocked to simulate the worse-case scenario at the beginning of the test. The flow rate was kept as 0.29 CFS to slowly reach the overtopping (approximately 14 min. to overtopping). Bedding material scour was found as the water level at the upstream side increased (Figure 24). Scour occurred around pipe when the flow rate was at 0.38 CFS, but no piping or seepage flow through the embankment were observed during the experiment (Figure 25). Significant surface scour was observed on both downstream and upstream sides after the embankment was overtopped (Figure 26The flow was kept running until most of the backfill material was eroded (Figure 27).

Figure 77: Bedding material scour under outlet

Figure 78 No piping or flow through the embankment in Test 24

Figure 79 Surface scour after overtopping on the downstream side

Figure 80 Erosion condition after completion of test

13.4. TEST 25 FLOWABLE FILL EMBANKMENT FOR CULVERT WITH PIPE BLOCKED

The flowable backfill embankment was constructed as described previously. Wood forms were set, and No.2A coarse aggregate was filled and compacted in the middle of the embankment before placing flowable backfill (Figure 28). Flowable backfill was mixed using the mix design No.3 in the concrete mixer (Figure 29). Figure 30a and b show the flowable backfill embankment after wood forms were removed.

Figure 81: Wood forms setup and No.2A coarse aggregate placement

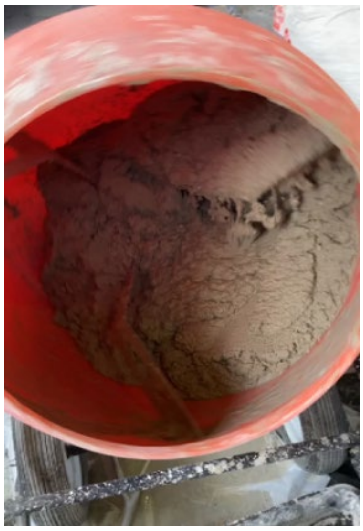

Figure 82: Flowable backfill mixed in the concrete mixer

(a)

(b)

Figure 83: Flowable backfill embankment (a) top view, and (b) downstream view

The pipe culvert was blocked during the experiment. The initial flow rate was set as the 0.77 CFS to reach the overtopping and increased up to 2.48 CFS after overtopping (3 mins). The flow velocity was measured as 1.8 ft/s on the top of the embankment and 3.5 ft/s on the downstream slope. Piping and no seepage flow went through the embankment. Besides, surface erosion, slope failure, and global failure were not observed on either the flowable backfill slopes or the middle of the embankment made by compacted No.2A coarse aggregate (Figure 31). Overtopping was kept under the high flood for 40 minutes, which was four times longer than any other tests conducted before, and no failure was found (Figure 32).

Figure 84: After overtopping

Figure 85: After 40 minutes of overtopping

14. RECOMMENDED CULVERT CONFIGURATION

As shown in the experimental program compacted No.2A coarse aggregate constructed in accordance with PennDOT Publication 408/2020, and PennDOT 72M RC-Drawings-30M (PennDOT, 2019, 2020) provides good performance. The compaction recommendations can effectively mitigate piping and seepage erosion before overtopping. However, significant surface scour occurs after the embankment is overtopped. To provide resilience against erosion following overtopping, flowable backfill, as specified in the PennDOT Publication 408/2020, and the updated PennDOT 72M RC-Drawings-30M (sheet 5 of 5) (PennDOT, 2019, 2020) is recommended for the end sections of the embankments with culverts. Compacted No.2A coarse aggregate can be used in the mid-section of the embankment between the flowable fill end sections.

AASHTO, T. (2019). Standard Method of Test for Moisture-Density Relations of Soils Using a 2.5-kg (5.5-lb) Rammer and a 305-mm (12-in.) Drop. *Standard Specifications for Transportation Materials and Methods of Sampling and Testing, American Association of State Highway and Transportation Officials (AASHTO), Washington DC*.

Abedini, M., Said, M. A. M., & Ahmad, F. (2012). Effectiveness of check dam to control soil erosion in a tropical catchment (The Ulu Kinta Basin). *Catena*, *97*, 63–70.

Abt, S. R., & Johnson, T. L. (1991). Riprap design for overtopping flow. *Journal of Hydraulic Engineering*, *117*(8), 959–972.

Abu-Hejleh, N. M., Alzamora, D., Mohamed, K., Saad, T., & Anderson, S. (2014). *Implementation Guidance for Using Spread Footings on Soils to Support Highway Bridges*.

Adamo, N., Al-Ansari, N., Sissakian, V., Laue, J., & Knutsson, S. (2020). Dam Safety Problems Related to Seepage: Dam Safety Problems Related to Seepage. *Earth Sciences and Geotechnical Engineering*, *10*(6), 191–239.

Adams, M., Nicks, J., Stabile, T., Wu, J. T., Schlatter, W., & Hartmann, J. (2011). *Geosynthetic reinforced soil integrated bridge system, synthesis report*. United States. Federal Highway Administration.

ASTM. (2006a). ASTM D 4253-00: Standard test method for maximum index density and unit weight of soils using a vibratory table. *Annual Book of ASTM Standards*.

ASTM. (2006b). ASTM D 4254-00: Standard test method for minimum index density and unit weight of soils and calculation of relative density. *Annual Book of ASTM Standards. American Society for Testing and Materials*.

ASTM. (2012). ASTM C39/C39M-12: Standard Test Method for Compressive Strength of Cylindrical Concrete Specimens. *Annual Book of ASTM Standard*.

ASTM. (2015a). ASTM C127 – 15: Standard test method for relative density (specific gravity) and absorption of coarse aggregate. *West Conshohocken, PA: ASTM*.

ASTM. (2015b). ASTM C143: Standard test method for slump of hydraulic-cement concrete. *ASTM Annual Book of ASTM Standards*.

Atkinson, J. H., Charles, J. A., & Mhach, H. K. (1990). Examination of erosion resistance of clays in embankment dams. *Quarterly Journal of Engineering Geology and Hydrogeology*, *23*(2), 103–108.

Beben, D. (2017). The role of backfill quality on corrugated steel plate culvert behaviour. *The Baltic Journal of Road and Bridge Engineering*, *12*(1), 1–11.

Briaud, J.-L. (1997). *Settlement of bridge approaches* (Vol. 234). Transportation Research Board.

Briaud, J.-L. (2008). Case histories in soil and rock erosion: Woodrow wilson bridge, Brazos River Meander, Normandy Cliffs, and New Orleans Levees. *Journal of Geotechnical and Geoenvironmental Engineering*, *134*(10), 1425–1447.

Briaud, J.-L., Chen, H.-C., Govindasamy, A. V., & Storesund, R. (2008). Levee erosion by overtopping in New Orleans during the Katrina Hurricane. *Journal of Geotechnical and Geoenvironmental Engineering*, *134*(5), 618–632.

Briaud, J.-L., Ting, F. C. K., Chen, H. C., Cao, Y., Han, S. W., & Kwak, K. W. (2001). Erosion function apparatus for scour rate predictions. *Journal of Geotechnical and Geoenvironmental Engineering*, *127*(2), 105–113.

Briaud, Shafii, I., Chen, H.-C., & Medina-Cetina, Z. (2019). *Relationship Between Erodibility and Properties of Soils*. Transportation Research Board.

Carroll Jr, R. G., Rodencal, J., & Collin, J. G. (1992). Geosynthetics in erosion control—The principles. *Geotextiles and Geomembranes*, *11*(4–6), 523–534.

Chanson, H. (2015). Embankment overtopping protection systems. *Acta Geotechnica*, *10*(3), 305–318.

Cividini, A., Bonomi, S., Vignati, G. C., & Gioda, G. (2009). Seepage-induced erosion in granular soil and consequent settlements. *International Journal of Geomechanics*, *9*(4), 187–194.

DeGroot, G. (1976). *Bonding study on layered soil-cement* (Vol. 76, Issue 16). Department of the Interior, Bureau of Reclamation.

El Taher, M., & Moore, I. D. (2011). *Effect of wall corrosion and backfill erosion on the strength of deteriorated metal culverts*.

Fell, R., & Fry, J.-J. (2007). *Internal Erosion of Dams and Their Foundations: Selected and Reviewed Papers from the Workshop on Internal Erosion and Piping of Dams and their Foundations, Aussois, France, 25-27 April 2005*. CRC Press.

Fell, R., Wan, C. F., Cyganiewicz, J., & Foster, M. (2003). Time for development of internal erosion and piping in embankment dams. *Journal of Geotechnical and Geoenvironmental Engineering*, *129*(4), 307–314.

Foster, M., Fell, R., & Spannagle, M. (2000). A method for assessing the relative likelihood of failure of embankment dams by piping. *Canadian Geotechnical Journal*, *37*(5), 1025–1061.

Frankson, R., K., Kunkel, S., Champion, B., Stewart, A. T., DeGaetano, & Sweet, W. (2017). Pennsylvania State Climate Summary. *NOAA National Centers for Environmental Information, Available at Https://Statesummaries. Ncics. Org/De*.

Fread, D. L. (1988). *BREACH, an erosion model for earthen dam failures*. Hydrologic Research Laboratory, National Weather Service, NOAA.

Fujisawa, K., Kobayashi, A., & Aoyama, S. (2009). Theoretical description of embankment erosion owing to overflow. *Geotechnique*, *59*(8), 661–671.

Fujisawa, K., Murakami, A., & Nishimura, S.-I. (2012). Experimental investigation of erosion rates of sand-clay mixtures and embankment failure caused by overflow. *Transactions of The Japanese Society of Irrigation*, *79*(3), 195–205.

Gao, K., Naito, C., Sulieman, M., Weisman, R., & Crociata, N. (2021). *Bridge Resilience in Rain Events Task 1.1 Evaluation of Backfill Properties* (ATLSS Report No. 21-01; p. 48). Lehigh University.

GDOT. (2013). *Standard specifications: Construction of transportation systems*.

Haeri, S. M., Noorzad, R., & Oskoorouchi, A. M. (2000). Effect of Geotextile Reinforcement on the Mechanical Behavior of Sand. *Geotextiles and Geomembranes*, *18*, 385–402.

Han, J., & Akins, K. (2002). Use of Geogrid-Reinforced and Pile-Supported Earth Structures. *Deep Foundations 2002*, 668–679. https://doi.org/10.1061/40601(256)48

Han, J., Bhandari, A., & Wang, F. (2012). DEM Analysis of Stresses and Deformations of Geogrid-Reinforced Embankments over Piles. *International Journal of Geomechanics*, *12*(4), 340–350. https://doi.org/10.1061/(ASCE)GM.1943-5622.0000050

Han, J., & Gabr, M. A. (2002). Numerical Analysis of Geosynthetic-Reinforced and Pile-Supported Earth Platforms over Soft Soil. *Journal of Geotechnical and Geoenvironmental Engineering*, *128*(1), 44–53. https://doi.org/10.1061/(ASCE)1090-0241(2002)128:1(44)

Hanson, G. J., Cook, K. R., & Britton, S. L. (2003). Observed erosion processes during embankment overtopping tests. *2003 ASAE Annual Meeting*, 1.

Hanson, G. J., & Hunt, S. L. (2006). Determining the erodibility of compacted soils for embankment dams. *Proceedings of the 26th Annual USSD Conference*, 311–320.

Helwany, S., Koutnik, T. E., & Ghorbanpoor, A. (2007). *Evaluation of Bridge Approach Settlement Mitigation Methods*. Wisconsin Highway Research Program.

Hewitt, P. G. (2004). Bernoulli's Principle. *The Science Teacher*, *71*(7), 51.

Hewlett, H. W. M., Boorman, L. A., & Bramley, L. A. (1987). *Design of reinforced grass waterways*. Construction Industry Research and Information Association.

Holtz, R. D., Kovacs, W. D., & Sheahan, T. C. (1981). *An introduction to geotechnical engineering* (Vol. 733). Prentice-Hall Englewood Cliffs.

Hoppe, E. J. (1999). *Guidelines for the use, design, and construction of bridge approach slabs*.

Horvath, J. S. (2000). Integral-abutment bridges: Problems and innovative solutions using EPS geofoam and other geosynthetics. *Res. Rpt. No. CE/GE-00*, *2*.

Houghtalen, R. J., Osman, A., & Hwang, N. H. (2016). *Fundamentals of hydraulic engineering systems*. Prentice Hall New York, NY.

Howard, A. K., & Hitch, J. L. (1998). *The design and application of controlled low-strength materials (flowable fill)*.

Illinois DOT. (2016). *Standard Specifications for Road and Bridge Construction*.

Indiana DOT. (2013). *Indiana Department of Transportation 2013 Design Manual*.

Iowa, D. O. T. (2012). Standard specifications for highway and bridge construction. *Iowa Department of Transportation, Ames, IA*.

Jeong, H.-S., Ryu, J.-I., & An, S.-R. (1989). An experimental study on piping failure of earth embankment. *Geotechnical Engineering*, *5*(4), 17–26.

Kaneshiro, J., Navin, S., Wendel, L., & Snowden, H. (2001). Controlled low strength material for pipeline backfill—Specifications, case histories and lessons learned. In *Pipelines 2001: Advances in Pipelines Engineering and Construction* (pp. 1–13).

Kentucky Department of Transportation. (2012). *Standard Specifications for Road and Bridge Construction*.

Kimmerling, R. (2002). *Geotechnical Engineering Circular No. 6 Shallow Foundations*. United States. Federal Highway Administration. Office of Bridge Technology.

Korkut, R., Martinez, E. J., Morales, R., Ettema, R., & Barkdoll, B. (2007). Geobag performance as scour countermeasure for bridge abutments. *Journal of Hydraulic Engineering*, *133*(4), 431–439.

Kramer, S. L., & Sajer, P. (1991). *Bridge approach slab effectiveness*. Washington State Department of Transportation.

LaDOTD. (2014). *Louisiana standard specifications for roads and bridges*. LA DOTD Baton Rouge, LA, USA.

LaDOTD, L. (Louisiana D. of T. and. (2016). *Louisiana standard specifications for roads and bridges*. LA DOTD Baton Rouge, LA, USA.

Lee, J. W., Butalia, T. S., & Wolfe, W. E. (1999). *Potential Use of FGD as a Flowable-Fill*.

Leonards, G. A., Huang, A. B., & Ramos, J. (1991). Piping and erosion tests at Conner Run Dam. *Journal of Geotechnical Engineering*, *117*(1), 108–117.

Long, J. H., Olson, S. M., Stark, T. D., & Samara, E. A. (1998). Differential Movement at Embankment-Bridge Structure Interface in Illinois. *Transportation Research Record: Journal of the Transportation Research Board*, *1633*(1), 53–60. https://doi.org/10.3141/1633-07

McLean, F. G., & Hansen, K. D. (1993). Roller compacted concrete for embankment overtopping protection. *Geotechnical Practice in Dam Rehabilitation*, 188–209.

Meade, B. W., Hunsucker, D. Q., & Stone, M. D. (1994). *Use of Flowable Fill (CLSM) for Trench Backfill*.

Mekkawy, M., White, D. J., Souleiman, M. T., & Sritharan, S. (2005). Simple design alternatives to improve drainage and reduce erosion at bridge abutments. *Proceedings of the 2005 Mid-Continent Transportation Research Symposium*.

Meyer, W., Schuster, R. L., & Sabol, M. A. (1994). Potential for seepage erosion of landslide dam. *Journal of Geotechnical Engineering*, *120*(7), 1211–1229.

Minnesota Department of Transportation. (2018). *Standard Specifications for Construction*.

Mitchell, J. K., & Soga, K. (2005). *Fundamentals of soil behavior* (Vol. 3). John Wiley & Sons New York.

MoDOT. (2018). *2018 Missouri Standard Specifications for Highway Construction* (p. 777). Missouri Highways and Transportation Commission.

Moore, I. D. (2001). Buried pipes and culverts. In *Geotechnical and geoenvironmental engineering handbook* (pp. 541–567). Springer.

Morales, R., Ettema, R., & Barkdoll, B. (2008). Large-scale flume tests of riprap-apron performance at a bridge abutment on a floodplain. *Journal of Hydraulic Engineering*, *134*(6), 800–809.

Naik, T. R., & Singh, S. S. (1997). Permeability of flowable slurry materials containing foundry sand and fly ash. *Journal of Geotechnical and Geoenvironmental Engineering*, *123*(5), 446–452.

Najafi, M., & Bhattachar, D. V. (2011). Development of a culvert inventory and inspection framework for asset management of road structures. *Journal of King Saud University-Science*, *23*(3), 243–254.

Naji, M., Firoozi, A. A., & Firoozi, A. A. (2020). A Review: Study of Integral Abutment Bridge with Consideration of Soil-Structure Interaction. *Latin American Journal of Solids and Structures*, *17*(2).

ODOT. (2005). ODOT Bridge Design Manual. *Columbus, Ohio*.

Ojha, C. S. P., Singh, V. P., & Adrian, D. D. (2003). Determination of critical head in soil piping. *Journal of Hydraulic Engineering*, *129*(7), 511–518.

Oklahoma DOT. (2009). *Oklahoma Design Standards*.

Palmeira, E. M., & Gardoni, M. G. (2002). Drainage and filtration properties of non-woven geotextiles under confinement using different experimental techniques. *Geotextiles and Geomembranes*, *20*(2), 97–115. https://doi.org/10.1016/S0266-1144(02)00004-3

PennDOT. (2010). *COMMONWEALTH OF PENNSYLVANIA DEPARTMENT OF TRANSPORTATION BUREAU OF PROJECT DELIVERY STANDARDS FOR ROADWAY CONSTRUCTION SERIES RC-1M TO 100M*.

PennDOT. (2015). *Penndot Drainage Manual* (Pub 584). PennDOT.

PennDOT. (2019). *COMMONWEALTH OF PENNSYLVANIA DEPARTMENT OF TRANSPORTATION BUREAU OF PROJECT DELIVERY STANDARDS FOR ROADWAY CONSTRUCTION SERIES RC-1M TO 100M*.

PennDOT. (2020). *Commonwealth of Pennsylvania DEPARTMENT OF TRANSPORTATION Publication 408/2020 SPECIFICATIONS*.

Powledge, G. R., & Dodge, R. A. (1985). Overtopping of small dams—An alternative for dam safety. *Hydraulics and Hydrology in the Small Computer Age*, 1071–1076.

Powledge, G. R., Ralston, D. C., Miller, P., Chen, Y. H., Clopper, P. E., & Temple, D. M. (1989). Mechanics of overflow erosion on embankments. II: Hydraulic and design considerations. *Journal of Hydraulic Engineering*, *115*(8), 1056–1075.

Raj, M., & Sengupta, A. (2014). Rain-triggered slope failure of the railway embankment at Malda, India. *Acta Geotechnica*, *9*(5), 789–798.

Reidmiller, D. R., Avery, C. W., Easterling, D. R., Kunkel, K. E., Lewis, K. L., Maycock, T. K., & Stewart, B. C. (2017). *Impacts, risks, and adaptation in the United States: Fourth national climate assessment, volume II*.

Richards, K. S., & Reddy, K. R. (2007). Critical appraisal of piping phenomena in earth dams. *Bulletin of Engineering Geology and the Environment*, *66*(4), 381–402.

Samadi, A., & Herbert, R. (2003). Corrosiveness of Controlled Low Strength Materials vs. That of Encasement Sand. In *New Pipeline Technologies, Security, and Safety* (pp. 514–523).

Samtani, N. C., & Nowatzki, E. A. (2006). *Soils and Foundations: Reference Manual*. United States. Federal Highway Administration.

Shiotani, T., & Ohtsu, M. (1999). Prediction of slope failure based on AE activity. In *Acoustic emission: Standards and technology update*. ASTM International.

Singh, V. P., Scarlatos, P. D., Collins, J. G., & Jourdan, M. R. (1988). Breach erosion of earthfill dams (BEED) model. *Natural Hazards*, *1*(2), 161–180.

Stephenson, J. B., Zhou, W. F., Beck, B. F., & Green, T. S. (1999). Highway stormwater runoff in karst areas—Preliminary results of baseline monitoring and design of a treatment system for a sinkhole in Knoxville, Tennessee. *Engineering Geology*, *52*(1–2), 51–59.

Sterpi, D. (2003). Effects of the erosion and transport of fine particles due to seepage flow. *International Journal of Geomechanics*, *3*(1), 111–122.

Tennessee, D. O. T. (2015). Standard specifications for road and bridge construction. *Nashville, TN: Tennessee DOT*.

Tingsanchali, T., & Chinnarasri, C. (2001). Numerical modelling of dam failure due to flow overtopping. *Hydrological Sciences Journal*, *46*(1), 113–130.

Van Tol, J., Akpan, W., Kanuka, G., Ngesi, S., & Lange, D. (2016). Soil erosion and dam dividends: Science facts and rural 'fiction'around the Ntabelanga dam, Eastern Cape, South Africa. *South African Geographical Journal*, *98*(1), 169–181.

Wahls, H. E. (1990). *Design and construction of bridge approaches* (Vol. 159). Transportation Research Board.

Wan, C. F., & Fell, R. (2004). Investigation of Rate of Erosion of Soils in Embankment Dams. *Journal of Geotechnical and Geoenvironmental Engineering*, *130*(4), 373–380. https://doi.org/10.1061/(ASCE)1090-0241(2004)130:4(373)

Wang, Z., Li, Q., Zhang, N., Jin, Y., Qin, H., & Ding, J. (2020). Slope failure of biotreated sand embankments under rainfall conditions: Experimental investigation and numerical simulation. *Bulletin of Engineering Geology and the Environment*, *79*(9), 4683–4699.

White, D., Sritharan, S., Suleiman, M. T., & Chetlur, S. (2005). *Identification of the best practices for design, construction, and repair of bridge approaches*. Iowa. Dept. of Transportation.

Wisconsin DOT. (2021). *Standard Specifications for Highway and Sturcture Construction*.

Wu, J. Y. (2005). Soil-based flowable fill for pipeline construction. In *Pipelines 2005: Optimizing Pipeline Design, Operations, and Maintenance in Today's Economy* (pp. 925–938).

Xie, Q., Liu, J., Han, B., Li, H., Li, Y., & Jiang, Z. (2019). Experimental investigation of interfacial erosion on culvert-soil interface in earth dams. *Soils and Foundations*, *59*(3), 671–686.

Yang, J., Yin, Z.-Y., Laouafa, F., & Hicher, P.-Y. (2019). Modeling coupled erosion and filtration of fine particles in granular media. *Acta Geotechnica*, *14*(6), 1615–1627.

Yegian, M. K., Ghahraman, V. G., & Harutiunyan, R. N. (1994). Liquefaction and embankment failure case histories, 1988 Armenia earthquake. *Journal of Geotechnical Engineering*, *120*(3), 581–596.

Yuan, S., Li, L., Amini, F., & Tang, H. (2014). Numerical study of turbulence and erosion of an HPTRM-strengthened levee under combined storm surge overflow and wave overtopping. *Journal of Coastal Research*, *30*(1), 142–157.

Zevgolis, I., & Bourdeau, P. L. (2007). *Mechanically stabilized earth wall abutments for bridge support*.